

BLM LIBRARY



88006432

AIRBORNE INFRARED
DETECTION OF DEER

H. Parker, Jr., 1972

Published on demand by
UNIVERSITY MICROFILMS
University Microfilms Limited, High Wycomb, England
A Xerox Company, Ann Arbor, Michigan, U.S.A.

88006432

AREA OIL SHALE OFFICE
CENTRAL LIBRARY,

QL
737
.U55
P37
1972

BLM Library
D-553A, Building 50
Denver Federal Center
P. O. Box 25047
Denver, CO 80225-0047

1. The first of these is the
fact that the system is
not a simple one, and
that it is not a simple
one.

**This is an authorized facsimile
and was produced by microfilm-xerography
in 1975 by
Xerox University Microfilms,
Ann Arbor, Michigan,
U.S.A.**

72-31,335

PARKER, Jr., H. Dennison, 1941-
AIRBORNE INFRARED DETECTION OF DEER.

Colorado State University, Ph.D., 1972
Agriculture, forestry & wildlife

University Microfilms, A XEROX Company, Ann Arbor, Michigan

DISSERTATION

AIRBORNE INFRARED DETECTION OF DEER

Submitted by

H. Dennison Parker, Jr.

In partial fulfillment of the requirements

for the Degree of Doctor of Philosophy

Colorado State University

Fort Collins, Colorado

May, 1972

COLORADO STATE UNIVERSITY

May 17

1972

WE HEREBY RECOMMEND THAT THE DISSERTATION PREPARED UNDER OUR
SUPERVISION BY H. DENNISON PARKER, JR.
ENTITLED AIRBORNE INFRARED DETECTION OF DEER
BE ACCEPTED AS FULFILLING IN PART REQUIREMENTS FOR THE DEGREE OF
DOCTOR OF PHILOSOPHY

Committee on Graduate Work

Richard J. Dinnel

W E Frazer

Charles J. Furr
Adviser

W E Frazer

C. J. Frazer

Head of Department

ABSTRACT OF DISSERTATION

AIRBORNE INFRARED DETECTION OF DEER

A study of airborne infrared deer detection was conducted in two phases. Phase I was an investigation of the radiant temperatures of mule deer and their surroundings on winter range in Colorado. Radiant temperatures of tame deer, sagebrush, snow, and rock were measured with an infrared radiometer during the winter of 1970. Air temperature, solar radiation, windspeed, and humidity were recorded simultaneously with each radiant temperature measurement.

All radiant temperatures were closely associated with and always exceeded, air temperature. Direct-beam solar radiation had a strong, but erratic effect on the radiant temperatures of all surfaces measured, except snow. Thermal contrast, the difference between deer and background radiant temperatures, was inversely related to air temperature. Although thermal contrast was greater during the daytime, the potential detection error due to solar heating of environmental substrata suggests that periods of no direct-beam solar radiation and low air temperatures are best for deer detection.

Phase II consisted of two flight tests of airborne thermal scanners for deer detection. The first test, in summer near Fort Collins, Colorado, resulted in 97 to 98.5% accurate detection of deer and antelope in pens. The second test, in winter over a larger area in Middle Park, Colorado produced successful detection of some deer, but not all.

Exact error figures were not available due to the failure of aerial photography, flown simultaneously to provide a control on the number of animals thermally detected, to image animals.

The author concludes that, based on the radiometric data, wild mule deer are probably detectable in their winter environment in Colorado, but that scanning equipment more sophisticated than that used in this study will be required except under conditions of total snow cover and little topographic relief. Technical limitations of thermal scanners are discussed in relation to deer detection.

H. Dennison Parker, Jr.

Range Science Department

Colorado State University

Fort Collins, Colorado 80521

June, 1972

ACKNOWLEDGEMENTS

In the interest of brevity, I am tempted to reduce these acknowledgements to the bare minimum. But I cannot, in fairness to all the people and organizations that made this study possible. Therefore, my thanks to:

Dr. Phil Weber and other personnel of the Forest Service Pacific Southwest Forest and Range Experiment Station, Berkeley, California, for the loan of equipment, and for advice and consultation on various aspects of the study.

R. Bruce Gill, Wildlife Researcher, and Paul F. Gilbert, Area Supervisor, Colorado Division of Game, Fish and Parks, Middle Park, Colorado, for permitting me the use of Division facilities, including the deer pen and trailer used in Phase I of the study, and for expert advice and counsel on the Middle Park deer population. Thanks is also due the Colorado Division of Game, Fish and Parks generally, for its interest and financial cooperation in this study.

Dr. O. C. Wallmo, project leader, and his colleagues in Wildlife Habitat Management Research at the Rocky Mountain Forest and Range Experiment Station, Fort Collins, Colorado, for the use of their tame deer, and for assistance and advice throughout the study.

Dr. Mario Martinelli and Mr. Marvin D. Hoover, project leaders, and their associates in Watershed Management Research, Rocky Mountain Forest and Range Experiment Station, for their loan of equipment during Phase I of the study.

Mr. Jim Elms and Mr. John Voth of the Aerial Fire Depot, Forest Service Region 1, Missoula, Montana, and Mr. Ralph Wilson of the Forest Service Firelab at Missoula, for valuable assistance in the planning and execution of the Middle Park deer detection test.

Dr. Aaron N. Moen, Assistant Professor, Cornell University, and Dr. David M. Gates, Director, Missouri Botanical Garden, for reviews of the original study plan.

The U. S. Department of Agriculture, Forest Service, and the National Aeronautics and Space Administration for sponsoring this research. Without the far-sighted interest of both these organizations in remote sensing of earth resources, this study would not have been made.

Mrs. Alice Wierman for typing, and advice on typographical form, of the final manuscript, and to Dr. Harold A. Paulsen, Assistant Director, Range and Wildlife Habitat Management Research, for allowing me Mrs. Wierman's services.

My graduate committee, Dr. Richard S. Driscoll, Dr. Warren E. Frayer, Dr. William E. Marlatt, and Dr. Charles F. Terwilliger,

my major professor, for the usual guidance in my graduate program, but also for the unusual liberty to pursue my research and studies unencumbered by a demand for adherence to pre-conceived ideas of appropriate curricula or study design. I could not have achieved my goals of either education or research in such a diverse field as remote sensing without that freedom and trust.

Special thanks are due Dick Driscoll, my literal mentor throughout the whole program. As a scientist, counselor, committee chairman and huntin' buddy, Dick was the personification of the ideal - no graduate student could ask for more.

Finally, thanks to my wife, Debbie, my son Jeff, and daughter, Kim. Deb knows what for....the kids will.

TABLE OF CONTENTS

<u>Chapter</u>	<u>Page</u>
I. <u>INTRODUCTION</u>	1
THE NEED FOR DEER DETECTION	1
COMMON METHODS OF DIRECT DETECTION	3
<u>Visual Detection</u>	3
<u>Photographic Detection</u>	4
PURPOSE OF THE STUDY	5
DETECTION OF INFRARED RADIATION	7
<u>Infrared Photography</u>	7
<u>Long-wave Infrared Detection</u>	7
Radiometers	10
Optical-Mechanical Scanners	10
II. <u>LITERATURE REVIEW</u>	27
INFRARED BIG GAME CENSUS	27
THE DEER AS AN ENERGY SYSTEM	33
<u>General Energy Budget</u>	33
<u>Metabolic Heat Production</u>	35
<u>Absorbed Radiant Energy</u>	37
<u>Conductive Heat Loss</u>	40
<u>Convective Cooling</u>	46
BACKGROUND TEMPERATURE	47

TABLE OF CONTENTS (continued)

<u>Chapter</u>	<u>Page</u>
III. <u>PHASE I: RADIOMETRIC INVESTIGATIONS</u>	51
EXPERIMENTAL PROCEDURE	51
<u>The Study Area</u>	51
<u>Materials and Instrumentation</u>	54
<u>Sampling Procedure</u>	58
<u>Data Analysis</u>	59
RESULTS AND DISCUSSION	60
<u>Deer ERT Variation</u>	60
<u>Background ERT Variation</u>	77
<u>Thermal Contrast</u>	105
<u>Potential Error Sources</u>	121
CONCLUSIONS	122
IV. <u>PHASE II: THERMAL SCANNING TESTS</u>	126
EXPERIMENTAL PROCEDURE	126
<u>Fort Collins Test</u>	126
<u>Middle Park Test</u>	129
Test Site Descriptions	129
Equipment	135
Procedure	138
RESULTS AND DISCUSSION	144
<u>Fort Collins Test</u>	144
<u>Middle Park Test</u>	148

TABLE OF CONTENTS (continued)

<u>Chapter</u>	<u>Page</u>
Radiant Temperatures	148
Aerial Photography	148
Thermal Imagery	152
V. <u>OVERALL CONCLUSIONS</u>	162
LITERATURE CITED	170
APPENDIX A - Properties of Infrared Radiation	176
APPENDIX B - Modes of Heat Transfer	183

LIST OF TABLES

<u>Table</u>	<u>Page</u>
1 George Reserve ground radiometer data from Croon, 1967	30
2 Total emittance of pelts from several mammals, at constant skin temperature of 38°C. (From Birkebak, 1966)	41
3 Solar reflectance (ρ) and absorptance (α) of several mammal pelts. (From Birkebak, 1966) . .	42
4 Results of stepwise multiple, linear regressions	61
5 ERT measurements at Junction Butte on January 26, 1972, 6:00 a.m.	149
6 The effect of wind speed on the ERT of snow	151
7 The effect of wind speed on the ERT of snow	151
8 The effect of wind speed on the ERT of snow	151
9 The effect of wind speed on the ERT of snow	151
10 The effect of wind speed on the ERT of snow	151
11 The effect of wind speed on the ERT of snow	151
12 The effect of wind speed on the ERT of snow	151
13 The effect of wind speed on the ERT of snow	151
14 The effect of wind speed on the ERT of snow	151
15 The effect of wind speed on the ERT of snow	151
16 The effect of wind speed on the ERT of snow	151
17 The effect of wind speed on the ERT of snow	151
18 The effect of wind speed on the ERT of snow	151
19 The effect of wind speed on the ERT of snow	151
20 The effect of wind speed on the ERT of snow	151
21 The effect of wind speed on the ERT of snow	151
22 The effect of wind speed on the ERT of snow	151
23 The effect of wind speed on the ERT of snow	151
24 The effect of wind speed on the ERT of snow	151
25 The effect of wind speed on the ERT of snow	151
26 The effect of wind speed on the ERT of snow	151
27 The effect of wind speed on the ERT of snow	151
28 The effect of wind speed on the ERT of snow	151
29 The effect of wind speed on the ERT of snow	151
30 The effect of wind speed on the ERT of snow	151
31 The effect of wind speed on the ERT of snow	151
32 The effect of wind speed on the ERT of snow	151
33 The effect of wind speed on the ERT of snow	151
34 The effect of wind speed on the ERT of snow	151
35 The effect of wind speed on the ERT of snow	151
36 The effect of wind speed on the ERT of snow	151
37 The effect of wind speed on the ERT of snow	151
38 The effect of wind speed on the ERT of snow	151
39 The effect of wind speed on the ERT of snow	151
40 The effect of wind speed on the ERT of snow	151
41 The effect of wind speed on the ERT of snow	151
42 The effect of wind speed on the ERT of snow	151
43 The effect of wind speed on the ERT of snow	151
44 The effect of wind speed on the ERT of snow	151
45 The effect of wind speed on the ERT of snow	151
46 The effect of wind speed on the ERT of snow	151
47 The effect of wind speed on the ERT of snow	151
48 The effect of wind speed on the ERT of snow	151
49 The effect of wind speed on the ERT of snow	151
50 The effect of wind speed on the ERT of snow	151
51 The effect of wind speed on the ERT of snow	151
52 The effect of wind speed on the ERT of snow	151
53 The effect of wind speed on the ERT of snow	151
54 The effect of wind speed on the ERT of snow	151
55 The effect of wind speed on the ERT of snow	151
56 The effect of wind speed on the ERT of snow	151
57 The effect of wind speed on the ERT of snow	151
58 The effect of wind speed on the ERT of snow	151
59 The effect of wind speed on the ERT of snow	151
60 The effect of wind speed on the ERT of snow	151
61 The effect of wind speed on the ERT of snow	151
62 The effect of wind speed on the ERT of snow	151
63 The effect of wind speed on the ERT of snow	151
64 The effect of wind speed on the ERT of snow	151
65 The effect of wind speed on the ERT of snow	151
66 The effect of wind speed on the ERT of snow	151
67 The effect of wind speed on the ERT of snow	151
68 The effect of wind speed on the ERT of snow	151
69 The effect of wind speed on the ERT of snow	151
70 The effect of wind speed on the ERT of snow	151
71 The effect of wind speed on the ERT of snow	151
72 The effect of wind speed on the ERT of snow	151
73 The effect of wind speed on the ERT of snow	151
74 The effect of wind speed on the ERT of snow	151
75 The effect of wind speed on the ERT of snow	151
76 The effect of wind speed on the ERT of snow	151
77 The effect of wind speed on the ERT of snow	151
78 The effect of wind speed on the ERT of snow	151
79 The effect of wind speed on the ERT of snow	151
80 The effect of wind speed on the ERT of snow	151
81 The effect of wind speed on the ERT of snow	151
82 The effect of wind speed on the ERT of snow	151
83 The effect of wind speed on the ERT of snow	151
84 The effect of wind speed on the ERT of snow	151
85 The effect of wind speed on the ERT of snow	151
86 The effect of wind speed on the ERT of snow	151
87 The effect of wind speed on the ERT of snow	151
88 The effect of wind speed on the ERT of snow	151
89 The effect of wind speed on the ERT of snow	151
90 The effect of wind speed on the ERT of snow	151
91 The effect of wind speed on the ERT of snow	151
92 The effect of wind speed on the ERT of snow	151
93 The effect of wind speed on the ERT of snow	151
94 The effect of wind speed on the ERT of snow	151
95 The effect of wind speed on the ERT of snow	151
96 The effect of wind speed on the ERT of snow	151
97 The effect of wind speed on the ERT of snow	151
98 The effect of wind speed on the ERT of snow	151
99 The effect of wind speed on the ERT of snow	151
100 The effect of wind speed on the ERT of snow	151

LIST OF FIGURES

<u>Figure</u>	<u>Page</u>
1 The infrared spectrum. (redrawn from Hackforth, 1960)	8
2 Method of terrain coverage by optical-mechanical scanners. (From Hirsch, et al., 1968)	12
3 Image formation by an optical-mechanical scanner. (From Wilson, et al., 1971	15
4 Typical scanner optical system. (Texas Instruments, Inc., 1971).	17
5 Optical-mechanical scanning geometry. (From Hirsch, et al., 1968).	20
6 Deer winter range near the Junction Butte study area.	52
7 The platform from which all ERT values were measured. (Photo by Paul Gilbert, Colorado Division of Game, Fish and Parks).	56
8 The effect of passing clouds on the ERT of deer .	63
9 The effect of shading on the ERT of a deer hide. Shade applied at time = 0, and removed at time = 120. (From Parker and Harlan, 1972).	65
10 ERT decay following shading of a deer hide in three trials. (From Parker and Harlan, 1972). . .	67
11 Regression lines of animal and snow ERT from Marble (1967), Moen (1968), and this study	74
12 Plot of sagebrush ERT vs. air temperature	78
13 Plot of sagebrush ERT vs. solar radiation	80
14 Plot of sagebrush ERT vs. time of day	82

LIST OF FIGURES (continued)

<u>Figure</u>		<u>Page</u>
15	Plot of snow ERT vs. air temperature	84
16	Plot of snow ERT vs. solar radiation	86
17	Plot of snow ERT vs. time of day	88
18	Plot of rock ERT vs. air temperature	90
19	Plot of rock ERT vs. solar radiation	92
20	Plot of rock ERT vs. time of day	94
21	Plot of deer ERT vs. air temperature	96
22	Plot of deer ERT vs. solar radiation	98
23	Plot of deer ERT vs. time of day	100
24	Plot of deer ERT vs. sagebrush ERT during same sample period. Deer ERT exceeded sagebrush ERT at all points above solid line.	107
25	Plot of deer ERT vs. snow ERT during same sample period. Deer ERT exceeded snow ERT at all points above solid line.	109
26	Mean thermal contrast between deer and sagebrush (ΔT_g), over 5°C air temperature classes.	111
27	Variation in ERT of deer, rock, soil, and sage- brush on a cloudless day. Rock, Soil, and sagebrush were all sunlit.	113
28	Variation in ERT of deer, rock, soil, and sage- brush on an overcast day.	115
29	Night regression lines of deer, snow, and sage- brush. Deer line calculated from nightclass deer data.	117
30	Day regression lines of deer, snow, and sage- brush. Deer line calculated from dayclass deer data.	119

LIST OF FIGURES (continued)

<u>Figures</u>	<u>Page</u>
31 Deer pens on the foothills campus at Colorado State University.	127
32 Mule deer on a portion of the Jensen Creek extensive site.	131
33 Variable topography in the Cedar Ridge area . .	133
34 Juniper overstory on the south side of Cedar Ridge.	133
35 Forest Service Kingair (foreground) and Aerocommander.	136
36 Flight line pattern on the Jensen Creek and Cedar Ridge sites.	139
37 Fluorescent panels marking initial points on flight lines.	142
38 Thermal imagery of deer in pens on Colorado State University foothills campus (enlarged approximately 11 times).	145
39 Part of one frame of aerial photography obtained over the Cedar Ridge site.	150
40 Thermal imagery of deer (white spots) on the Cedar Ridge site. Arrow indicates direction of flight. (Enlarged approximately 2.2 times)..	153
41 Thermal imagery of cattle (white spots) along Colorado River. (Enlarged approximately 2.2 times). This imagery was generated from the tape-recorded video data.	155
42 The contribution of deer ERT to integrated resolution element ERT, as a function of the instantaneous angular field of view (IFOV). . .	164
43 Blackbody radiation curves, 100°K to 1,000°K. .	177

Chapter I

INTRODUCTION

THE NEED FOR DEER DETECTION

Census information, in the very broadest sense, has long been recognized as a basic requirement for effective game management. Leopold (1933), gives four steps usually involved in the initiation of [game] management on any piece of land. The first step listed is census.

McCain and Taylor (1956), wrote, "It is unnecessary to point out the necessity of an inventory of the deer population on each unit of deer range. One needs only to remember the following problems, the solutions of which are possible only with some reliable idea of deer numbers: Are there too many deer on the range for the available forage? How do numbers of deer and their effects on the forage compare with numbers and influence of domestic livestock? Are the deer increasing or decreasing? How many and what kind (bucks, does, fawns) should be harvested each year?"

Stanley A. Cain, former Assistant Secretary for Fish, Wildlife and Parks, U.S. Department of the Interior, said in 1966: "There is need for information on population size, occurrence of subpopulations, and distribution in space and time of individual species and associations of different species. There is need for data on recruitment and mortality. Such inventory data are required for fishes, birds, and

mammals of importance to man if they are to be granted conservation management, that is, if man is to make nondepletive use of them by avoiding overharvest."

Thus, the need for census information has been acknowledged throughout the history of modern game management. Today, increased recreational demands on our game species, indeed, the very survival of some, are requiring an increase in management intensity to a degree which can only be speculated at this time. The principles of management are known and have not changed since they were first written by Leopold (1933). However, successful management based on these principles depends on the quality of the ecological information which is available. Heretofore, mistakes by game managers, due to a lack of this information, have been buffered somewhat by the high productivity of most game species--there was room for error. But the error margin is now decreasing rapidly.

Census information may be spatial, temporal, or both. Theoretically, a spatial census would yield information on animal numbers at a single point in time, over a specified area. In a temporal census, the spatial dimension is held constant while time is varied. There are many possible combinations and variations of these two basic categories, but there is one characteristic which is common to all--the presence of individual animals is to be known, i.e., the animals must be detected. In the usual sense, census amounts to quantitative detection of individuals in space, usually over the range or part of the range of the species under investigation. But detection may also be limited to a small area or include the time dimension, for the purpose of determining migratory patterns,

behavior, food preference, or any of a wide range of other species or population characteristics.

COMMON METHODS OF DIRECT DETECTION

Visual Detection

Historical methods of determining the whereabouts of deer may be considered in two categories, direct and indirect. Indirect methods, such as pellet group counting, do not detect deer. Rather, they detect evidence of deer use. Direct methods, however, detect the actual animals. With the indirect methods, the quantity which is detected must be related to the quantity of interest, deer numbers. Theoretically, direct detection methods are inherently simpler because this step is omitted. The quantity detected and the quantity of interest are the same. In fact, however, this theoretical simplicity has rarely been observed.

All direct deer detection methods of the past and probably of the future, must actually detect electromagnetic radiation emanating from the animals. The most common detector of this type of radiation is the eye, and visual counting of various big-game species from aircraft is standard management procedure in numerous states. However, there are serious limitations to the technique.

Evans, et al., (1966) reported, "The foremost problem in an aerial census, particularly of animals in a forested habitat, is to eliminate or evaluate visibility bias." Bergerud and Manuel (1969) reported



acceptable accuracy in moose counts, "...only because of pilot and observer experience." Watson and Scott (1956) realized that "... seldom, if ever, do aerial observers see all the animals they are attempting to count....," and estimated that 22% of the caribou population studied was missed in aerial counts. This same error source has been discussed by numerous other authors (Siniff and Skoog, 1964; Thomas, 1967; Pennycuik, 1968).

The importance of the background against which the animals are observed may also be a critical factor. In Colorado, Gilbert and Grieb (1957) concluded that "...snow cover is a great influence on the accuracy of aerial big game counts." Evans, et al., (1966) noted "...good snow cover is practically essential...." The importance of background characteristics in antelope counts was brought out by Bear (1970).

Other problems associated with aerial visual detection of big-game animals include light conditions (Turner and Watson, 1964; Grzimek and Grzimek, 1960; Siniff and Skoog, 1964; Gilbert and Grieb, 1957), delineation of sample area (Banfield, et al., 1955; Watson, et al., 1969), and eye fatigue.

Photographic Detection

Aerial photography has been used less than visual observation, probably because of its greater cost and equipment requirements. The main value of photography is the instantaneous recording of a scene which can be examined more closely at a later date. The advantage here is obvious when large herds of animals must be counted. However,

since conventional cameras and films "see" approximately the same as the human eye, some of the problems associated with visual observation also apply to aerial photography. In particular, the problem of visibility remains.

Siniff and Skoog (1964) cite the difficulty of locating animals on photographs where there is heavy vegetative cover or a poor background. Grzimek and Grzimek (1960) rejected photography because of the very large number of exposures which would have been required to cover the area they studied in Tanganyika. Thomas (1967) mentioned the importance of a snow background for aerial photographic counting of caribou.

PURPOSE OF THE STUDY

The possibility of detecting wild deer by their radiated "body heat" suggests solutions to several of the problems encountered in visual or photographic detection. The primary advantage is the reduction or elimination of visibility bias. Additionally, the prospect of automatic data interpretation, coupled with the rapid, wide area coverage capability of airborne thermal radiation detectors, offers a method for obtaining much larger, and therefore more meaningful samples from which to statistically estimate population size.

This study was both exploratory and applied. As shown in Chapter II, almost no work had been done on the detectability of big-game animals by an airborne thermal infrared scanner. Even less information was available on the basic radiation properties which determine such detectability. Therefore, this study was divided into two phases.

When measurement systems are taken into account, the results are not as simple as they seem. The results are often more complex than they appear. In particular, the results are often more complex than they appear. In particular, the results are often more complex than they appear.

There are many factors that can affect the results of a measurement. These factors can be divided into two main categories: systematic errors and random errors. Systematic errors are errors that are caused by a consistent bias in the measurement process. Random errors are errors that are caused by unpredictable variations in the measurement process. Both types of errors can lead to inaccurate results.

MEASUREMENT IN THE FUTURE

The possibility of measuring things in the future is a topic that has been discussed for many years. Some people believe that it is possible to measure things in the future, while others believe that it is not. The debate is still ongoing, and there is no clear answer at this time. However, it is clear that the possibility of measuring things in the future is a topic that is worth considering.

There are many reasons why it is difficult to measure things in the future. One of the main reasons is that the future is uncertain. We do not know what will happen in the future, and this makes it difficult to measure things in the future. Another reason is that the future is often very far away, and this makes it difficult to measure things in the future.

The first phase was an investigation of the environmental factors which were hypothesized to have important effects on the emission of thermal infrared radiation by wild, Rocky Mountain mule deer (Odocoileus hemionus hemionus, Raf.). These factors were air temperature, solar radiation, windspeed, relative humidity, and time of day. Specifically, the following questions were posed:

- 1) What is the relative importance of each of the environmental factors studied to the natural variation in surface radiant temperatures of mule deer?
- 2) How much thermal contrast is there between deer and their surroundings, and how does it vary in terms of the environmental factors?
- 3) When, in terms of the environmental factors studied, would detection be most likely?

Phase II consisted of flight testing of an airborne thermal infrared scanner under conditions of maximum theoretical deer detectability, as drawn from the results of Phase I. It would have been desirable to attempt detection under a variety of conditions to test in depth the results of Phase I, especially question 3, above. But, due to the difficulty and expense involved in gaining the use of the necessary scanning equipment, the testing schedule under Phase II consisted of two trials. The first test, near Fort Collins, was conducted to aid in the planning of the Middle Park test, in which the Phase I results were applied.

DETECTION OF INFRARED RADIATION

Infrared Photography

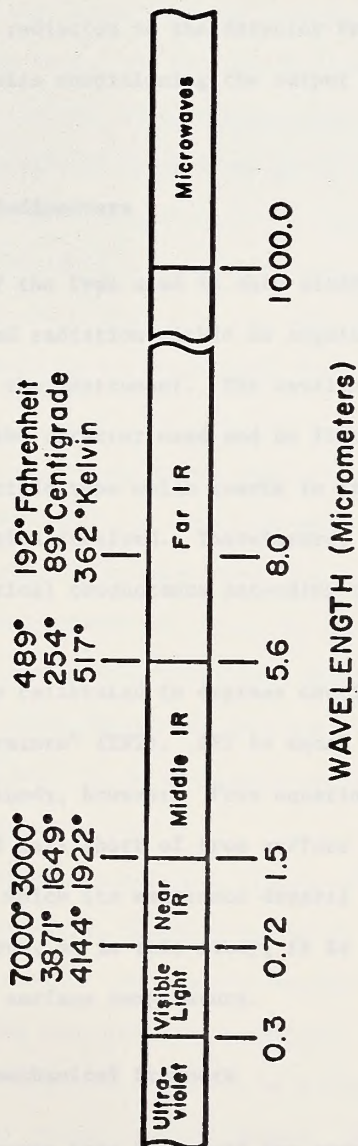
The infrared spectrum may be considered in three wavelength bands, the near infrared (0.7 to 1.5 micrometers), the middle infrared (1.5 to 5.6 micrometers), and the far infrared (> 5.6 micrometers) (Figure 1) (Hackforth, 1960). The near infrared band is also known as the "photographic" infrared band, because radiation in these wavelengths can be detected by certain photographic films (Kodak types 2443, 5424). Because of the high reflectance in this band by healthy green plants, infrared photographic films have been extensively used for vegetation analysis.

Longwave Infrared Detection

Detection of radiation at wavelengths longer than 1.5 micrometers requires electronic rather than photographic methods. In photography, each photo-sensitive grain in the emulsion reacts to the radiation which is incident on it, producing a change in the color or shading. Variation in the light intensity reaching different portions of the exposed film results in variation in reaction among individual grains, and an image is formed. Infrared radiation in the middle and far infrared bands, however, cannot be detected by any photographic films now available. In fact, even if such a hypothetical film were available, it would be exposed by the infrared radiation emitted by the camera in which it was being used. Therefore, at the heart of any longwave

Figure 1.--The infrared spectrum. (redrawn from Hackforth, 1960).

TEMPERATURE OF PEAK RADIATED ENERGY



infrared detection system is the detector, an electronic analog of the photo-sensitive film grain. The other components of these systems perform the tasks of directing radiation to the detector from the targets, and of amplifying and otherwise conditioning the output signal of the detector.

Radiometers

Infrared radiometers of the type used in this study detect and measure the longwave infrared radiation within an angular field of view determined by the optics of the instrument. The wavelengths of radiation detected are determined by the detector used and by filters. The detector is usually of the thermoelectric type which reacts to its own temperature changes caused by the radiation received. Thermistors, solid-state devices which vary in electrical conductance according to their temperature, are often used.

Radiometers are usually calibrated in degrees centigrade, a measure of "effective radiant temperature" (ERT). ERT is equal to true surface temperature only for a blackbody, however. From equation 31, (Appendix A), the ERT of a surface will fall short of true surface temperature in proportion to the amount by which its emittance departs from unity. However, for many applications, as in this study, it is the ERT which is of interest and not true surface temperature.

Optical-mechanical Scanners

Optical-mechanical scanners have been used for remote sensing in numerous wavelength bands, from the ultraviolet on through the far infrared.

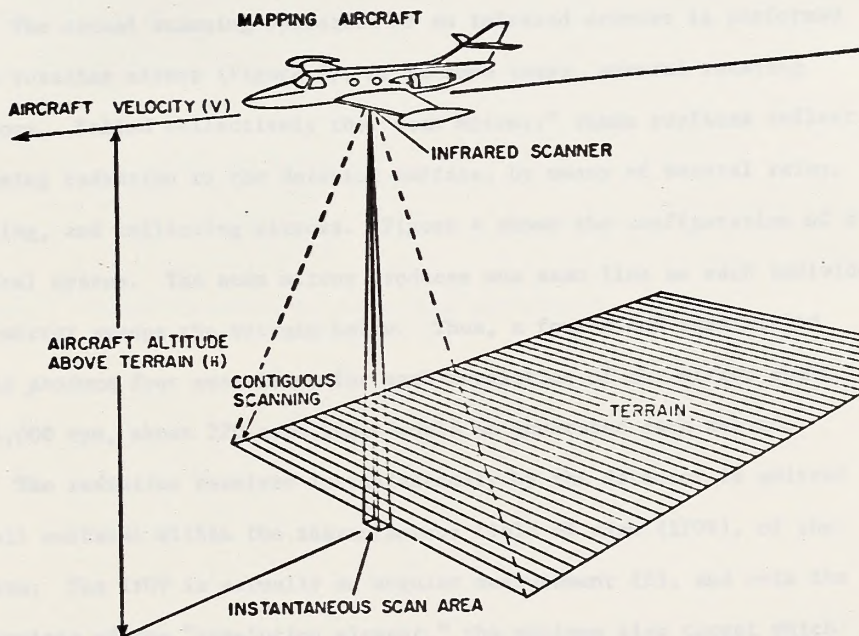
Normally operated from aircraft or satellites, these instruments produce imagery composed of contiguous scan lines (Figure 2). The main difference between systems operating in different wavelength bands is the type of detector used. The optical systems, mechanical assemblies, and electronics perform the same basic functions.

The detector is a transducer of radiant energy to electrical energy. There are two broad types of electronic detectors which have been used for longwave infrared detection, thermoelectric, and photoelectric detectors. The relatively slow response time of thermoelectric detectors limits their use to nonscanning devices, such as radiometers.

Photoelectric detectors are of two types, photovoltaic and photoconductive. Photovoltaic detectors are those which generate an electrical potential, or voltage difference, when irradiated. The voltage level varies with the intensity of radiation impinging on the detector surface and thus produces an output signal which is proportional to radiation received. The indium antimonide detector (InSb) is an example of this type of detector. It is in common use for remote sensing in the 3.0 to 5.0 micrometer band.

Photoconductive detectors do not generate voltage differences directly. Rather, incident radiation causes a change in electrical resistance of the detector material. In order to monitor these resistance changes, an external bias voltage is applied. As the resistance of the detector varies with variation in radiation intensity, the difference in bias voltage across the cell varies. Voltage or

**Figure 2.--Method of terrain coverage by optical-mechanical
scanners. (From Hirsch, et al., 1968).**



current across the detector is then an electrical record of radiant energy received. Longwave infrared scanners commonly use one of two detectors of the photoconductive type, mercury-doped germanium (Hg:Ge) or mercury-cadmium-telluride (MCT). Both of these detectors require cryogenic cooling to a temperature of around -200 C, or less, for operation in the 8.0 to 14.0 micrometer band.

The actual scanning operation of an infrared scanner is performed by a rotating mirror (Figure 3), or in some cases, several rotating mirrors. Called collectively the "scan mirror," these surfaces reflect incoming radiation to the detector surface, by means of several relay, folding, and collecting mirrors. Figure 4 shows the configuration of a typical system. The scan mirror produces one scan line as each individual mirror sweeps the terrain below. Thus, a four-sided scan mirror would produce four scan lines for each revolution of the mirror shaft. At 4,000 rpm, about 270 scan lines would be generated each second.

The radiation received instantaneously by the detector is emitted by all surfaces within the instantaneous field of view (IFOV), of the system. The IFOV is actually an angular measurement (β), and sets the dimensions of the "resolution element," the minimum size target which is detectable, at a given altitude. β is expressed in milliradians, units of angular measure, and is related to spatial resolution (resolution element size) by the altitude of the aircraft.

$$\omega = \beta h \quad (1)$$

ω = width of resolution element at the nadir

(in milliradians)

h = scanner-to-ground distance (in feet)

Figure 3.--Image formation by an optical-mechanical scanner.
(From Wilson, et al., 1971).



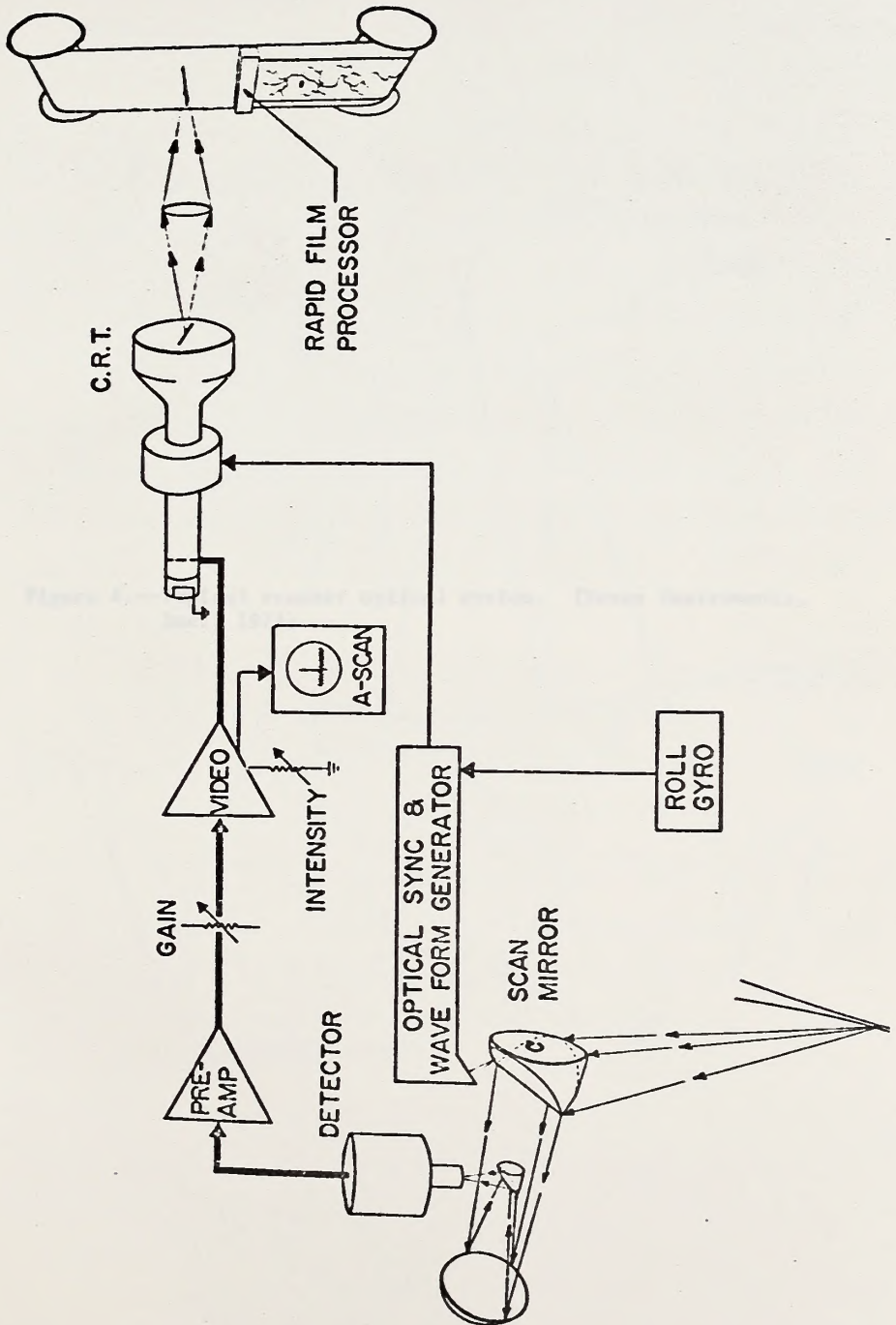
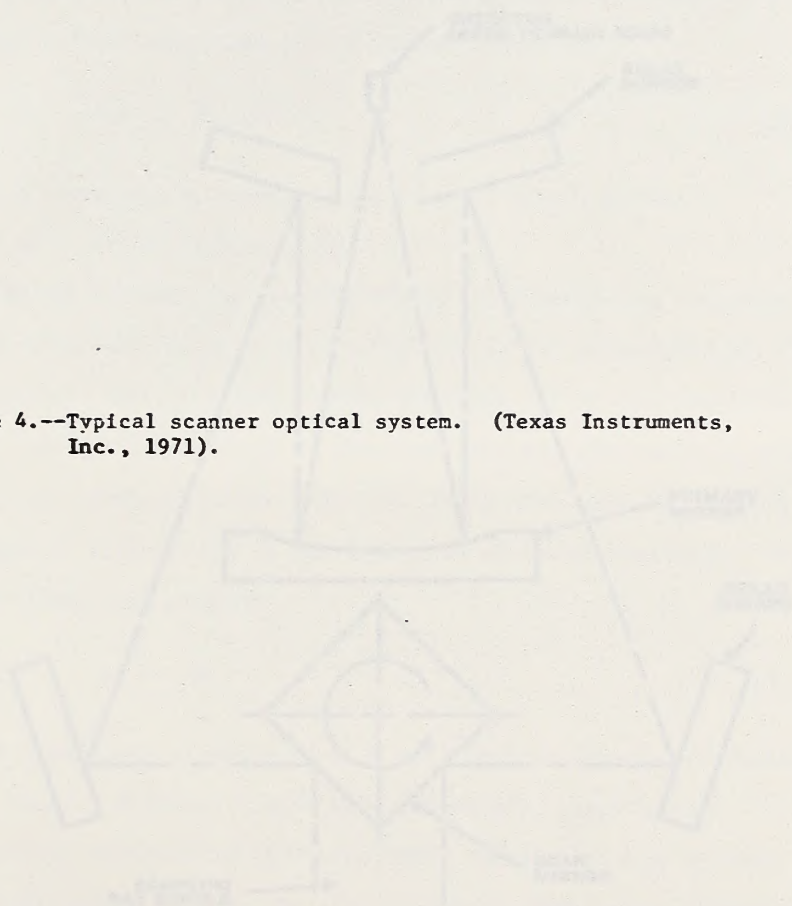
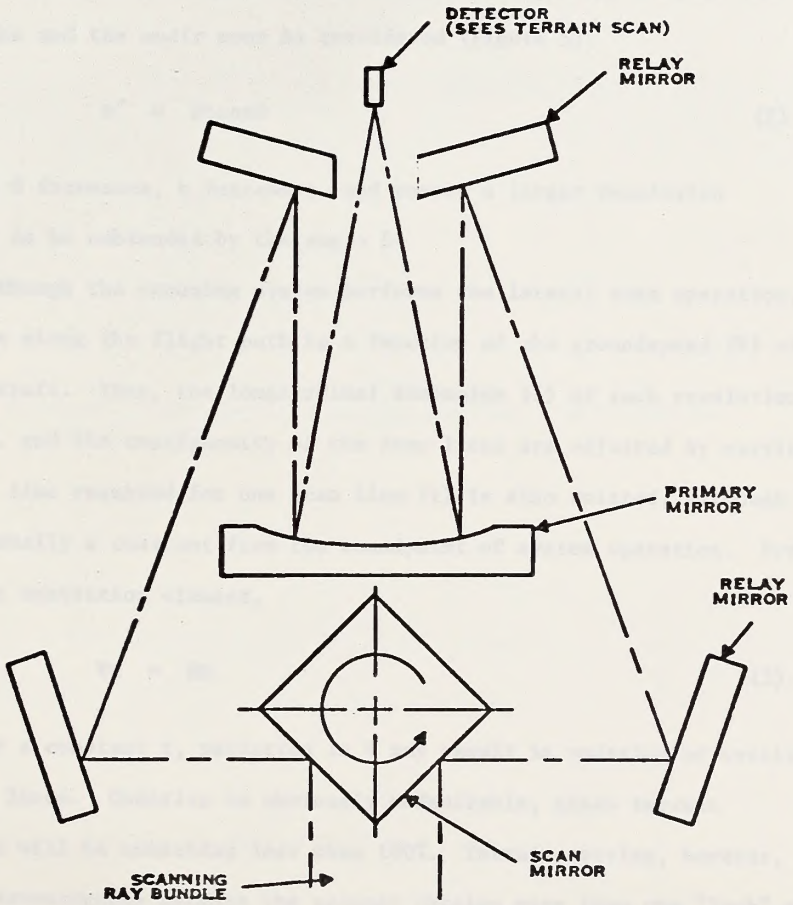


Figure 4.--Typical scanner optical system. (Texas Instruments, Inc., 1971).







Scanning systems with 1.0 to 3.0 milliradian IFOV are currently in declassified use.

Equation (1) holds only when applied at the nadir. To determine the size of off-nadir resolution elements, the angle (θ) between the view line and the nadir must be considered (Figure 5).

$$\omega' = \beta h \cos \theta \quad (2)$$

As θ increases, h increases, and causes a larger resolution element to be subtended by the angle β .

Although the scanning system performs the lateral scan operation, coverage along the flight path is a function of the groundspeed (V) of the aircraft. Thus, the longitudinal dimension (l) of each resolution element, and the contiguosity of the scan lines are adjusted by varying V . The time required for one scan line (t) is also related, although it is usually a constant from the standpoint of system operation. For a square resolution element,

$$Vt = \beta h \quad (3)$$

For a constant t , variation in V may result in underlap or overlap of scan lines. Underlap is obviously undesirable, since terrain coverage will be something less than 100%. Terrain overlap, however, may be advantageous because the scanner obtains more than one "look" at each point on the ground.

The overall resolution of a scanning system depends on thermal sensitivity, as well as spatial resolution. The signal generated by

...with 1.5 to 2.0 milligrams per 100 grams of ...

...the ...

...the ...

...the ...

...the ...

...

...

...the ...

...the ...

...the ...

...the ...

...the ...

...the ...

...the ...

...the ...

...the ...

...

...

...the ...

...the ...

...the ...

...the ...

...the ...

...the ...

...the ...

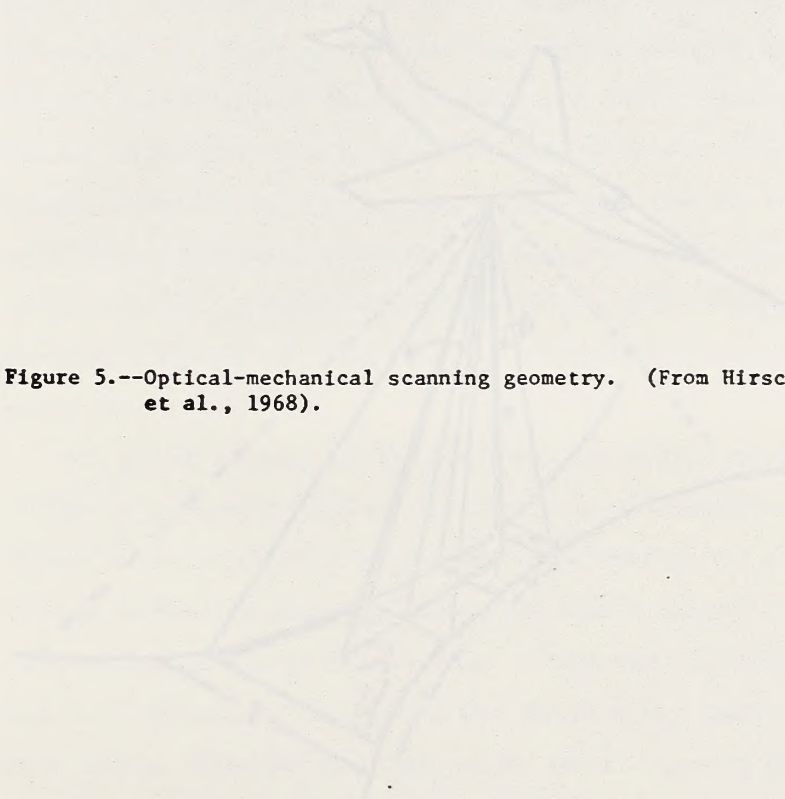
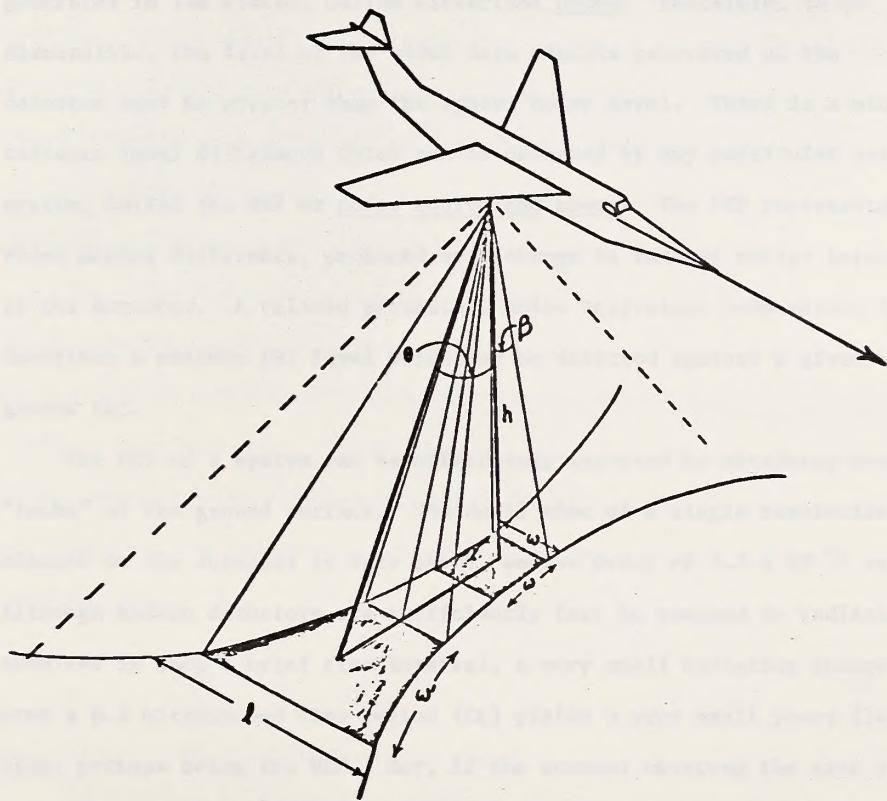


**Figure 5.--Optical-mechanical scanning geometry. (From Hirsch,
et al., 1968).**

Figure 2—Statistical analysis of the data. (75% of 1000)



the detector is amplified and otherwise conditioned by the electronics of the system, to produce a video signal. Changes in radiation intensity at the detector produce variations in the output video signal. But the video may also contain extraneous voltage or current fluctuations generated in the system, called electrical noise. Therefore, to be discernible, the level of the video data signals generated at the detector must be greater than the system noise level. There is a minimum radiance level difference which can be detected by any particular scanning system, called the NEP or noise equivalent power. The NEP represents a video signal difference, produced by a change in radiant energy intensity at the detector. A related parameter, noise equivalent temperature (NET), describes a minimum ERT level which can be detected against a given background ERT.

The NEP of a system can be effectively improved by obtaining more "looks" at the ground surface. The dwell time of a single resolution element on the detector is very short, on the order of 0.3×10^{-6} seconds. Although modern detectors are sufficiently fast to respond to radiation received in such a brief time interval, a very small radiation change (dT) over a 0.3 microsecond time period (dt) yields a very small power fluctuation, perhaps below the NEP. But, if the scanner observes the same spot several times, temporal integration of dT results in an overall higher video signal. Of course, the noise is similarly integrated. But due to the temporally random distribution of some types of noise, the integration may result in less overall video noise, since signals which are positive and negative around a zero level reference are integrated together, causing the resultant noise to be less than the original noise on a single scan line.

Some infrared scanners are quantitative. That is, they not only detect radiation, they also determine what ERT is represented by a given radiation intensity level. Calibration is achieved by means of temperature reference sources positioned near the scan mirror, one each for the highest and lowest expected target temperatures. The detector "sees" each of the reference sources once on each scan line. The video signals from the references then represent the highest and lowest temperatures detected. Actual video calibration may be accomplished electrically in real time, or later by other means, using the recorded reference video.

The video output from a scanner may be recorded on film, tape, or other recording media. The most versatile film-recording method is to expose film to the face of a cathode-ray tube (CRT), which sequentially displays each scan line. Normally, the film is pulled past the CRT at a rate such that the longitudinal scale of the terrain is maintained in the imagery. The relationship is expressed, for constant altitude, by equation (4).

$$\frac{fS}{t} = \frac{V}{t} \quad (4)$$

f = film transport speed

S = scale factor (constant with constant altitude)

V = aircraft speed

t = time for one scan line

Therefore, if the scanner is operating fast enough to overlap successive scan lines, the film must be moved at a speed slow enough that the scan lines displayed on the CRT will overlap on the film. Lack of

synchronization between scanning speed and film speed will cause incorrect aspect ratio in the imagery; i.e., longitudinal distortion of the imagery, either compression or expansion. Of more importance in some applications, however, disparity between the film speed and scanner speed can result in information loss. For example, if the film is moved past the CRT too slowly, multiple scan lines of different terrain may be stacked on one another and obliterate valuable data.

As a practical matter, V is not usually known with the precision required for exact adjustment of f . Additionally, overlap is often desirable because of the effectively decreased NEP. Therefore, most scanners are designed with a t small enough to intentionally produce overlap. It should be noted, however, that equation (4) only relates film transport speed (f) to aircraft groundspeed (V), at a fixed altitude. The amount of terrain overlap, or number of "looks," is also a function of altitude (equation (3)). A decrease in altitude reduces the overlap.

Although convenient, film-recorded imagery has several important disadvantages. First, present hardware limitations dictate the use of black and white film in most cases. Target ERT variations are represented by varying shades of gray, from black to white. Therefore, the number of temperature levels which can be distinguished is limited by the ability of the human eye to distinguish between these shades of gray. Although the scanner may be capable of detecting ERT differences as small as 0.5 C, the human imagery interpreter probably cannot.

A related problem is the inability of the film to resolve small ERT variations because of the limited number of discrete temperature levels which can be represented on the film. If, for example, the full range of

grays, from black to white, is spread over a 10° temperature range, then a single degree of difference can probably be seen in the imagery. If however, the gray scale is spread over, say 30° , then a difference of 3° may be the least which can be seen. Although the equipment operator can vary the intensity and gain of the system to produce emphasis in a particular portion of the temperature range, doing so may result in a complete loss of information in another portion of the scale. His alternative is to spread the total gray scale over a wider band of temperatures, but then small temperature variations will not be recorded.

A final disadvantage of film recording is the lack of adaptability to automatic (computer) processing. There are instruments, such as the microdensitometer, isodensitracer, and various types of flying spot scanners, which can measure the density of film, and produce a proportional electrical output which can then be processed by computer. However, the resolution of the final analysis is still limited by the original film resolution. Also, because of additional error, expense, time, and equipment requirements, this approach probably is not justified except for very small data loads.

Tape recording is another common method of recording scanner data. Unlike film, tape can preserve all the video information generated by the scanner. The full range of temperatures may be recorded without any loss of system resolution. Once recorded, the data record is permanent and may be converted to film imagery later, if desired. Tape recorded data may also be processed by digital computers, an important consideration when large quantities of data are involved.

The potential data output of optical-mechanical scanners is very great, however, and high quality, wideband recorders are necessary to preserve it. Commonly, greater than 200,000 data points per second may be generated. In terms of a thermal infrared scanner, this rate corresponds to 200,000 ERT differences (ΔT 's) per second. To record this data, a recorder must have a bandwidth of at least 200 KHz. Modern instrumentation recorders have no difficulty in meeting this requirement. But the analysis, whether manual or automatic, may be a problem if the maximum data rate must be preserved.

Chapter II

LITERATURE REVIEW

INFRARED BIG GAME CENSUS

Only two reports were found on previous attempts to detect big-game animals by airborne, thermal infrared scanners. The first was by Garvin, et al., (1964) in an experiment on the feasibility of detecting moose (Alces americana americana, Clinton) on Isle Royale, Michigan. Using a Reconofax VI scanner manufactured by the H. R. B. Singer Company, simultaneously with black and white aerial photography, they came to the following conclusions:

1. Filters are required on all daylight infrared flights to obtain proper contrast.
2. Tree falls, rocks, and moose appear as the only relatively high radiating sources and of these the moose are the most difficult to detect on daylight IR.
3. It is concluded that during daylight hours moose can be detected and identified on Reconofax VI imagery under specialized conditions.
4. With the aid of simultaneous aerial photography, it was determined that moose signals were recorded by the IR system in daylight at altitudes of 1,000 ft or less provided the animals are situated in areas of no cover or very sparse unfoliated vegetation.

5. Altitudes of 500 ft or less are required for the unaided identification of moose on IR imagery if the animals are situated in open areas during daylight hours.
6. Suspected moose signals can be verified by using only infrared imagery if comparative infrared records exist. The displacement or absence of the suspected signal(s) would indicate that the source was mobile, hence an animal. The size and shape would provide proof of identity, i.e., large signals would be moose.
7. Moose cannot be detected under dense unfoliated deciduous vegetation on IR imagery acquired above 500 ft during daylight hours.
8. Moose cannot be detected under dense coniferous vegetation on imagery acquired during daylight hours with either an aerial camera or infrared sensor.
9. Preliminary results indicate that correlation between IR and visual photography is required for detecting moose at 1,000 ft on daylight IR because of the similarity of target signatures from moose, rocks, and tree falls.
10. Night flights should allow moose to be detected more easily because the exposed rocks and tree falls would rapidly cool off, leaving the moose as the only significant radiating source.

On January 4, 1967 a test was conducted for detection of white-tailed deer (Odocoileus virginianus) on the Edwin S. George Reserve in Michigan (Croon, 1967). A report of this experiment was also

published in the Journal of Wildlife Management (Croon, et al., 1968). The thermal imagery was obtained by the Infrared Physics Laboratory of the University of Michigan. Radiometric measurements of various background temperatures were recorded with a Stoll-Hardy radiometer immediately following the test and are listed in Table 1. These measurements indicated approximately a 7°C ERT difference between the deer and their snow background.

The video data from the test were recorded both directly on film and on electrical tape. The deer identifications were made from film imagery which was generated from the tape recordings after the flight. The original, direct-recorded film imagery was not used because of variation in gain and contrast on the film, produced by the equipment operator as a part of the test.

Examination of the thermal imagery revealed 93 positive and five probable deer identifications. This count compared with an estimate of 101 deer which were believed to be in the area.

In conclusion, the author presented the following advantages and disadvantages of infrared big-game inventories:

ADVANTAGES. The primary advantages in the use of infrared line scanner for big-game inventories are the high percentages of animals detected and the large area covered per unit time.

Although the detection percentages obtained by infrared scanners may vary with areas and their corresponding conditions, it is felt that the resulting figures could match those obtained by other inventory means in a relatively open environment. At the same time

Table 1.--George Reserve ground radiometer data from Croon, 1967.

Object	Time ¹	Measurement
		- -°C - -
Background along side of road	1210	-4.8
Background under leafless canopy	1211	-5.1
Turkey	1309	3.6
Background near turkeys	1310	-4.4
Background by deer under hardwood canopy	1320	-5.0
Deer under hardwood canopy	1324	2.2
Zenith above deer in hardwoods	1330	12.6
Deer under conifer canopy	1338	0.4
Background under conifer canopy	1339	-5.6
Man's coat under conifer canopy	1340	1.4
Man's face under conifer canopy	1340	14.4
Deer in open	1352	3.5
Background near deer in open	1354	-5.3
Zenith at open deer site	1355	22.0
Cedar tree near deer in open	1356	3.8

¹ Time expressed on 24-hour basis.

it would not only be a census, but also an inventory because animals, numbers, and locations could be obtained at a given instant.

The area covered in an infrared survey depends upon the scanner angle, flight altitude, and aircraft velocity. As better detection equipment is developed and aircraft altitudes and velocities are increased, the area traversed would rapidly increase.

The problem created by false targets would diminish as the imagery interpreter became more familiar with a given region. For example, the difficulty in differentiating deer and open water or springs would be eliminated after the spring locations had been marked on accompanying maps. On following flights, the targets that are previously marked spring locations could be disregarded.

Specific examples of application include detection of animals in the open range such as antelope and bison; detection of bear, moose, and caribou in the Alaskan environments; detection of most big-game animals in brush fields throughout the year; and detection of deer and moose in hardwood stands in the winter.

DISADVANTAGES. At the present time, the disadvantages in the use of the infrared line scanner for big-game inventories include the following: security classification, cost, reduction in detection by screening material, and inability to distinguish between kinds and sizes of animals.

The infrared line scanner used in the George Reserve test was developed under military contract and was considered "Classified."

The only unclassified scanner on the market is being produced by Bendix Aerospace Systems Division and first models will be available to the public this spring, [1967].

The cost of an infrared line scanning system is above \$50,000. In order to cover the initial investment and high operating cost, a time-share program would have to be established among several agencies. This would be feasible because the scanner has many applications in fields such as agriculture, forestry, geography, and geology.

Foliage between the target and the airborne sensor screens the emitted radiation from the target and thus prevents detection. Solution of this problem is not immediately foreseen.

The inability to distinguish between kind and sizes of animals is an inherent disadvantage of the infrared scanner and is related to thermal and spatial resolving power in the infrared portion of the spectrum. Increased temperature sensitivity and higher spatial resolution will help minimize this problem in the future.

One study was found on the radiant temperature relationships which determine the detectability of big-game animals by a thermal scanner. Marble (1967) measured radiant temperatures of bison (Bison bison Smith), pronghorn antelope (Antilocapra americana americana, Ord.), white-tailed deer, mule deer, and of various background materials. She found a much higher variation in animal ERT during the daytime, than at night. She also noted the uniform background temperatures under conditions of snow cover, which were mentioned by Croon (1967).

Little differences were noted between the ERT's of the various animal species studied.

Marble reported less thermal contrast between the animals and their background during the night than during the day, and concluded that high overcast conditions during the daytime offered the best opportunity for detection.

McCullough et al. (1969) reported on work at the George Reserve in Michigan, subsequent to that reported by Croon (1967). Attempts were made to detect deer using scanners filtered to the 3.5 - 5.5 micrometer and 3.5 - 15.0 micrometer wavelength bands, but they were unsuccessful. The authors suspected a masking effect due to larger amounts of energy available from a greater variety of sources in the 3.5 - 14.0 micrometer band. The 3.5 - 5.5 micrometer test probably was unsuccessful because of the relatively low amounts of radiation emitted in that band by sources at the temperature of the deer during the test.

THE DEER AS AN ENERGY SYSTEM

General Energy Budget

As with all terrestrial organisms, the mule deer lives within, and only by virtue of, an extremely complex and dynamic energy field. The many energy sources, receptors, and vectors in the field, together with its dynamism preclude detailed in vivo analysis and quantification of its many variables. Likewise, in vitro duplication is virtually impossible. Yet, many problems such as the one investigated in this

study, can be better understood and analyzed when approached from the energy standpoint. Doing so, however, requires that energy systems be viewed rather simply in the initial stages of investigation.

Detection of wild deer by airborne thermal infrared scanning depends on the surface temperature relationships between the animals and their surroundings. In turn, these temperatures are dependent on the energy flow mechanisms which operate in and around the animals. Therefore, the literature was reviewed from the mechanistic viewpoint to better understand the processes which determine surface temperature.

The energy radiated by a deer surface may originate internally or externally. Internally, metabolic heat is generated by the various life processes of the animal. Externally, solar radiation or longwave radiation from various environmental substrata are absorbed by the animal. Examination of the overall energy budget for wild deer yields insight into the relative importance of each of these heat sources.

The steady-state energy budget of a deer standing in sunlight may be generally represented by the following equation, adapted from Gates (1962), Birkebak (1966), and Porter and Gates (1968):

$$M + Q + q + R_L = r(Q+q) + A_n \epsilon \sigma T_s^4 + \sum A_i K_i \left(\frac{T_i - T_{i+1}}{x_i} \right) + h A_n (T_s - T_a) + E_e + E_r + W \quad (5)$$

M = metabolic heat produced

Q = direct-beam solar radiation absorbed

q = diffuse solar radiation absorbed

R_L = longwave radiation absorbed

- r = shortwave reflectance of the deer surface
 A_n = surface area
 ϵ = infrared surface emittance
 σ = Stefan-Boltzmann constant
 T_s = surface temperature
 A_i = area of i^{th} tissue layer
 K_i = thermal conductance of i^{th} tissue layer
 T_i = temperature of i^{th} tissue layer
 X_i = thickness of i^{th} tissue layer
 h = convective heat transfer coefficient
 T_A = air temperature
 E_e = evaporative heat loss
 E_r = respiratory heat loss
 W = work done by the animal

Equation (5) is more illustrative than analytical, to be sure. However, it shows the major sources of energy gain and loss for a deer and provides a basis for examining the processes which affect T_s , the critical variable in this investigation.

Metabolic Heat Production

No published results were found on measurement of heat production in mule deer. However, heat production in white-tailed deer has been studied by Silver et al. (1959). They reported basal metabolic rates

for four, recumbent white-tailed deer as 24.6, 29.0, 24.8, and 25.9 Kcal day⁻¹ kg⁻¹ of body weight. No difference was found between basal metabolism in summer and winter.

A more realistic approach to natural heat production in wild deer is measurement of fasting metabolic rate. This quantity (FMR), considers heat production due to basal metabolism as well as heat production due to normal activity, since it is measured on confined, but active animals which are not lying down. Silver, et al. (1969) observed seasonal changes in FMR for adult white-tailed deer. They reported an average of 33.8 Kcal day⁻¹ kg⁻¹ of body weight for deer in winter coats from September through April. From May through August, however, heat production averaged 52.2 Kcal. Measurement of FMR in red deer (Cervus elaphus) by Brockway and Maloiy (1967) and by Maloiy (1968), showed no seasonal trend, however. Seasonal variation in FMR is not normal in domestic animals according to Silver et al. (1969).

Heat production, as a function of air temperature, was studied by Silver, et al. (1971). Mean heat production of deer in winter coats increased 91% as air temperature decreased 29.4°C over a period of 6 hours. For deer in summer coats, heat production increased 110% during a decrease in air temperature of 28.5°C. These and other data by the same authors indicate a stronger coupling between heat production and air temperature in summer than in winter. They suggest that this difference is due to physical differences, mainly insulation, in deer at different seasons.

Hart, et al. (1961) reported increased heat production in caribou calves as air temperature lowered, over a range of zero to 20°C, with

a further increase when exposed to a 12 to 21.5 m.p.h. wind. Blackster et al., (1958) reported virtual constancy of heat production in unclipped sheep from 12 to 31°C.

Absorbed Radiant Energy

Besides metabolic heat production, most of the heat input to a deer is radiant energy from three sources: direct-beam solar radiation, diffuse solar radiation, and longwave radiation from the atmosphere and other environmental substrata. The degree to which each of these energy components contributes to the heat load on a deer depends on the intensity of the radiation, and on the absorptance of the animal's surface, both in terms of wavelength, (Appendix A).

The solar radiation incident at the earth's surface occurs in two major components, direct-beam (Q) and diffuse (q) radiation. At the top of the earth's atmosphere, the rate of solar radiation is about $2.0 \text{ cal cm}^{-2} \text{ min}^{-1}$, the solar constant. According to Sellers (1965), the wavelength of peak solar radiation is about 0.5 micrometers, and about 99% of the sun's total radiation occurs between 0.15 and 4.0 micrometers. Gates (1962), however, points out that plotting energy against frequency, instead of against wavelength, results in a wavelength of peak radiation at about 1.0 micrometers. Most of the solar radiation reaching the earth's surface occurs between 0.4 and 4.0 micrometers, due to atmospheric absorption of the ultraviolet wavelengths by ozone and oxygen. An approximation of the direct-beam solar radiation incident on a surface between 30° and 50° latitude may be calculated from tables prepared by Frank and Lee (1966).

Sellers (1965) shows diffuse radiation (q) to average from about one-half to two-thirds of direct-beam radiation (Q) at temperate latitudes. For a standard cloudless atmosphere, Brooks (1959) gives $0.16 \text{ cal cm}^{-2} \text{ min}^{-1}$ for q and $1.33 \text{ cal cm}^{-2} \text{ min}^{-1}$ for Q . According to Reifsnyder and Lull (1965), diffuse radiation amounts to about 15% of total incoming solar radiation on a clear day. They also present a table of percent radiation penetration of various types of cloud masses from List (1958). On overcast or hazy days, all the incoming solar radiation may be diffuse.

Longwave environmental radiation (R_L) may be considered in two categories, terrestrial and atmospheric. Terrestrial radiation is emitted by all surfaces in wavelengths and intensity proportional to temperature and surface emittance (equation 31). Both the atmosphere and the terrain are relatively low temperature sources, radiating at wavelengths greater than 4 micrometers.

Atmospheric longwave radiation is emitted by all atmospheric constituents, including water vapor, dust particles, clouds, and various atmospheric gases. The magnitude of radiation at any time and point is a complex result of differential absorption and re-radiation by each of these components. However, "sky" ERT, measured with a long-wave infrared radiometer, has been used to obtain information on the magnitude and variability of atmospheric radiation.

Hardy and Stoll (1954) recorded an average zenith ERT of -42.6°C in winter at Fairbanks, Alaska. The average summer zenith ERT was 4.9°C . They also demonstrated the strong correlations which exist between sky ERT and cloud cover, and between sky ERT and atmospheric water vapor content. These correlations would be expected as a

consequence of the increase in radiating surface area under these conditions. Gates (1961) reported similar results.

Only limited information was found on specific values for long-wave atmospheric radiation on a surface. Kelly, et al., (1954) reported $5.33 \times 10^{-4} \text{ cal cm}^{-2} \text{ min}^{-1}$ for longwave atmospheric and diffuse solar radiation combined, during the daytime at Davis, California. Sauberer and Dirmhirn (1958) reported $0.5 \text{ cal cm}^{-2} \text{ min}^{-1}$ during the day and $0.47 \text{ cal cm}^{-2} \text{ min}^{-1}$ at night, in Vienna at mid-summer.

Most of the longwave radiation from a night sky is emitted by water vapor in the lowest few hundred feet (Reifsnyder and Lull, 1966). Goss and Brooks (1956) give the following empirical relationship:

$$R = (0.660 + 0.039 \sqrt{e}) \sigma T^4 \quad (6)$$

where R = total (hemispherical) sky radiation in $\text{cal cm}^{-2} \text{ min}^{-1}$

e = vapor pressure at 1400 hours in millibars

T = air temperature in $^{\circ}\text{K}$

Sky ERT may be roughly converted to radiant intensity per unit radiating surface area (W_T) by assuming $E = 1.0$ and applying equation 31. Conversion of the data from Hardy and Stoll (1954) gives:

$$\text{at } -42.6^{\circ}\text{C} \quad W_T = 0.23 \text{ cal cm}^{-2} \text{ min}^{-1}$$

$$\text{at } +4.9^{\circ}\text{C} \quad W_T = 0.49 \text{ cal cm}^{-2} \text{ min}^{-1}$$

These figures represent approximate total emission per unit surface area of the radiating source and are not intended to show incident radiation on a terrestrial surface. Nevertheless, they do

serve as a basis for comparison between sky radiation levels across different seasons, times, and weather conditions.

The importance of solar radiation to the energy level of a surface depends on the absorptance of the surface for radiant energy at those wavelengths (0.04 - 4.0 micrometers). A rough idea of absorptance in the visible wavelengths (0.4 - 0.7 micrometers) can be gained from color. The darker the color, the greater the absorptance. However, color gives no information about absorptance in the infrared wavelengths.

Hammel (1956) measured total emittance in the infrared for pelts from 10 arctic mammals and reported values of 0.98 to 1.00 for all pelts. Birkebak (1966) obtained similar results on skins from several rodents and lagomorphs, when the skins were at uniform temperature throughout (Table 2). The same author reported total solar reflectance (r) and absorptance for several mammal species, using both dry and fresh skins. Absorptance for all species was in excess of 73% on the dorsal surfaces. No difference was found between measurements of dry and fresh skins (Table 3).

Conductive Heat Loss

Conductive heat loss only occurs between solid surfaces in contact, (Appendix B). Therefore, conduction from a standing deer can only occur across a relatively small surface area, from the feet to the ground surface. If the animal is lying down, or is otherwise in contact with an additional area of external surface, conductive heat loss would increase. In either case, however, there must be a temperature difference

Table 2.--Total emittance¹ of pelts from several mammals, at constant skin temperature of 38° C. (From Birkebak, 1966)

Animal	Dorsal	Ventral
Flying squirrel (<i>Glaucomys volans</i>)	0.95	0.95-0.99
Cottontail rabbit (<i>Sylvilagus floridanus</i>)	0.97-0.98	0.92-0.93
Woodchuck (<i>Marmota monax</i>)	0.98	--
Red squirrel (<i>Taxiasciurus hudsonicus</i>)	0.95-0.98	0.97-1.0
Gray squirrel (<i>Sciurus carolinensis</i>)	0.99	0.99
Mole (<i>Scalopus aquaticus</i>)	0.97	--
Deer mouse (<i>Peromyscus</i> sp.)	--	0.94

¹ Emittance is unitless, and expresses emittance of a surface as a fraction of blackbody (perfect) emittance, (See Appendix A).

Table 3.—Solar reflectance (ρ) and absorptance (α) of several mammal pelts. (From Birkebak, 1966)¹

Animal	Dorsal		Ventral	
	ρ	α	ρ	α
Cottontail rabbit (<i>Sylvilagus floridanus</i>)			0.52	0.48
White-footed mouse (<i>Peromyscus</i> sp.)	0.15	0.85	0.39	0.61
Red squirrel (<i>Tamiasciurus hudsonicus</i>)	0.27	0.73	0.22	0.78
Fox squirrel (<i>Sciurus niger</i>)	0.18	0.82	0.41	0.59
Gray squirrel (<i>Sciurus carolinensis</i>)	0.22	0.87	0.39	0.61
Striped ground squirrel (<i>Citellus tridecemlineatus</i>)	0.16	0.84	0.28	0.72
Field mouse (<i>Microtus pennsylvanicus</i>)	0.11	0.89	0.17	0.83
Pocket gopher (<i>Geomys bursarius</i>)	0.22	0.78	0.24	0.76
Short-tailed weasel (<i>Mustela erminea</i>)	0.26	0.74	0.58	0.42
Red-backed mouse (<i>Clethrionomys gapperi</i>)	0.13	0.87	0.24	0.76
Eastern chipmunk (<i>Tamias striatus</i>)	0.15	0.85	0.41	0.59
Shrew (<i>Sorex</i> sp.)	0.19	0.81	0.26	0.74
Common mole (<i>Scalopus aquaticus</i>)	0.19	0.81	0.19	0.81

¹ Reflectance and absorptance are unitless (See Appendix A).

for heat transfer to occur, and heat loss would only take place if the animal's surface was warmer than the substrate surface. Therefore, most heat lost by conduction from a standing deer must be limited by the rate of convective heat transfer away from the skin surface. The temperature of the skin, however, is a function of the rate of heat conduction through the various tissue layers from the internal body.

Heat loss by conductance depends on the thermal conductance and thermal gradient across each body tissue layer. A planar representation of conductance (C) through a single tissue layer is

$$C = A_i K_i \left(\frac{T_{i+1} - T_i}{X_i} \right) \quad (7)$$

For conductance through several (i) layers of tissue (i.e., fat, muscle, skin, fur) equation 7 becomes a summation of single-layer conductances, as shown by the conductance term in equation 5.

Birkebak (1966) suggests heat conduction in animals can be more realistically represented as conduction through a series of concentric, cylindrical shells

$$C = \frac{2\pi L K_i (T_{i+1} - T_i)}{\ln \left(\frac{X_i}{X_{i+1}} \right)} \quad (8)$$

where C = conductive heat loss, L = cylinder lengths.

If animal size and thermal conductance are considered constants, conductive heat loss reduces to dependency on the temperature differences which exist between each tissue layer (T_i), under steady-state conditions.

Further, the temperature of each tissue layer is dependent on central body temperature (T_I) and air temperature (T_A). Therefore, internal temperature (T_I) may be a variable of some importance in the determination of heat loss.

Although mammals are thermoregulatory by definition, the degree to which their internal temperature can vary may be greater than 1°C as has been generally accepted (Scholander, et al., 1950). Bligh and Harthoorn (1964) found nycthemeral variation of 1° to 3°C in the deep-body radiotelemetric temperature of several African mammals. Sheep (Ovis aires) were the most thermally stable of animals studied. Camels (Camelus dromedarius) and buffalo (Syncaerus caffer) were the least stable. Others have also found sheep to be thermally stable within about 1°C (Bligh, et al. 1964; Eyal, 1963).

Hart, et al. (1961) recorded variation of about 3°C in the rectal temperature of infant caribou under a variety of environmental conditions. Rectal temperatures of reindeer (Rangifer tarandus) varied about 2°C and of caribou, about 1.5°C in studies by Irving and Krog (1955). McEwan, et al. (1965) found normal rectal temperature variation of about 1.5°C in barren-ground caribou (Rangifer tarandus groenlandicus) with elevations of up to 2.2°C as a result of activity.

Franzmann and Herbert (1971) reported rectal temperatures of Bighorn sheep (Ovis canadensis) varied directly with excitability and ambient air temperature.

Little information was found on the temperature variation between tissue layers. McGinnis, et al. (1970) measured deep muscle, and subcutaneous temperatures in three species of African ungulates. The

maximum mean temperature difference between the two locations was 1.1°C . The two temperatures varied concurrently, but the magnitude of variation was greater in the subcutaneous measurements. Also, mean muscle temperatures were not always greater than subcutaneous temperatures, as might be suggested by equation 5.

In spite of the lack of information, it seems reasonable to assume that the variation of temperatures between tissue layers is small in comparison to the gradient which exists between skin temperature and air temperature.

Subcutaneous fat is a poor insulator, compared to fur (Scholander, et al. 1950). Hatfield and Pugh (1951) reported the conductance of fat to be $0.0294 \text{ cal cm}^{-1} \text{ min}^{-1} ^{\circ}\text{C}^{-1}$. According to Hammel (1955), the thermal conductance of fur fibers is negligible compared to the conductance of the trapped air between the fibers. Therefore, the conductance of still air may be used to approximate fur conductance, under conditions of free convection. Gates (1962) gives $0.0036 \text{ cal cm}^{-1} \text{ min}^{-1} ^{\circ}\text{C}^{-1}$ for the conductance of air at 20°C . The variation in conductance of air as a function of temperature is about $1.10 \times 10^{-5} \text{ cal cm}^{-1} \text{ min}^{-1} ^{\circ}\text{C}^{-1}$ (Hammel, 1955). Extrapolating Gates' figure to 100°C ., the conductance of fur is still an order of magnitude less than the conductance of fat. Therefore, the skin to air gradient would be expected to exceed the gradient from internal body to skin.

Irving and Krog (1955) reported that the temperature difference from the center of the body to the skin surface was never more than 10°C in various arctic mammals and birds, but the difference between skin temperature and air temperature was as much as 70°C .

Convective Cooling

Heat transfer by convection is proportional to the temperature difference between the deer surface and the air (equation 33, Appendix B). Therefore, heat transfer will be away from a deer's surface whenever the animal's surface temperature exceeds air temperature. This heat loss results in a decreased surface temperature and, therefore, a decrease in thermal radiation from the surface.

According to Birkebak, et al. (1966), free convection heat transfer is a minor factor in the overall heat transfer process from fur.

Forced convection is a complex process, especially in a natural setting from a surface as irregular as that of a deer. The convective heat transfer coefficient (h) attempts to account for the geometrical and textural properties of the surface, wind velocity, and physical properties of the air.

Porter and Gates (1968) considered an animal's body to be roughly cylindrical and used the following formulation for h:

$$h = K \left(\frac{V^{\frac{1}{3}}}{D^{\frac{1}{3}}} \right) \quad (9)$$

where V is the windspeed, D is body diameter, and K is a constant.

Birkebak (1966) points out the difficulty or impossibility of determining h for complex biological systems and gives several semiempirical methods which have been used.

Theoretically, a boundary layer must always exist above a solid surface. However, a deer's surface of hair is not solid. It is a complex of cylindrical surfaces separated by air spaces. Stephens



and Moen (1968) investigated the effect of wind on a deer surface simulator in a wind tunnel. They found that the boundary layer was completely confined within the hair layer of the simulator at windspeeds of 10 m.p.h. or greater. Thus, there was no thermal gradient between the hair surface and the air above a windspeed of 10 m.p.h. They also observed the nonlinear effect of windspeed on surface temperature described by Gates (1962) for flat plates.

Birkebak (1966) measured radiometric surface temperature of a cottontail rabbit pelt (Sylvilagus floridanus) under windspeed variation of 0 to 40 m.p.h. He reported that radiant temperatures were insensitive to windspeed, but varied directly with air temperature. He concludes, from the work of Moote (1955) and Lentz and Hart (1960), that a main effect of wind is to increase the thermal conductance of the hair layer by ventilation of the skin and flattening of the hair.

BACKGROUND TEMPERATURE

Because the detection of wild deer by an airborne thermal scanner depends in part on scene contrast, specifically thermal scene contrast, it is important to consider what radiant temperatures may be expected from background materials such as vegetation, soil, and rock. Unlike homeothermic animals, these background materials do not generate internal heat, at least to a degree which can be identified in a natural situation.

Abiotic materials lose heat by conduction, convection, and radiation only, (Appendix B). Obviously there is no internal mechanism

which reacts to an increasing heat load by dissipating more heat in some manner. Rocks, soil, snow, and other nonliving materials gain and lose heat strictly in accordance with the three physical processes of heat energy exchange, in a magnitude dependent on the temperature regime of the environment.

Higher plants, on the other hand, possess a degree of control over the amount of heat gained or lost from their surfaces. Change in evapotranspiration rate by stomatal control, and adjustment of solar energy absorbed by leaf orientation, are the two primary mechanisms involved.

Gates (1970) states that a typical vegetative surface will have temperatures considerably lower than adjacent bare soil areas during periods of strong solar irradiation, due to the ability of the plants to lose heat by transpiration. Temperatures of the plant surfaces will be near or below air temperature, while soil temperatures may be 20°C higher than air temperature.

Elsewhere, Gates (1969) discusses plant reaction to temperature increase, pointing out the direct relationship which exists between leaf temperature and transpiration rate. A related physiological relationship was suggested by Olson (1967), who said that difference in moisture stress was a major factor affecting the appearance of vegetation on thermal infrared imagery. After further work, Weaver, et al. (1969) concluded that nighttime imagery provided the greatest thermal contrast between vegetation in swamps and other wet areas where the water table was close to the surface, but that daytime imagery is best in high ground locations, including agricultural land.

Gates (1961) reported that radiant temperatures of moss, grass, soil, and snow, all varied directly with air temperature and cloud cover. Temperatures of all materials except snow exceeded air temperature, over the air temperature range of about -22 to 0°C .

In studies relating temperature to leaf shape and size, Tibbals et al. (1964) concluded that leaves of broadleaf species will be warmer than leaves of coniferous species under similar conditions.

Lambert (1970) studied the effect of variation in solar radiation caused by cloud cover, on the surface temperatures of smooth sumac (Rhus glabra L.), measured with thermocouples. Surface temperature of the plants varied with air temperature, and solar radiation, but not always directly. Plant surface temperatures exceeded air temperature during the day, but dropped below it at night, over a range of 10 to 34°C . The amplitude of change in plant surface temperatures as a reaction to shading or unshading, varied with the duration of exposure to direct solar radiation, within limits apparently set by air temperature.

Monteith and Szeicz (1962) reported ERT's of short grass were 3 to 5°C below air temperature at night, but exceeded air temperature during the day, over an air temperature range of 8.1 to 23.4°C . A similar trend was found in the ERT of bare soil, although the range of soil temperatures was greater than the range of any plant materials measured. Soil temperature exceeded air temperature by as much as 20°C . Water showed the smallest ERT range, varying only 4 to 6°C around a mean of 19.3°C .

These three species were feeding independently of each other.

With one exception, all species associated with the vegetation and ground.

Temperature of all habitats was recorded as follows:

Temperature, near the air temperature range of 10 to 15°C.

It was noted that temperature in the shade and sun, relative

to air (10°C) indicated that there is probably greater air in

some than in others as indicated by the relative humidity.

Temperature (10°C) indicated that there is relative humidity in some

than in others as indicated by the relative humidity of some

than in others as indicated by the relative humidity of some

than in others as indicated by the relative humidity of some

than in others as indicated by the relative humidity of some

than in others as indicated by the relative humidity of some

than in others as indicated by the relative humidity of some

than in others as indicated by the relative humidity of some

than in others as indicated by the relative humidity of some

than in others.

Temperature and relative humidity of some species were 10

10°C below the temperature in the air, but recorded the temperature during

the day, near the temperature range of 10 to 15°C, 1°C below

that was found in the air of some birds, although the range of air

temperature was greater than the range of air temperature recorded.

That temperature recorded the temperature of air was 10°C, 10°C

below the highest air temperature recorded, 10°C below the range of

10°C.

Myers and Heilman (1969) found correlations between soil texture and surface temperature and between soil moisture and surface temperature. Although the amount of contrast varied with time of day, the difference between the temperatures of sandy soils versus clayey soils was found to vary from 3 to 38°C, the sandy soils being warmer. Soil moisture was found to have an effect on diurnal temperature variation of the soils of 51° and 45° in a dry field, and of 42°, 41°, and 40° in a field with more moisture. Werner and Schmer (1971) also found surface temperature differences between moist and dry sites with an airborne thermal scanner.

Chapter III

PHASE I: RADIOMETRIC INVESTIGATIONS

EXPERIMENTAL PROCEDURE

The Study Area

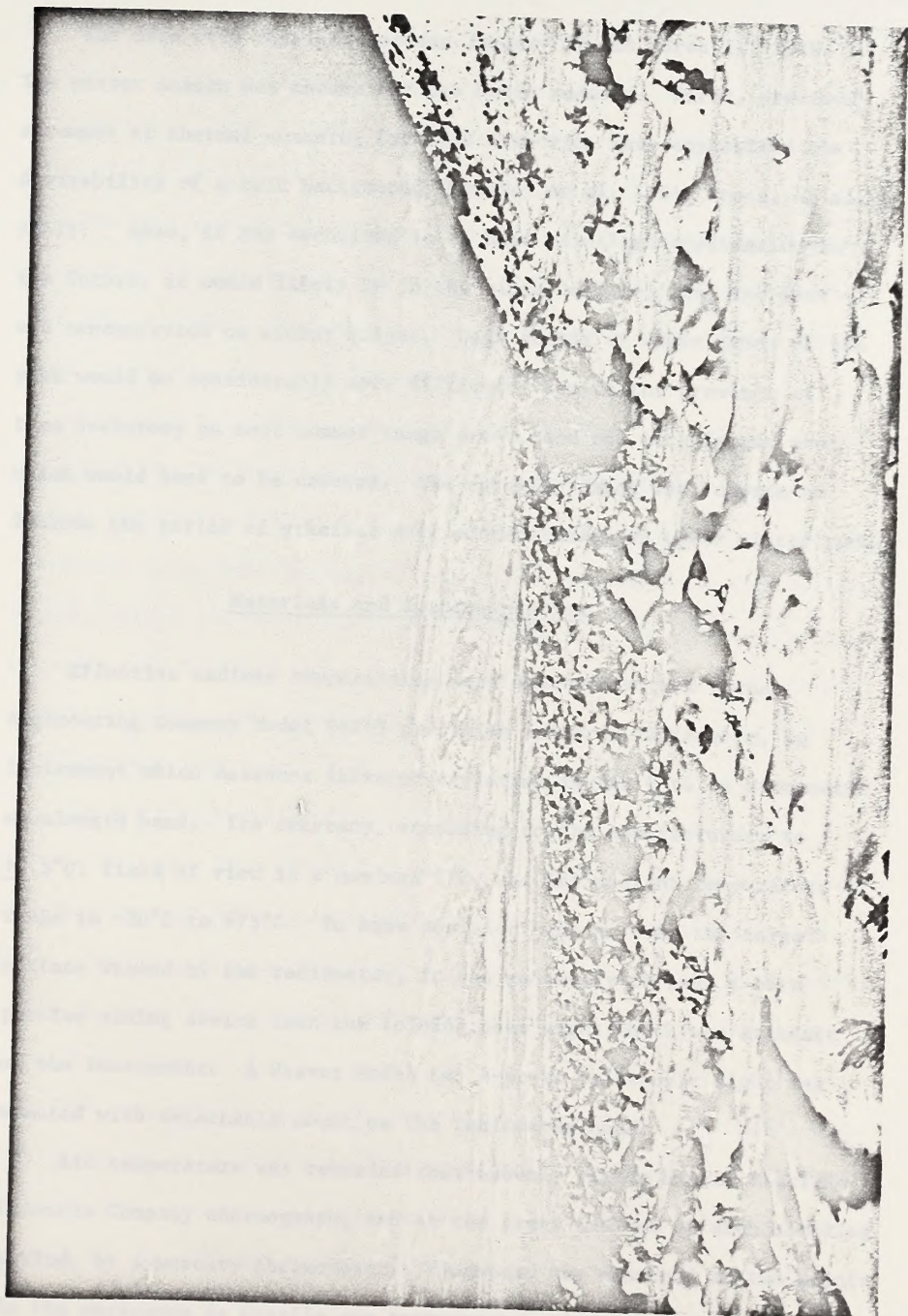
The field data were obtained at a site on the southwest slope of Junction Butte, a prominent hill of 8,700-ft elevation about 5 miles south of Kremmling, Colorado. The study area was at an elevation of about 7,700 ft with an approximate slope of 17% and a southwesterly aspect.

The area was typical of much of Colorado's deer winter range. Characterized by big sagebrush (Artemisia tridentata Nutt.), the vegetation included other low, shrubby species, grasses, and forbs, but no tree overstory (Figure 6).

The site was selected partly because a deer enclosure was available which could be used to contain the tame mule deer used in the study. The 100 X 200 ft enclosure was built in 1968 by the Colorado Division of Game, Fish and Parks. Additionally, the area was similar in vegetation, elevation, and weather conditions to much of the State's critical mule deer winter range. It was believed that the results would, therefore, have a more direct application to the deer census problem in Colorado, than would data from other areas.

Figure 6.--Deer winter range near the Junction Butte study area.

Figure 2—Data source: 1990 Census of the United States.





The data were obtained between January 27 and March 11, 1970. The winter season was chosen for two basic reasons. First, previous attempts at thermal scanning for deer detection have emphasized the desirability of a cold background (Garvin, et al. 1964; Croon, et al. 1967). Also, if the technique is to have practical application in the future, it would likely be in the winter season, when the deer are concentrated on winter ranges. Deer census at other times of the year would be considerably more difficult, due to the presence of tree overstory on most summer range areas, and the much larger area which would have to be covered. The specific dates were chosen to include the period of greatest deer concentration on their winter range.

Materials and Instrumentation

Effective radiant temperatures were measured with a Barnes Engineering Company Model PRT-5 precision infrared radiometer, an instrument which measures infrared radiation in the 8 to 14 micrometer wavelength band. Its accuracy, according to the manufacturer, is $\pm 0.5^{\circ}\text{C}$, field of view is a nominal 2°C , and its radiant temperature range is -20°C to $+75^{\circ}\text{C}$. To have positive control over the target surface viewed by the radiometer, it was necessary to have a more precise aiming device than the folding peep sight which was standard on the instrument. A Weaver Model K4, 4-power telescopic sight was mounted with detachable mount on the radiometer head.

Air temperature was recorded continuously with a United Electric Controls Company thermograph, and at the start and end of each sampling period, by a mercury thermometer. Windspeed was measured at two points in the enclosure by Casella cup anemometers. Atmospheric water vapor

pressure was measured with a sling psychrometer without a wick on the wet bulb, using a technique suggested by William E. Marlatt (Private communication, 1969). Solar radiation was measured with a Kahl Scientific star pyranometer.

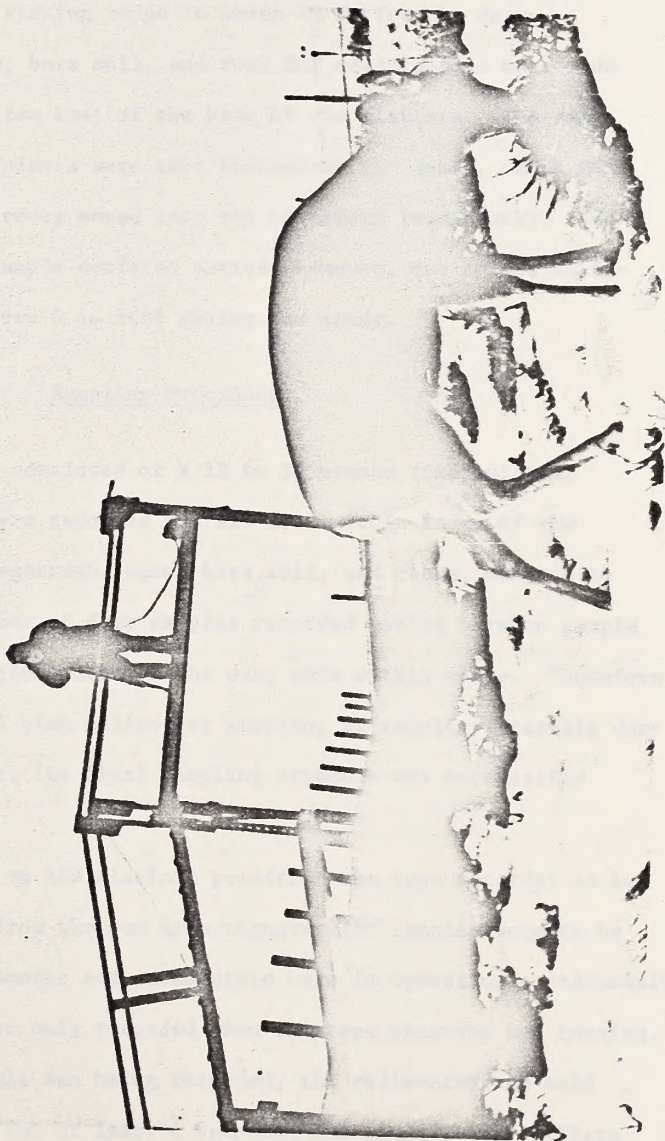
The data from the radiometer, anemometers, and pyranometer were recorded on FM, analog tape recording equipment, located in a trailer near the enclosure. Air temperature, psychrometer bulb temperatures, cloud cover estimates, and time were recorded by hand.

Four tame mule deer, three bucks and one doe, were placed in the enclosure for the duration of the study. The unrestrained animals were at liberty to browse on the natural vegetation growing in the enclosure, or to eat the special deer ration provided. The composition of this ration was described by Reichert (1972). The animals were also provided with drinking water, kept unfrozen by a propane tank heater. The only shelter was a small shed in one corner of the pen. It was used little by the deer.

The 8-ft high enclosure was constructed of wooden posts and woven wire. Due to previous harassment of research deer by feral dogs in the area, the fence was covered with burlap to a height of about 6 ft. This measure was suggested by O. C. Wallmo (Private communication, 1970) to reduce the animals' tendency to attempt jumping through the fence when frightened.

ERT measurements were made from a platform, built 8 ft above the ground in the enclosure to provide an elevated angle of view (Figure 7). The elevation was desirable to simulate, as closely as possible, the view angle of a thermal scanner flying over the terrain. Deer ERT's

Figure 7.--The platform from which all ERT values were measured.
(Photo by Paul Gilbert, Colorado Division of Game,
Fish and Parks).



were measured whenever, during a sample period, the animals moved within range of the radiometer. The radiometer's 2° field of view limited the maximum viewing range to about 40 ft for the deer.

Sagebrush, snow, bare soil, and rock ERT measurements were made on samples within a few feet of the base of the platform. The same two, live sagebrush plants were used throughout the study. Rock ERT was measured on two rocks moved into the enclosure from nearby. The snow and bare soil sample surfaces varied, however, due to the variation in snow cover from 0 to 100% during the study.

Sampling Procedure

A sample period consisted of a 15 to 30 minute time interval during which ERT's were recorded for all deer within range of the radiometer, and of sagebrush, snow, bare soil, and rocks, subject to snow cover. The number of deer samples recorded varied between sample periods; in a few periods none of the deer were within range. Therefore, although the original plan called for sampling at regular intervals during the day and night, the final sampling schedule was necessarily irregular.

Remote controls on the platform permitted the tape recorder to be stopped and started from the pen area whenever ERT samples were to be recorded. The pyranometer and anemometers were in operation continuously, but their outputs were only recorded when the tape recorder was running.

When an ERT sample was being recorded, the radiometer was held steady on the target for at least 4 seconds, and often longer. There was no problem in obtaining a long, continuous sample on the inanimate targets, but the deer did not often remain still for more than 4 or 5 seconds.

Data Analysis

The taped data from the radiometer, pyranometer, and anemometers were converted to a digital format with the aid and equipment of Dr. John R. Morgan, Assistant Professor of Physics, Colorado State University. The digital record length was 4 seconds, and the sampling rate was 5,000 samples per second. The digital records were written on digital tapes in a format compatible with the CDC 6400 computer on the Colorado State University campus.

The hand-recorded data on air temperature, vapor pressure, and time of day, together with the taped data, were placed on punched cards for the analyses.

Stepwise, multiple linear regression techniques were used to measure the association between each environmental variable and the ERT of deer, sagebrush, and snow. In each case, the ERT value was used as the "dependent" variable, and air temperature, solar radiation, windspeed, and relative humidity were the "independent" variables. Regressions were also run on the thermal contrast (ΔT) which existed between deer and sagebrush and between deer and snow, using the same "independent" variables mentioned above.

RESULTS AND DISCUSSION

Deer ERT Variation

The R^2 values generated by multiple regression indicated air temperature was the environmental variable most valuable for prediction of deer ERT. Despite numerous variable transformations, tests of interactions, and reordering of the variable insertion sequence, air temperature consistently accounted for more of the ERT variation than any other variable. The R^2 contributions of each environmental factor, developed by the stepwise procedure, are given in Table 4.

An analysis of the variance of the deer ERT values as a function of solar radiation revealed a marked reduction in variation during periods when solar radiation was less than $0.14 \text{ cal cm}^{-2} \text{ min}^{-1}$, the solar radiation rate which corresponded approximately to 7:45 p.m. and 5:15 p.m. Therefore, the deer data was divided into "dayclass" and "nightclass" groups, on the basis of solar radiation rates greater or less than $0.14 \text{ cal cm}^{-2} \text{ min}^{-1}$. From Table 4, the increase in predictability of nightclass ERT was appreciable. Note that the nightclass data was not only night-time data, but also included records obtained during those crepuscular periods immediately following sunset and just before sunrise. The nightclass data also included a few records obtained during the daytime, when a dense overcast caused the solar radiation rate to drop below $0.14 \text{ cal cm}^{-2} \text{ min}^{-1}$.

Table 4.--Results of stepwise multiple, linear regressions.

Target Category	Sample Size	Mean (°K)	Multiple Correlation Coefficients (R)	Coefficient of Determinations (R ²)	Additional Contribution to Total R ² ¹				Standard Error of Estimate
					X ₁	X ₂	X ₃	X ₄	
Deer-all data	140	279.9	0.72	0.52	.2.10(2)	.33(1)	.05(3)	.04(4)	4.98
Deer-dayclass	88	282.8	0.62	0.39	.15(1)	.04(4)	.08(3)	.12(2)	5.80
Deer-nightclass	52	274.9	0.91	0.82	.66(1)	.07(2)	.04(4)	.05(3)	1.67
Sagebrush-all hours	46	271.5	0.94	0.88	.75(1)	.13(2)	0	0	1.97
Snow-all hours	39	269.0	0.87	0.76	.61(1)	.10(2)	.05(3)	0	1.68
Rock-all hours	45	276.0	0.87	0.76	.41(1)	.35(2)	0	0	3.17
ΔT_S -all hours	130	7.7	0.56	0.31	.07(3)	.11(2)	.13(1)	0	4.98
ΔT_N -all hours	92	10.2	0.64	0.41	.06(3)	.24(1)	.11(2)	0	5.35

X₁ = air temperature; λ_2 = solar radiation; X₃ = relative humidity; X₄ = windspeed

ΔT_S = ERT difference between deer and sagebrush; ΔT_N = ERT difference between deer and snow

¹ Values of 0 indicate an additional R² contribution less than .04

² Numbers in parentheses indicate order of variable insertion

The effects of the other environmental variables were mixed, accounting for ERT variations up to 35% beyond the variation absorbed by the air temperature term.

The effect of direct solar radiation is not shown clearly by the regression results. A strong effect was observed in the field, however, when the abrupt shading or unshading of a deer caused a rapid ERT change of as much as 20°C (Figure 8).

In 1971 an additional experiment, reported by Parker and Harlan (1972), was performed to examine the shading effect. In that test, abrupt shading of a tanned, furred mule deer hide caused the rapid declines in ERT shown in Figure 9. ERT decreases of 19.9°, 17.2°, and 17.3° were recorded in three trials. After removal of the shade, radiant temperatures increased at a rate similar to the decay rate and stabilized at approximately the same temperatures which existed prior to shading (Figure 10).

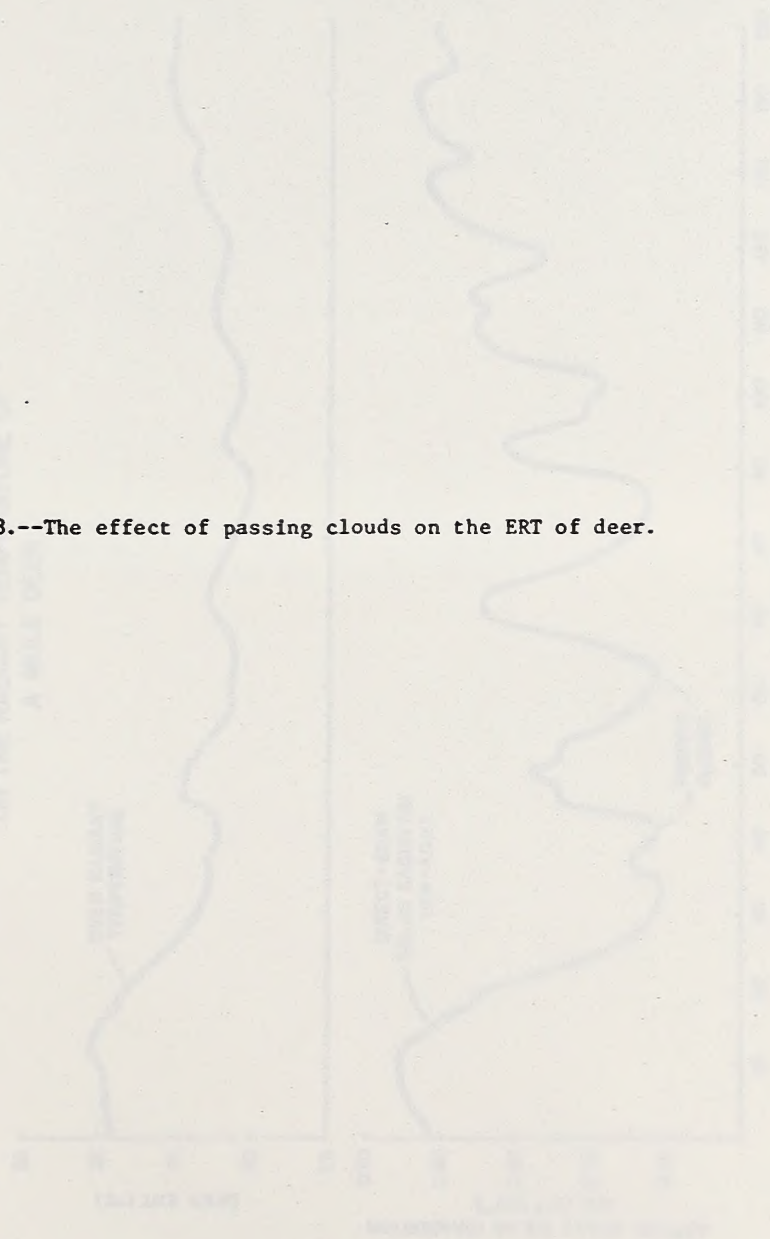
The lack of a strong solar radiation effect in the deer regression results was believed to have been related primarily to the mobility of the animals. The radiation flux incident on a surface (I_s) is proportional to the angle of incidence (δ) of the radiation beam to the surface (i.e., the angle between the radiation beam and a perpendicular to the surface).

$$I_s = I_o \cos \delta \quad (10)$$

Where I_o is the flux density perpendicular to the beam.

Being free to move about, the deer were almost constantly changing the angle δ for any point on their surfaces. Additionally, the shading

Figure 8.--The effect of passing clouds on the ERT of deer.



EFFECT OF VARIATION IN SOLAR RADIATION ON THE RADIANT TEMPERATURE OF A MULE DEER

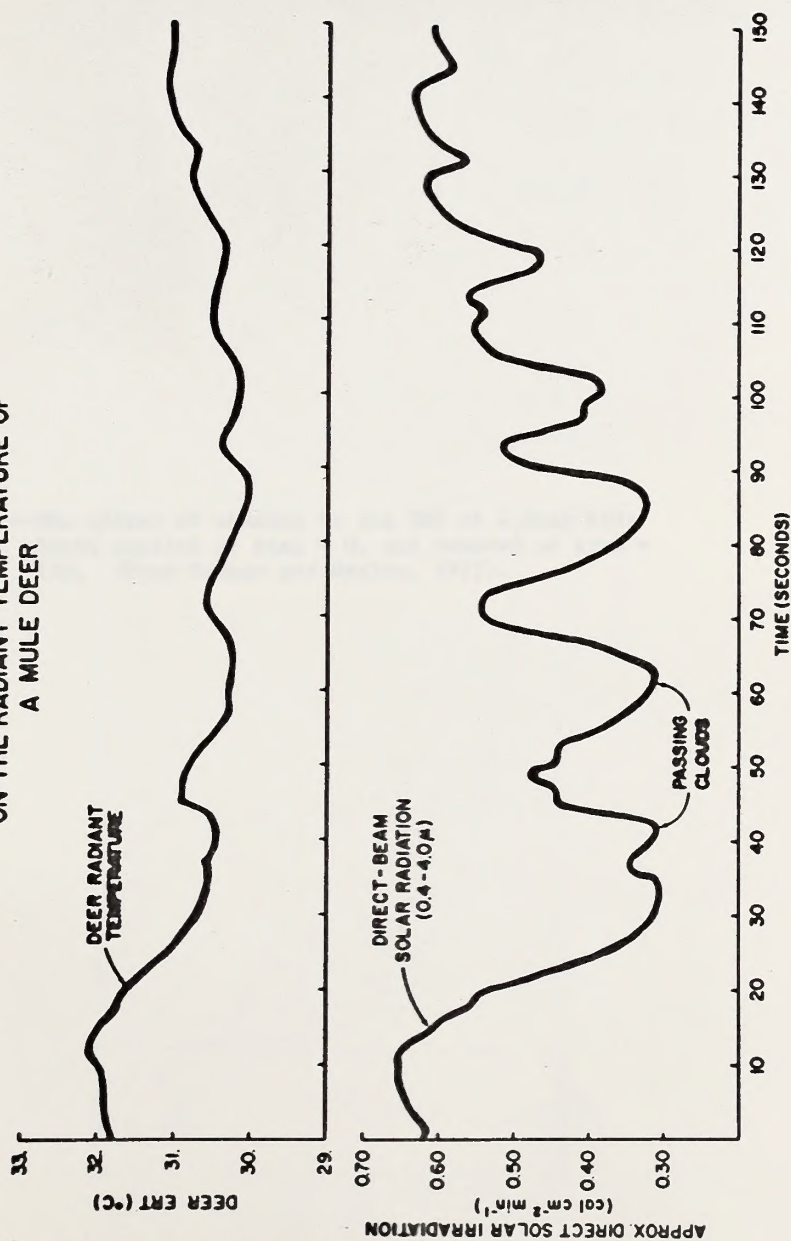


Figure 9.--The effect of shading on the ERT of a deer hide.
 Shade applied at time = 0, and removed at time =
 120. (From Parker and Harlan, 1972).

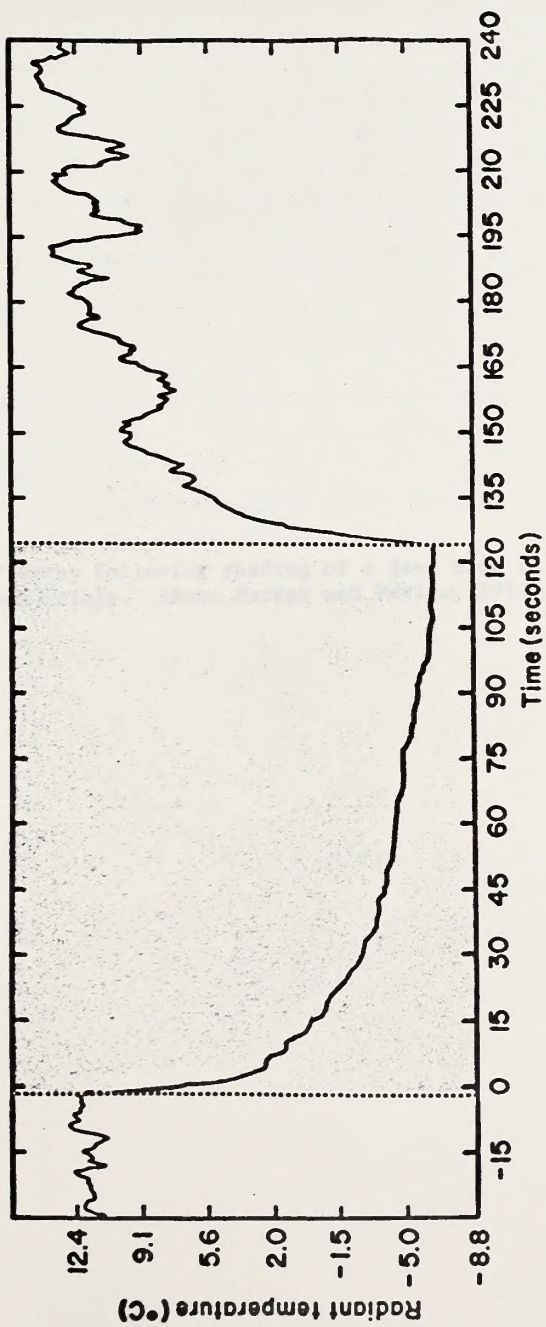
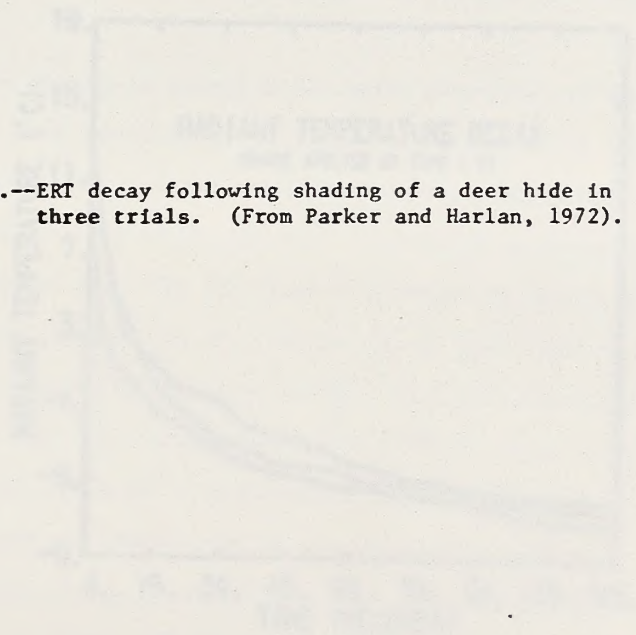
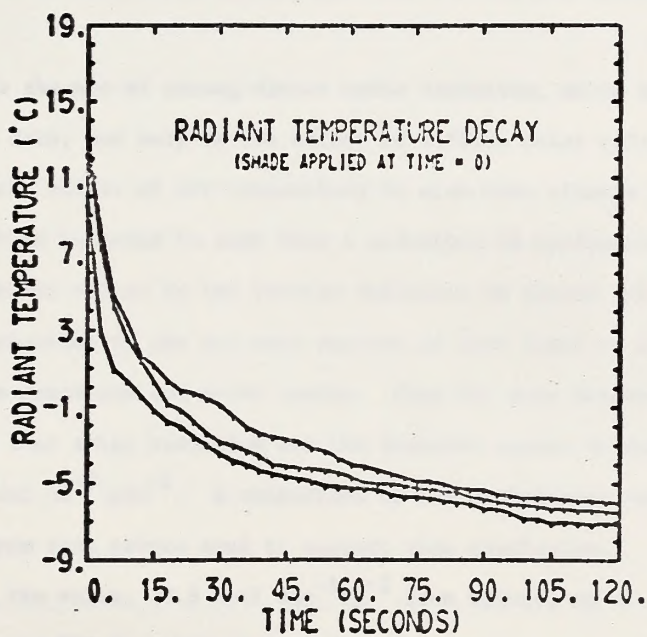


Figure 10.--ERT decay following shading of a deer hide in three trials. (From Parker and Harlan, 1972).





effect must have been considerable, as the animals moved around, irregularly exposing various portions of their bodies to the sun's direct beam. Consequently, any point on the animals' surfaces was absorbing a varying amount of direct solar energy, and differential surface heating, both spatially and temporally, was the result. Although the pyranometer measured direct and diffuse solar radiation incident on a horizontal surface, it could not describe the irradiation of a particular area on an animal's surface as each ERT measurement was made.

In the absence of strong direct solar radiation, as in the night-class deer data, not only is the effect of diffuse solar radiation more apparent, the effect of air temperature is also more clearly shown. This result is believed to stem from a reduction in confounding of the air temperature effect by the erratic influence of direct solar radiation.

From equation 5, the two main sources of heat input to the deer surface are metabolic and solar energy. From the data presented here, it appears that solar radiation was the dominant source at rates greater than $0.14 \text{ cal cm}^{-2} \text{ min}^{-1}$. A comparison of the approximate energy supplied from each source tend to support this conclusion.

Using the value, $33.8 \text{ Kcal day}^{-1} \text{ Kg}^{-1}$ from Silver, et al. (1969), as the average FMR for white-tailed deer in a winter coat and applying it to a deer weighing 68.0 Kg, the average rate of metabolic heat production per minute (E_M) may be approximated:

$$E_M = \frac{(33.8 \text{ Kcal day}^{-1} \text{ Kg}^{-1}) (68.0 \text{ Kg})}{1440 \text{ Min day}^{-1}} \times 1000$$

$$E_M = 1596.1 \text{ cal min}^{-1} \quad (11)$$

The rate of radiant energy absorption by the deer surface (E_A) is a function of radiation available for absorption, absorptance of the surface, and absorbing surface area.

In this study, the total rate of shortwave, hemispherical, direct, and diffuse solar radiation on a horizontal surface was approximately $0.90 \text{ cal cm}^{-2} \text{ min}^{-1}$, at noon on February 1.

Birkebak (1966) measured shortwave solar absorptance for a number of mammals (Table 2, Page 41). Although he did not measure absorptance of a deer surface, an assumed value of 0.85 is probably within reason, considering the relatively high absorptance found for other furred species of similar coloration.

According to Reifsnnyder and Lull (1965), diffuse radiation (Q_d) is about 15% of direct-beam radiation (Q_D). Therefore, Q_d may be found as follows:

$$Q_D + .15 Q_D = 0.90 \text{ cal cm}^{-2} \text{ min}^{-1} \quad (12)$$

$$Q_D = 0.78 \text{ cal cm}^{-2} \text{ min}^{-1}$$

$$Q_d = 0.90 - 0.78 = 0.12 \text{ cal cm}^{-2} \text{ min}^{-1}$$

To determine surface area (A), a regression equation from Moen (1968), relating surface area to body weight, gives the following:

$$A = 1.375 + .0091(68.0) = 19,940 \text{ cm}^2 \quad (13)$$

Considering the trunk of the animal's body to be a cylinder, Porter and Gates (1968) used the following equation to compute the solar irradiance (\bar{S}) on a simulated animal surface:

$$\bar{S} = \frac{2S \int_0^{\frac{\pi}{2}} \cos \delta d\delta}{\pi} \quad (14)$$

where S = incident direct solar radiation

δ = angle between solar direction and a
perpendicular to the cylinder surface

Integrated over a 90° quadrant of the cylinder, and multiplying by 2 to get hemispherical surface exposed, equation 14 becomes:

$$\bar{S} = \frac{2S}{\pi} \quad (15)$$

From equation 12, $S = Q_D = 0.78 \text{ cal cm}^{-2} \text{ min}^{-1}$

$$\text{and } \bar{S} = \frac{2(0.78)}{\pi} = 0.50 \text{ cal cm}^{-2} \text{ min}^{-1}$$

Here, \bar{S} is the average direct-beam solar radiation incident on the deer surface, per square centimeter. From equation 13 the total surface area is $19,940 \text{ cm}^2$. Applying \bar{S} to one-half the total surface area (upper half of the cylinder), and using 0.85 for absorptance, the total direct-beam radiation absorbed (E_D) is obtained:

$$E_D = \frac{(19940 \text{ cm}^2) (0.50 \text{ cal cm}^{-2} \text{ min}^{-1}) (0.85)}{2} \quad (16)$$

$$E_D = 4237.2 \text{ cal min}^{-1}$$

Assuming diffuse radiation to be incident on the whole surface, total diffuse radiation absorbed (E_d) may be found by multiplying total surface area by the rate of diffuse radiation (Q_d):

$$E_d = (19940 \text{ cm}^2)(0.12 \text{ cal cm}^{-2} \text{ min}^{-1}) \quad (17)$$

$$E_d = 2392.8 \text{ cal min}^{-1}$$

By adding E_D and E_d , the total shortwave radiation absorbed per minute (E_A) is found:

$$E_A = 4237.2 + 2392.8 = 6630.0 \text{ cal min}^{-1} \quad (18)$$

Thus, E_A is greater than 4 times E_M , suggesting the heat generated by absorbed solar radiation dominates the total heat energy input to the animal during periods of greatest solar radiation flux.

To find the rate of total solar radiation at which E_M is equal to E_A , the following calculations were performed:

$$E_M = E_A \quad (19)$$

$$1596.1 \text{ cal min}^{-1} = E_D + E_d$$

from equation 16.

$$E_D = \frac{(\text{surface area}) (\bar{S}) (\text{absorptance})}{2} \quad (20)$$

where surface area and absorptance are considered constant, and

$$\bar{S} = \frac{2(Q_D)}{\pi}$$

From equation 17,

$$E_d = (\text{surface area}) (Q_d)$$

$$E_d = (19,940) (.15 Q_D) \quad (21)$$

Expanding equation 19,

$$1596.1 = \frac{(19940)(Q_D)(0.85)}{\pi} + (19940)(.15 Q_D) \quad (22)$$

Solving for Q_D ,

$$Q_D = 0.19 \text{ cal cm}^{-2} \text{ min}^{-1}$$

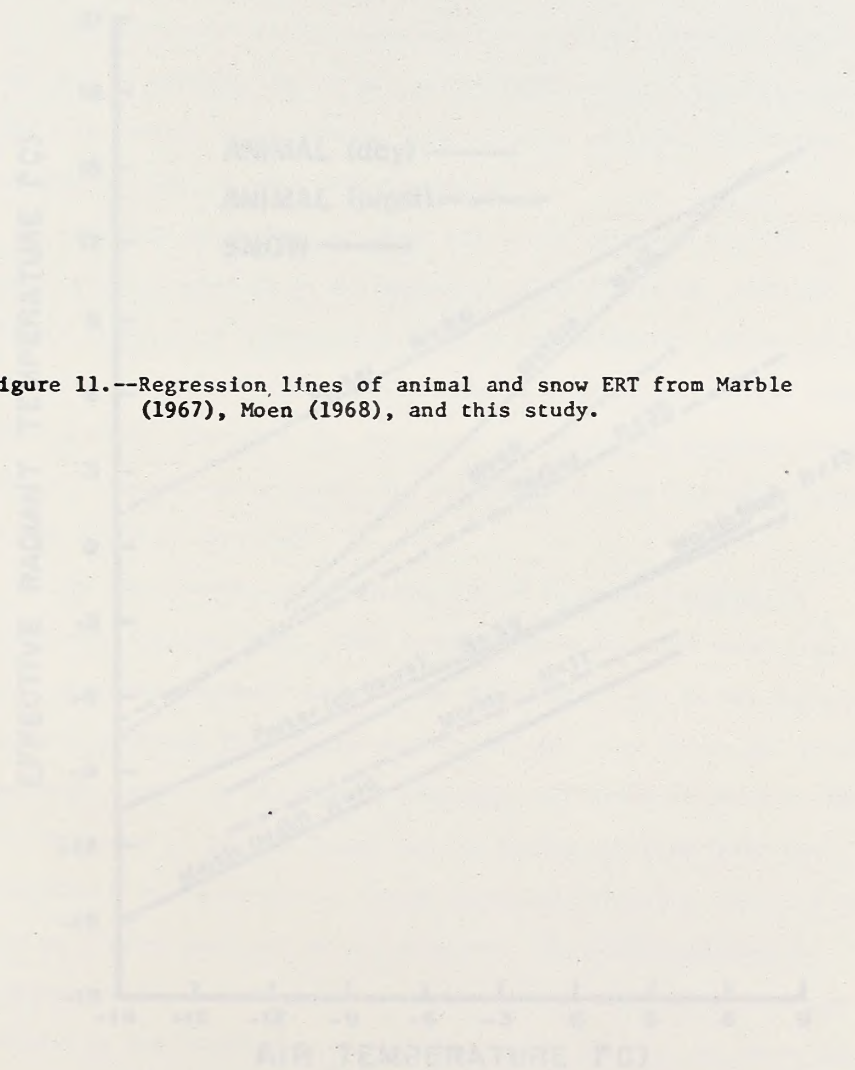
Therefore, when solar radiation drops to $0.19 \text{ cal cm}^{-2} \text{ min}^{-1}$, metabolic heat production equals radiation absorbed. At solar radiation levels below $0.19 \text{ cal cm}^{-2} \text{ min}^{-1}$, metabolic energy is the dominant energy source. This figure agrees approximately with the experimental evidence in this study, where a solar radiation level of $0.14 \text{ cal cm}^{-2} \text{ min}^{-1}$ was the point of division between deer ERT data of very high variance and data of comparatively low variance, i.e., the division between nightclass and dayclass data wherein the difference in variance was believed due to the erratic effect of direct solar radiation.

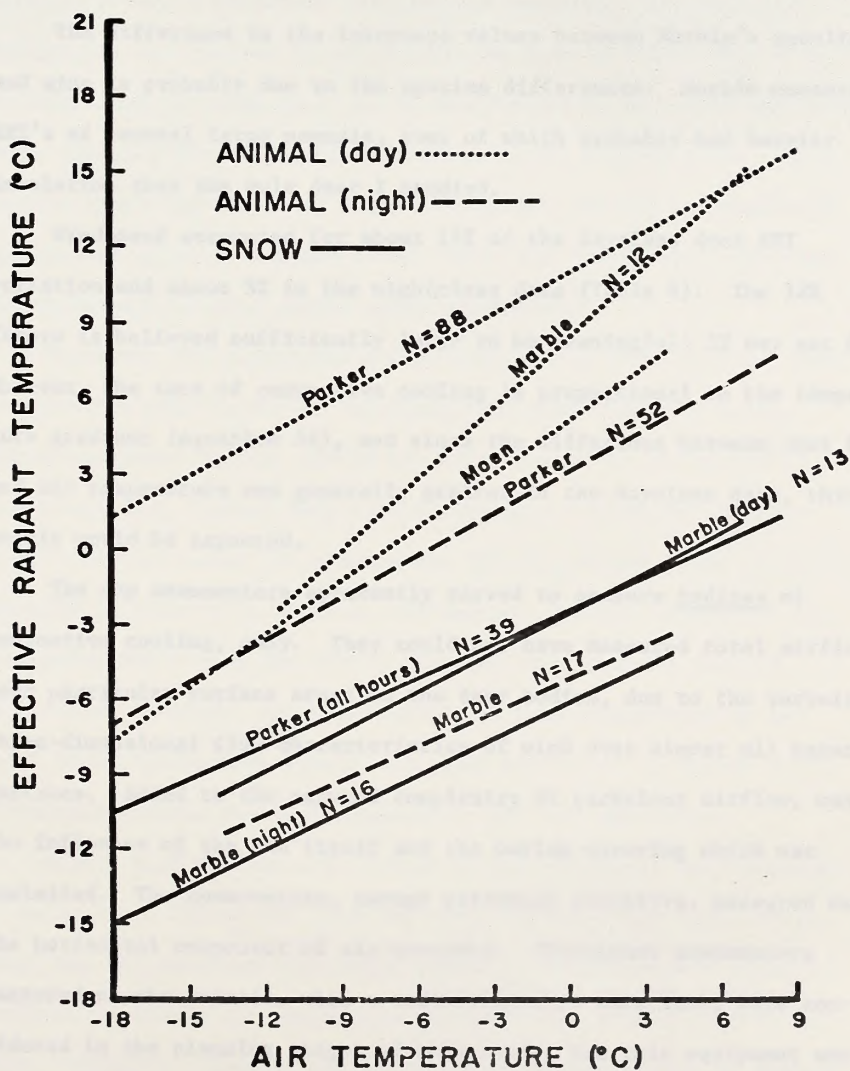
During periods of no direct solar irradiation of the deer surface, metabolic energy production was the major heat source and it was relatively constant.

These results agree well with the results of Marble (1967) and McCullough, et al. (1969), both of whom commented on the erraticism of deer radiant temperatures on clear days.

Figure 11 shows regression lines of animal radiant temperatures against air temperature. The lines from Marble (1967), for several different mammal species, were actually constructed by McCullough, et al. (1969), using Marble's data. Moen (1968) used a deer simulator.

Figure 11.--Regression lines of animal and snow ERT from Marble (1967), Moen (1968), and this study.





The regression lines shown from this study were obtained by simple linear regression of deer ERT against air temperature. There is good agreement between slope of the night regression lines and the daytime slopes are very close.

The difference in the intercept values between Marble's results and mine is probably due to the species differences. Marble measured ERT's of several large mammals, some of which probably had heavier insulation than the mule deer I studied.

Windspeed accounted for about 12% of the dayclass deer ERT variation and about 5% in the nightclass data (Table 4). The 12% figure is believed sufficiently large to be meaningful; 5% may not be. However, the rate of convective cooling is proportional to the temperature gradient (equation 34), and since the difference between deer ERT and air temperature was generally greater in the dayclass data, this result would be expected.

The cup anemometers apparently served to measure indices of convective cooling, only. They could not have measured total airflow over particular surface areas on the deer bodies, due to the turbulent, three-dimensional flow characteristics of wind over almost all natural surfaces. Added to the natural complexity of turbulent airflow, was the influence of the pen itself and the burlap covering which was installed. The anemometers, though extremely sensitive, measured only the horizontal component of air movement. Thermistor anemometers fastened on the animals, with a radiotelemetric data link, were considered in the planning stages of this study, but this equipment was not available.

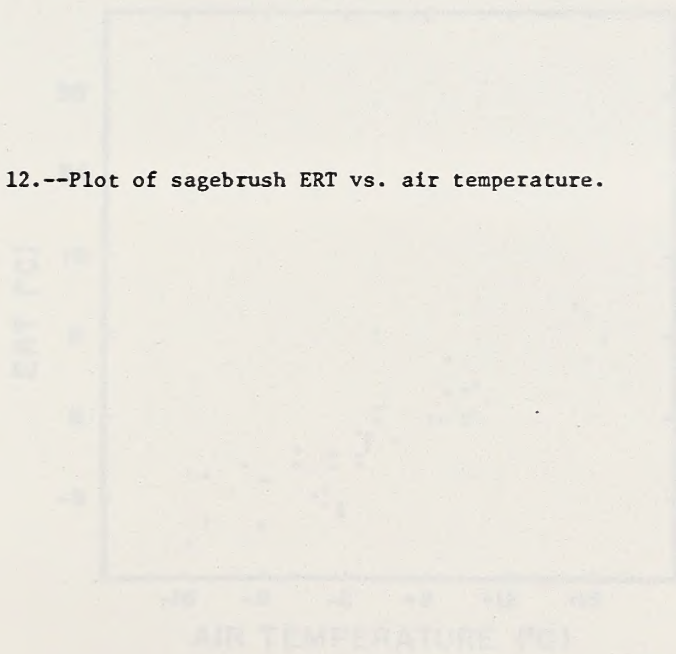
Background ERT Variation

Sagebrush ERT exhibited the lowest variation about regression, the strongest correlation with air temperature, and the largest multiple R^2 value of any of the surfaces measured. The high air temperature correlation ($R = 0.87$) can be seen in Figure 12. With an additional increase in R^2 of 7% contributed by the solar radiation term, the multiple correlation coefficient (R) reaches 0.94. These results agree with those of Gates (1961), but are not comparable to the results of other studies found, since all others were conducted during periods of more active plant metabolism.

Sagebrush ERT measurements were made over a field of view which included not only leaves of the plant, but also the woody stems. Therefore, these results should not be construed as indicative of individual leaf surface temperature variation. Since an airborne thermal scanner could not measure the ERT of a single leaf, no attempt was made to measure it with the radiometer. Rather, values for the integrated ERT's over the entire field of view were the desired objectives. However, the contribution of leaf temperature to the total field temperature should have been sufficient to detect a 1°C difference between the leaf temperature and air temperature.

Actual leaf surface area viewed by the radiometer was estimated to be at least 50% of the field of view. If the woody stems of the plant may be considered thermally inert, their temperature would be expected to follow air temperature linearly when shaded from direct solar radiation. Most of the sagebrush stems were shaded by leaves.

Figure 12.--Plot of sagebrush ERT vs. air temperature.



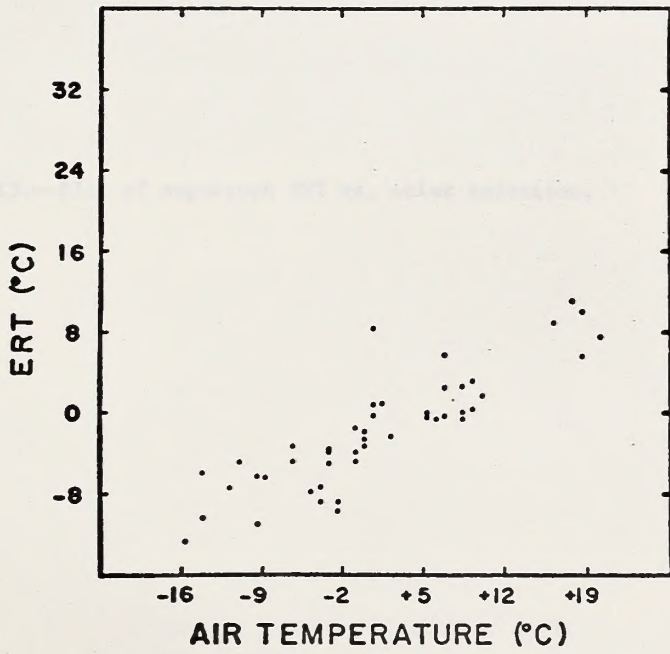
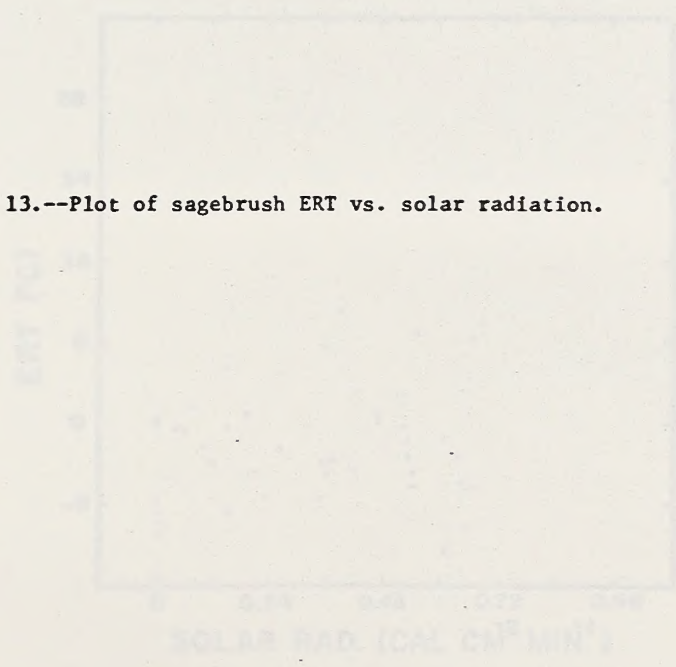


Figure 13.--Plot of sagebrush ERT vs. solar radiation.



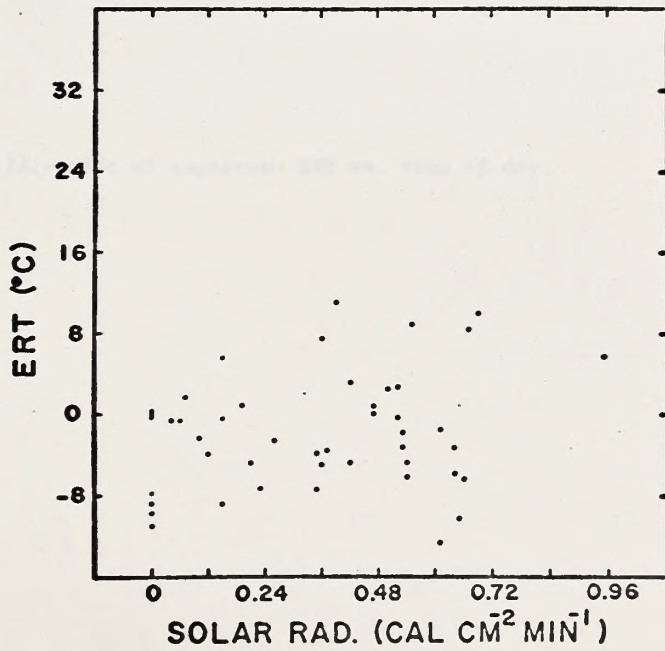
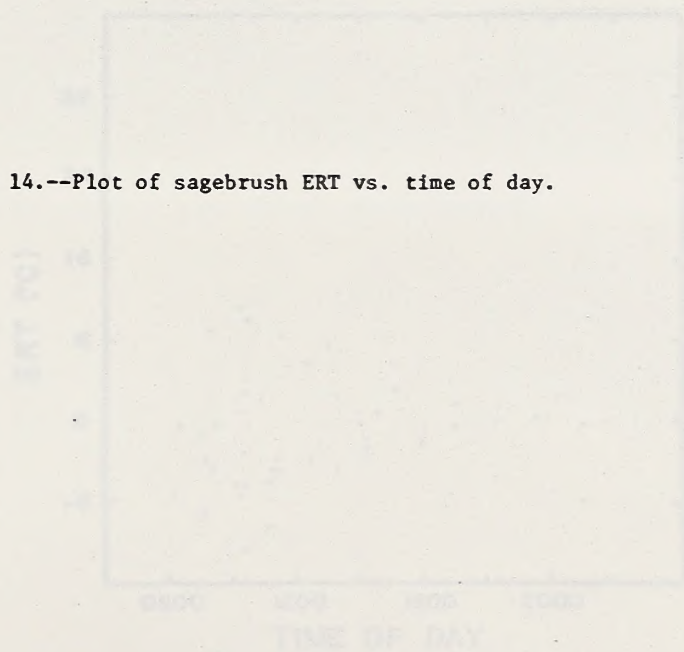


Figure 14.--Plot of sagebrush ERT vs. time of day.



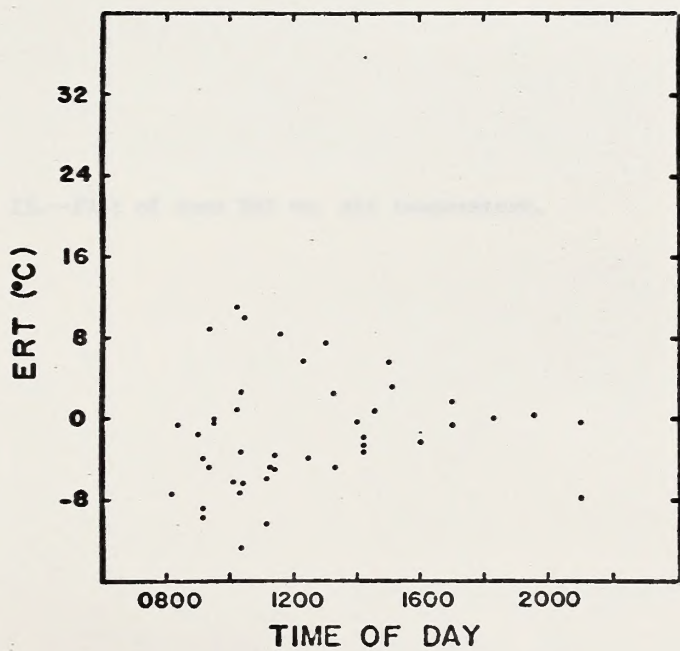
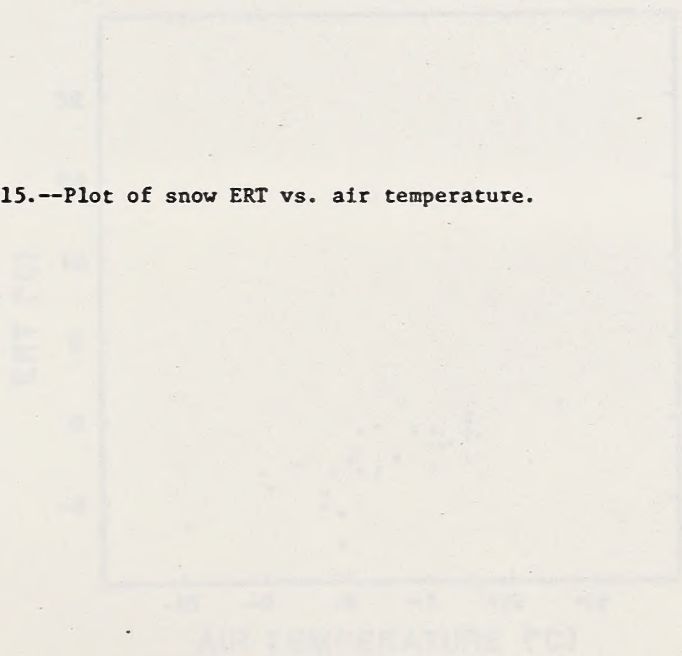
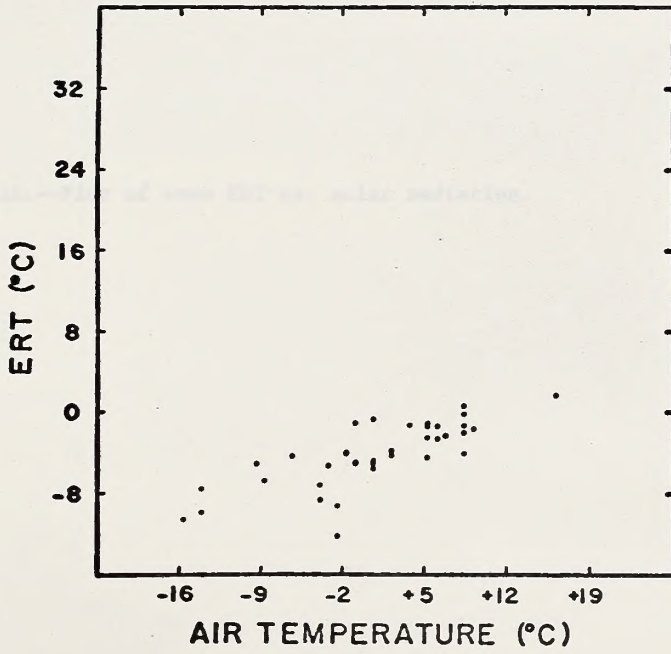


Figure 15.--Plot of snow ERT vs. air temperature.





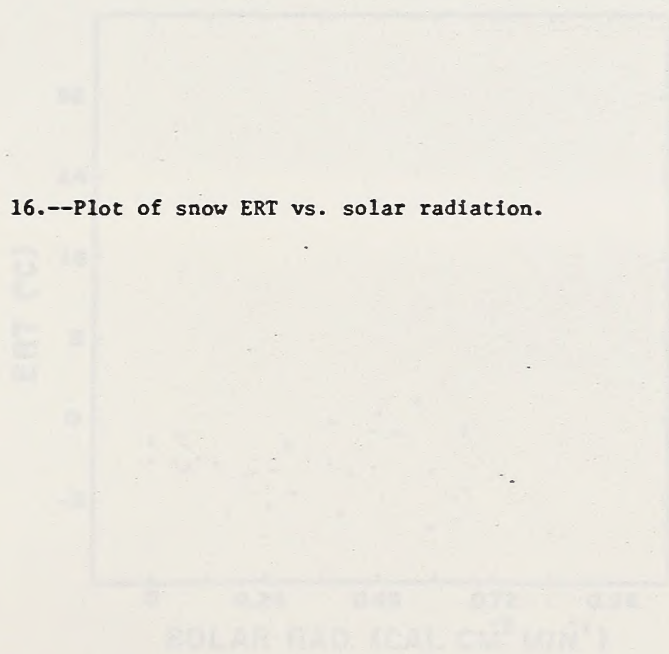


Figure 16.--Plot of snow ERT vs. solar radiation.

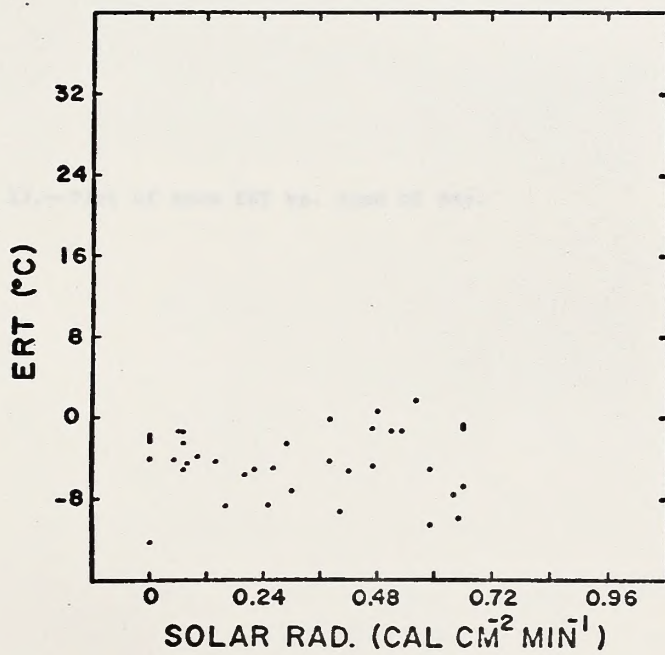
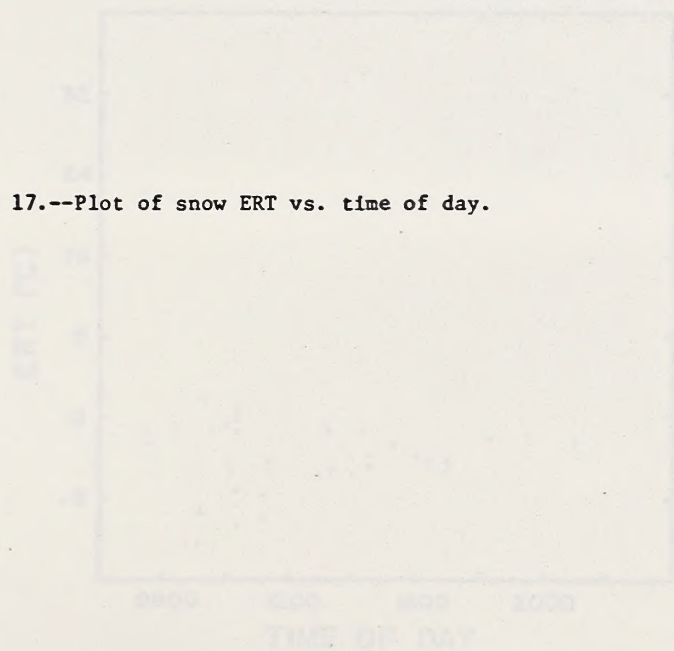


Figure 17.--Plot of snow ERT vs. time of day.



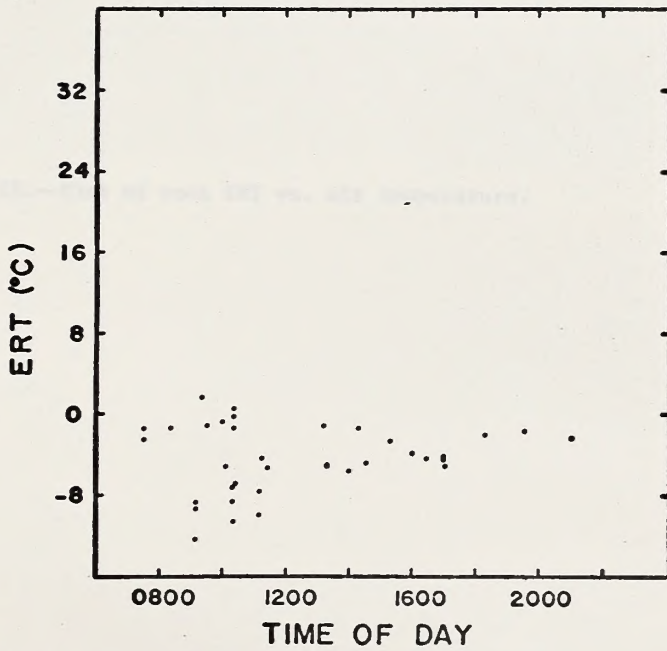
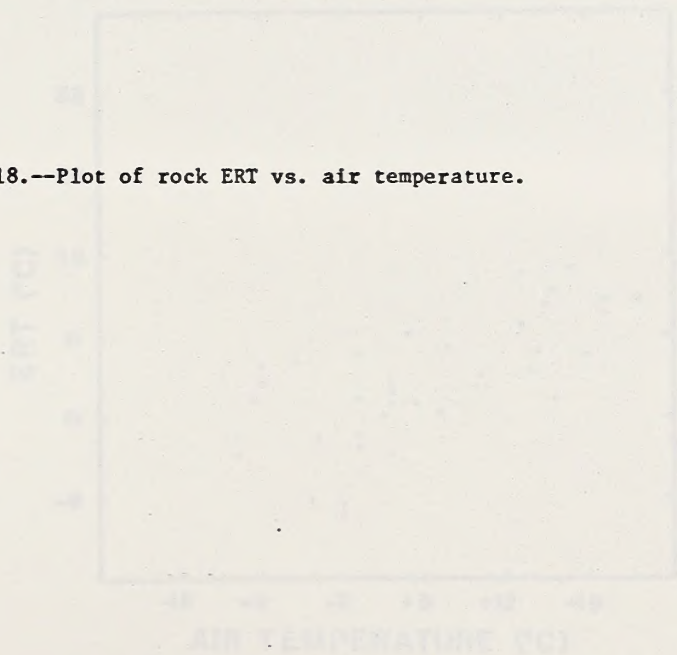


Figure 18.--Plot of rock ERT vs. air temperature.



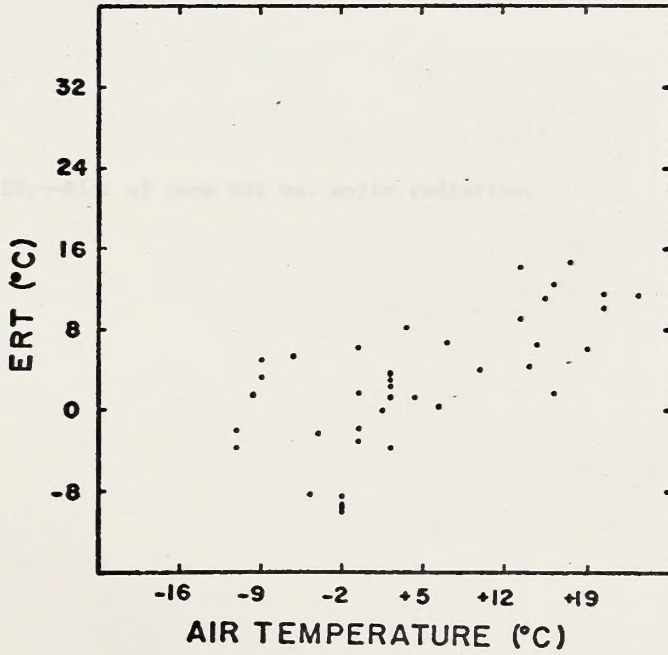
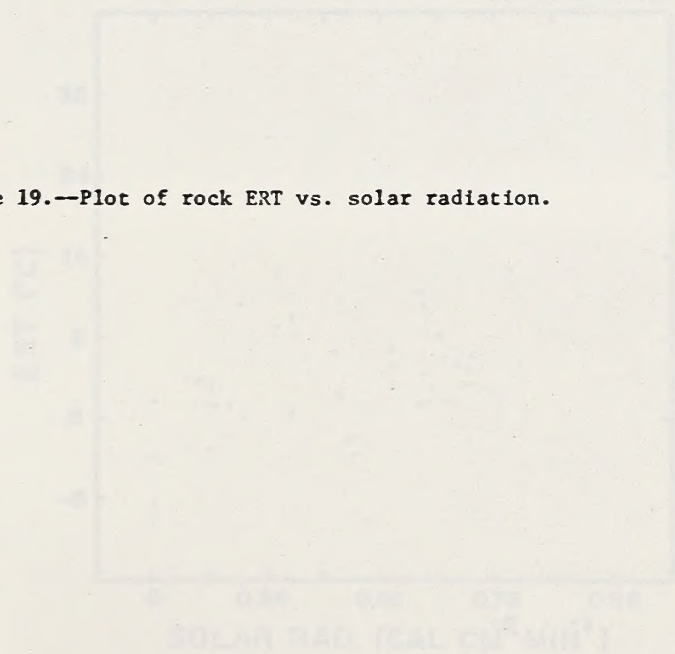


Figure 19.—Plot of rock ERT vs. solar radiation.



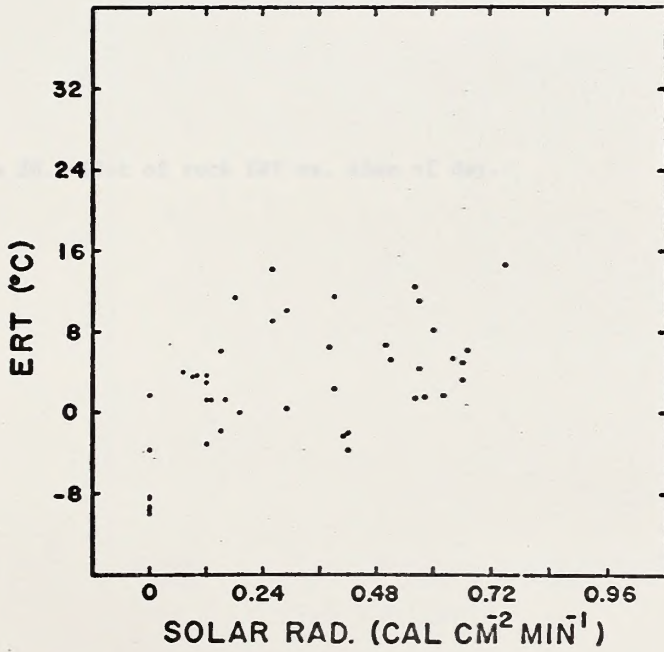
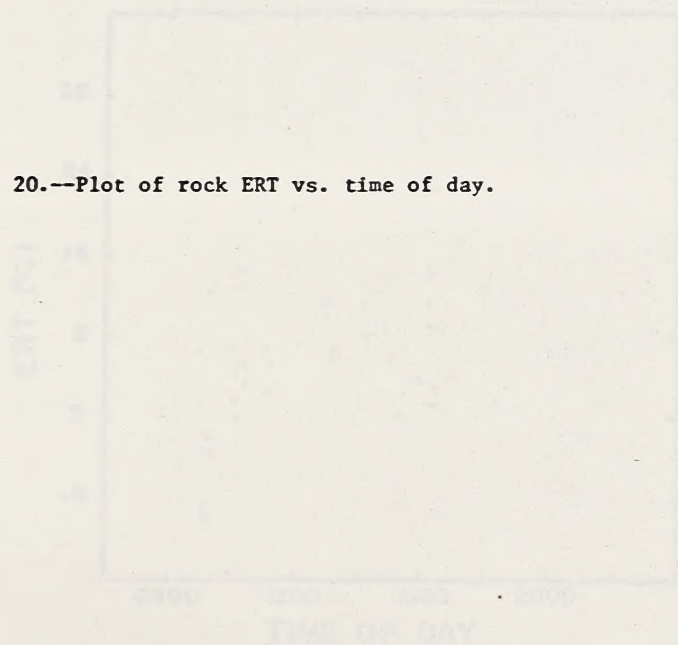


Figure 20.--Plot of rock ERT vs. time of day.



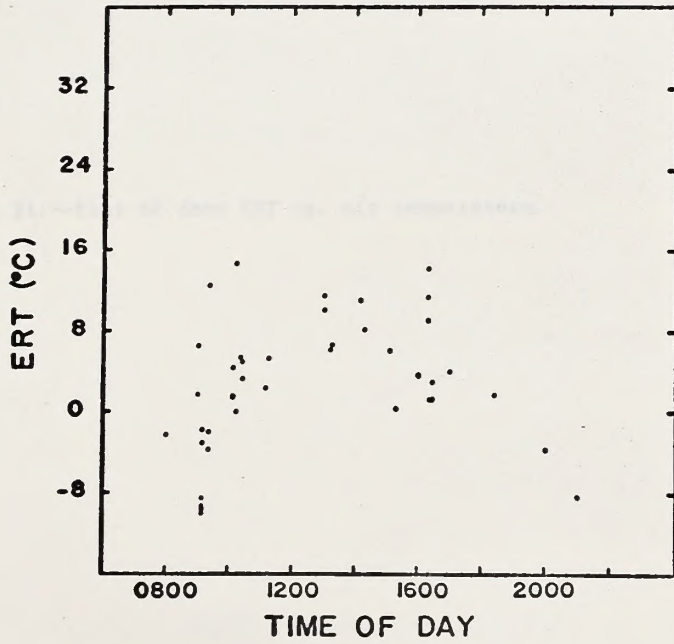
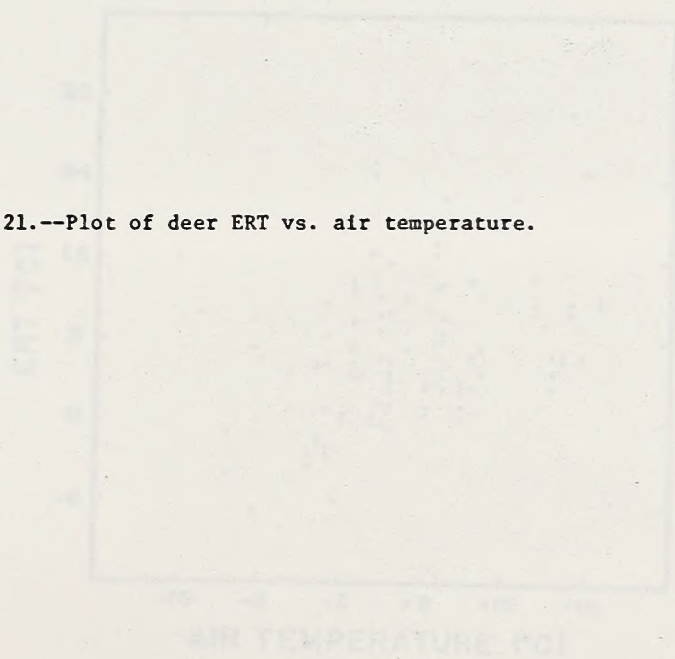


Figure 21.--Plot of deer ERT vs. air temperature.



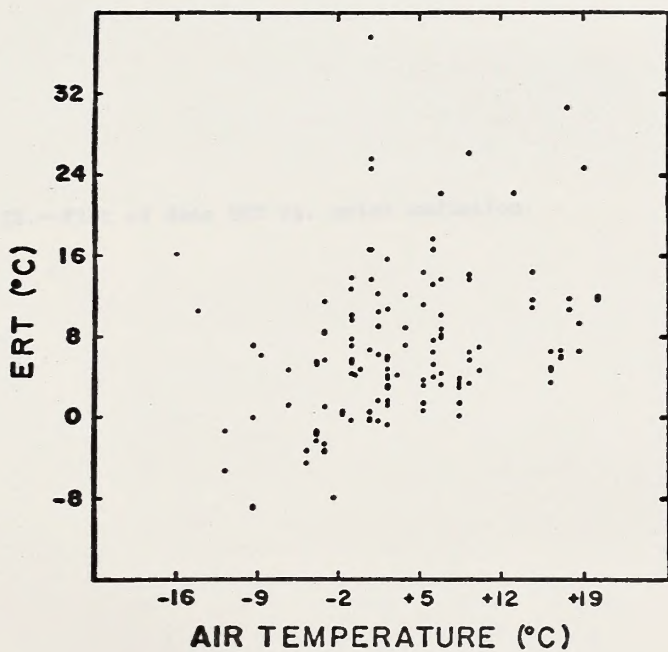
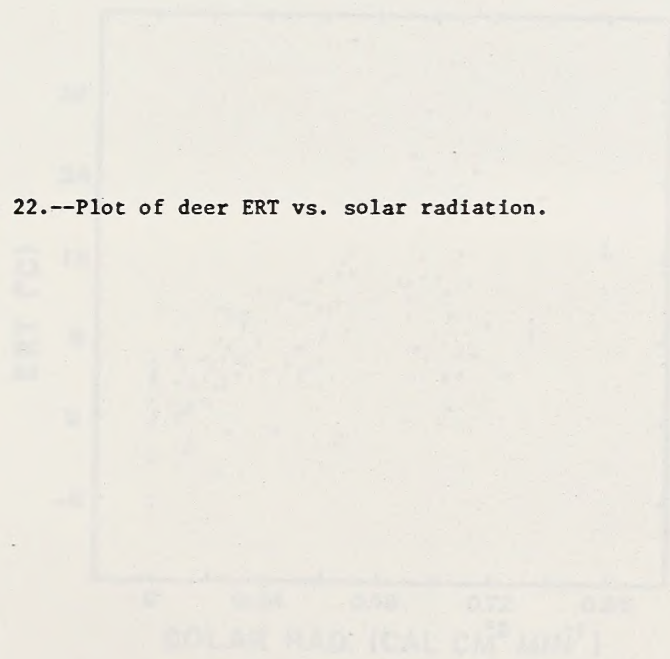


Figure 22.--Plot of deer ERT vs. solar radiation.



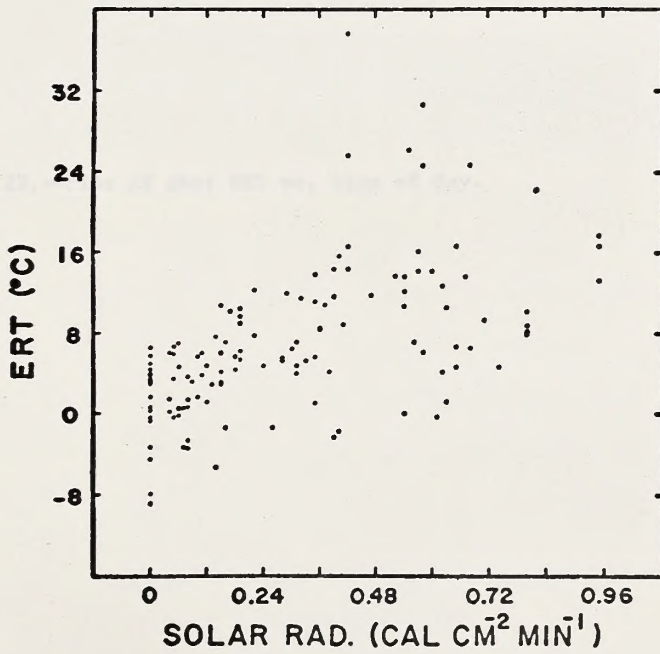
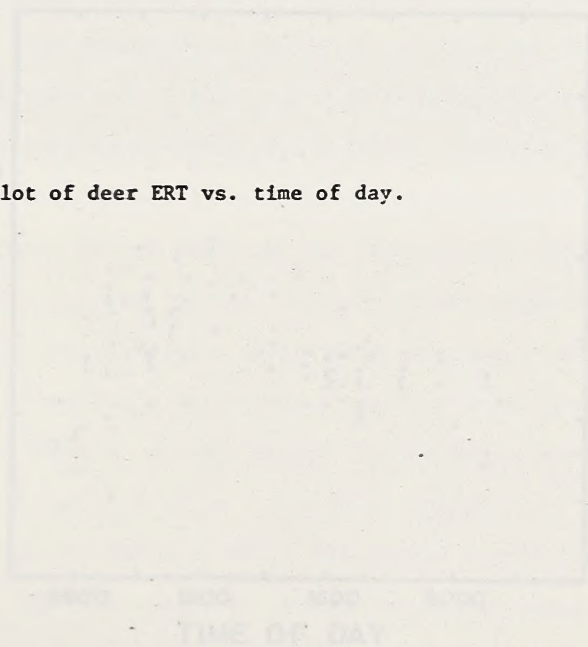
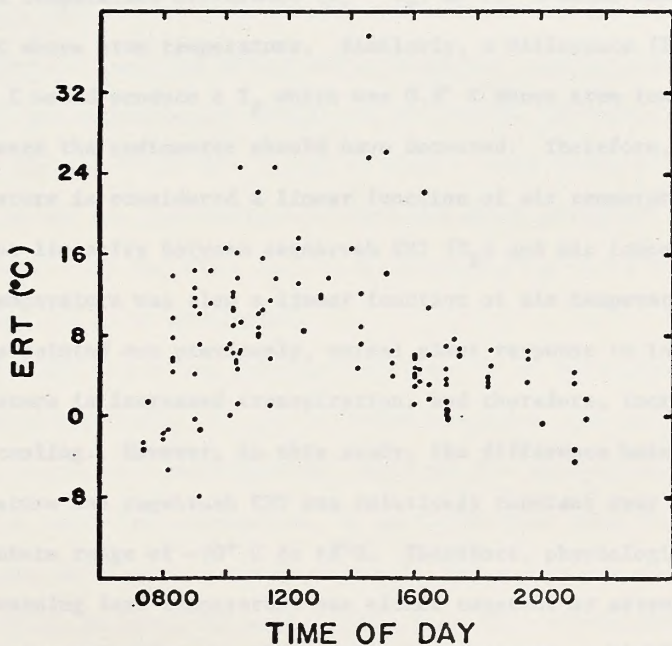


Figure 23.--Plot of deer ERT vs. time of day.





Using 50% as the approximate proportion of the radiometer's field of view occupied by leaves, and 50% by stems, the average ERT of the whole field (T_F) of area A may be estimated as follows:

$$(.5)(A)(T_L) + .5(A)(T_S) = T_F \quad (23)$$

where T_L = leaf temperature

T_S = stem temperature

Thus, a temperature difference ($T_L - T_S$) of -2° C would cause T_F to be 1° C above stem temperature. Similarly, a difference ($T_L - T_S$) of -1° C would produce a T_F which was 0.5° C above stem temperature, a difference the radiometer should have detected. Therefore, if stem temperature is considered a linear function of air temperature, the apparent linearity between sagebrush ERT (T_F) and air temperature implies leaf temperature was also a linear function of air temperature.

As pointed out previously, normal plant response to increasing air temperature is increased transpiration, and therefore, increased evaporative cooling. However, in this study, the difference between air temperature and sagebrush ERT was relatively constant over the air temperature range of -20° C to $+8^\circ$ C. Therefore, physiological response to increasing leaf temperature was either constant or absent. Constancy implies transpiration at sub-freezing temperatures, a highly unlikely conclusion. Therefore, there must have been no detectable evaporative cooling at all.

The air temperature range over which these sagebrush ERT values were measured should be noted carefully. A constant difference between

plant ERT and air temperature cannot be maintained at much higher air temperatures. Whether transpiration occurs in winter from an evergreen broadleaf species such as sagebrush is not known. However, it apparently did not in this study, at least in a magnitude sufficient to cause any significant leaf surface cooling.

Snow ERT was also most closely associated with air temperature, although not as closely as was sagebrush ERT (Table 4, page 61). Snow consistently exhibited the most uniform ERT at a particular time than any other surface. This uniformity was believed due to the high reflectance of snow for direct solar radiation. Little absorptance occurred and consequently, little of the erratic ERT variation found in deer and sagebrush ERT, caused by direct solar radiation.

Snow was the only background material which exhibited any association with humidity, but the R^2 contribution (0.05) was probably still too low to be meaningful.

Rock ERT showed the greatest relationship to solar radiation of all background materials. R^2 due to solar radiation was nearly as high as the air temperature contribution. Although the absorptance of the rocks for solar radiation was unknown, it must have been quite high, considering the strong solar heating which occurred. The retention of heat by rocks was noted on at least two nights, when rock ERT exceeded deer ERT as late as 9:00 p.m.

Bare soil ERT measurements were not made as planned, due to frequent coverage of the selected surface area by snow. Even when clear of snow, the soil varied from mud to dry or frozen, and repeat measurements under similar conditions were few.

The variations in ERT of sagebrush, snow, rock, and deer, as functions of air temperature, solar radiation, and time of day, are shown in figures 12 through 23, pages 70-101. These plots graphically illustrate the strength of the associations between time, air temperature, and solar radiation, and the ERT of all surfaces measured.

Atmospheric water vapor pressure had no important effect on the ERT of any surface. The data was run both as vapor pressure (in. Hg), and as relative humidity, with no definite effect found.

The lack of any humidity effect detected may be due to error in measurement. Atmospheric water vapor content, even at saturation levels, is very low and difficult to measure in the air temperature range included.

However, there are two potential effects of vapor pressure on ERT. One is the variation in surface temperature due to change in the thermal conductance of air as a function of water vapor content. Increased conductance of air would allow more heat loss in the convective mode. But, since the thermal conductance of air is so low, it is doubtful that this effect could be measured in company with the many other variables present.

The other potential effect of vapor pressure is the attenuation of radiation in the 8-14 micrometer band by water vapor. From Gates (1962) precipitable water vapor (w) over a distance (L) may be calculated as follows:

$$w(\text{cm}) = \frac{p(\text{gm cm}^{-3})}{d(\text{gm cm}^{-3})} \times L(\text{cm}) \quad (24)$$

where d = density of liquid water = 1.0, p = mass of water vapor along the path.

The mass of water vapor in saturated air at -20°C is about $.9 \times 10^{-6} \text{ gm cm}^{-3}$, and at $+10^{\circ}\text{C}$, it is about $9.0 \times 10^{-6} \text{ gm cm}^{-3}$.

The maximum value for L was about 1,220 cm. Applying these figures to equation 24, the extremes of precipitable water during this study were:

$$\text{At } -20^{\circ}\text{C} \quad W = \frac{.9 \times 10^{-6}}{1.0} \times 1220.0 = 1098 \times 10^{-6} \text{ cm}$$

$$\text{At } +10^{\circ}\text{C} \quad W = 1098.0 \times 10^{-5} \text{ cm}$$

Yates, et al. (1960) shows atmospheric transmission in the 6.0 to 15.0 micrometer band is 60% at a precipitable water content of 1.0 mm, and almost 100% over a 0.3 Km path containing 5.7 mm of precipitable water. A collection of data on atmospheric transmission in various wavelengths was found in Wolfe (1965). Although no information was found on transmission through paths containing less than 1.0 mm of precipitable water, it is reasonable to assume negligible absorption and scattering by water vapor over a 1220 cm path containing a maximum of .1098 mm of water, as found in this study.

Thermal Contrast

The results of the multiple regressions of thermal contrast between deer and sagebrush (ΔT_s) and between deer and snow (ΔT_N) indicated thermal contrast was less predictable than most ERT values taken alone (Table 4, page 61). This result is, again, believed attributable to the erratic solar radiation effect, especially on the deer surfaces.

More meaningful representations of ΔT are shown in figures 24 and 25, where deer ERT is plotted against mean snow and sagebrush ERT during the same sample periods. Deer ERT exceeded the existing mean sagebrush ERT in all but one case, which occurred when the deer was shaded and the plant was sunlit. Mean snow ERT never exceeded deer ERT.

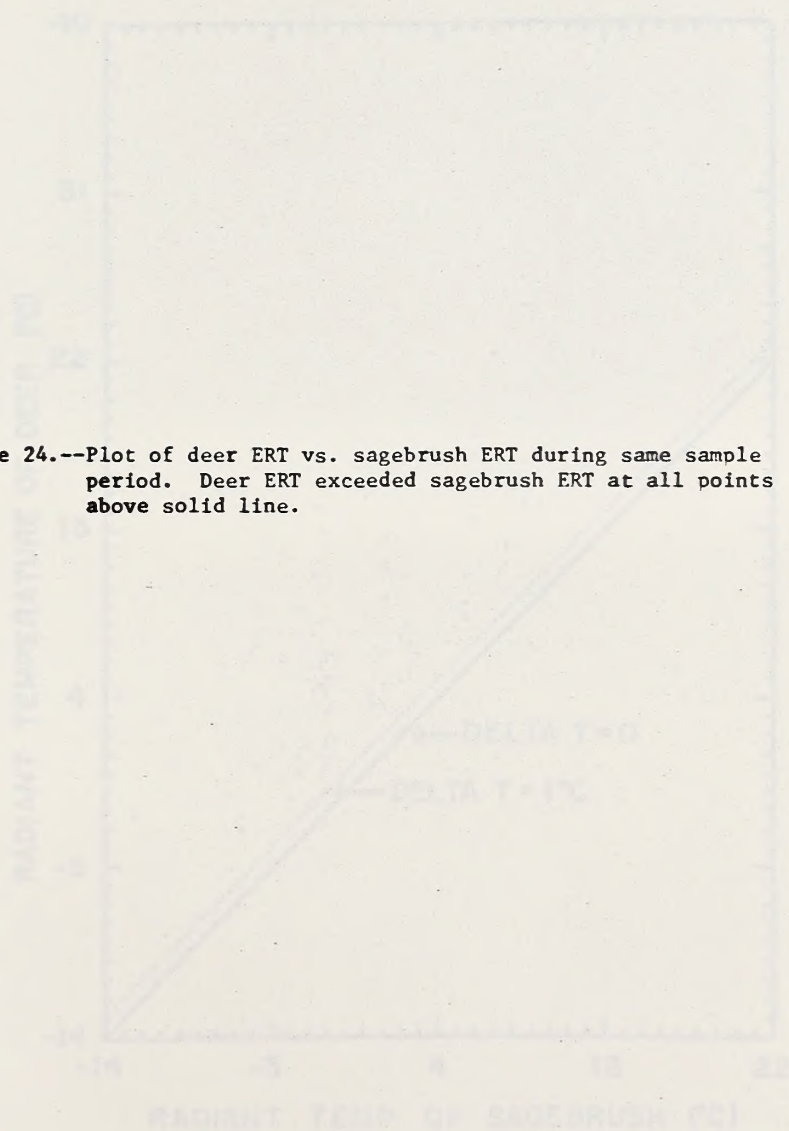
Thermal contrast between deer and sagebrush, plotted in 5°C air temperature classes (Figure 26), illustrates the overall dependence of ΔT_s on air temperature.

Thermal contrast between deer and rock was frequently negative during daylight hours. The strong influence of solar radiation on the ERT of rock and other surfaces can be seen in Figure 27, where ERT variation on a clear day is shown. Figure 28 shows ERT variation on an overcast day.

The general trend in thermal contrast between deer, sagebrush, and snow, the two primary background materials in the study area, can be judged from the regression lines in Figures 29 and 30. Three-variable multiple regression equations, ERT against air temperature and solar radiation, were used to generate these lines. For the lines in Figure 29, solar radiation was held constant at 0, to represent night. In Figure 30, solar radiation was set at $0.90\text{ cal cm}^{-2}\text{ min}^{-1}$ to represent maximum sunlight.

Although these lines indicate greater thermal contrast during the daytime, the statistical value of each line must be considered (Table 4, page 61). Also, the daytime lines do not show the extremes, caused by solar heating, which occurred.

Figure 24.--Plot of deer ERT vs. sagebrush ERT during same sample period. Deer ERT exceeded sagebrush ERT at all points above solid line.



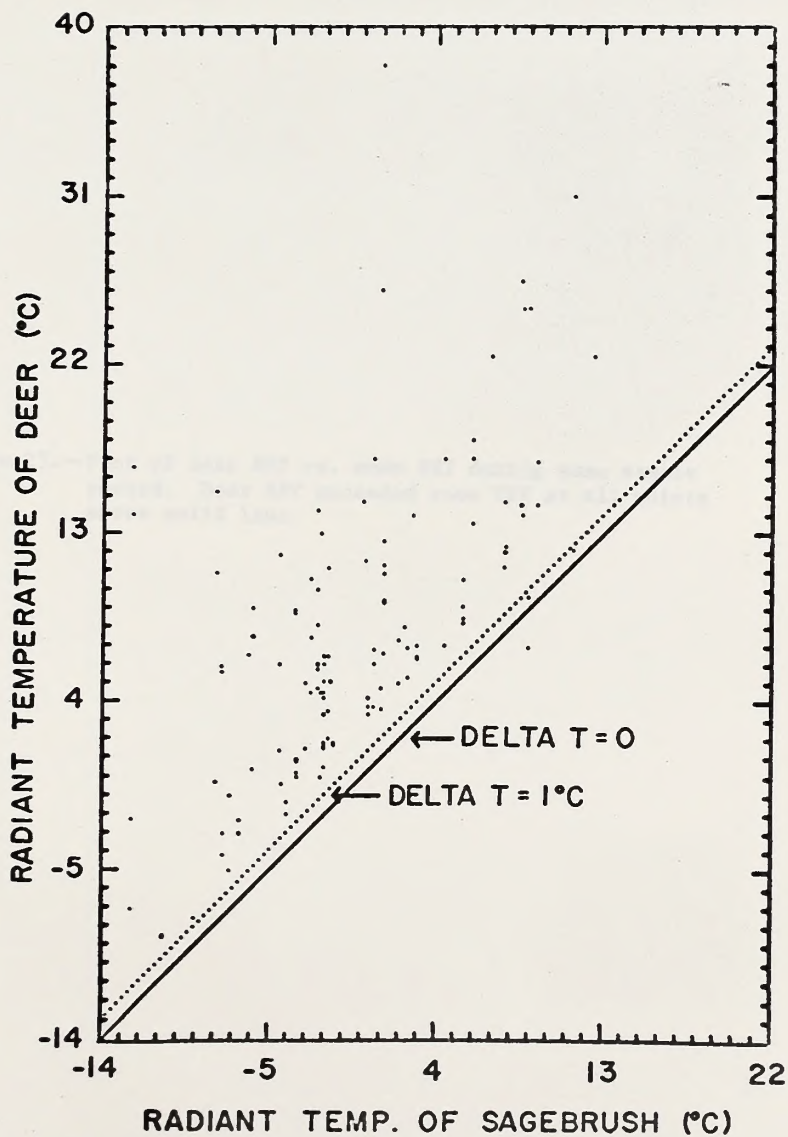
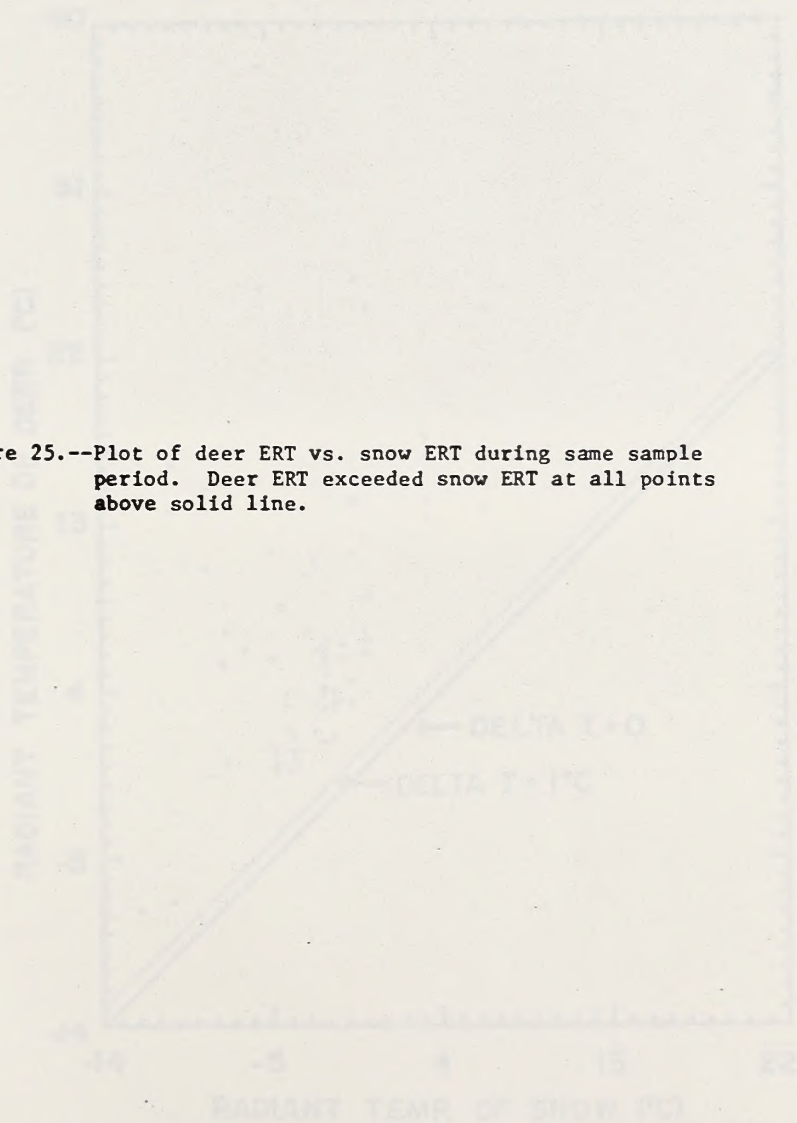


Figure 25.--Plot of deer ERT vs. snow ERT during same sample period. Deer ERT exceeded snow ERT at all points above solid line.



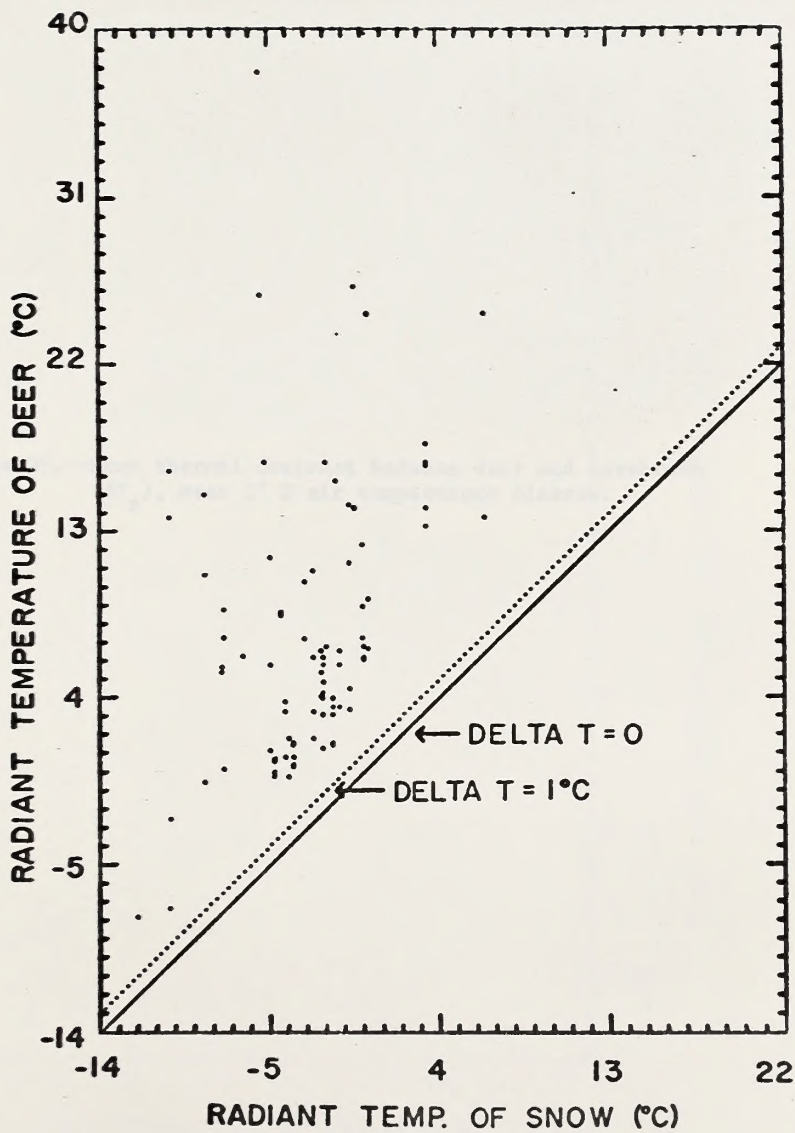
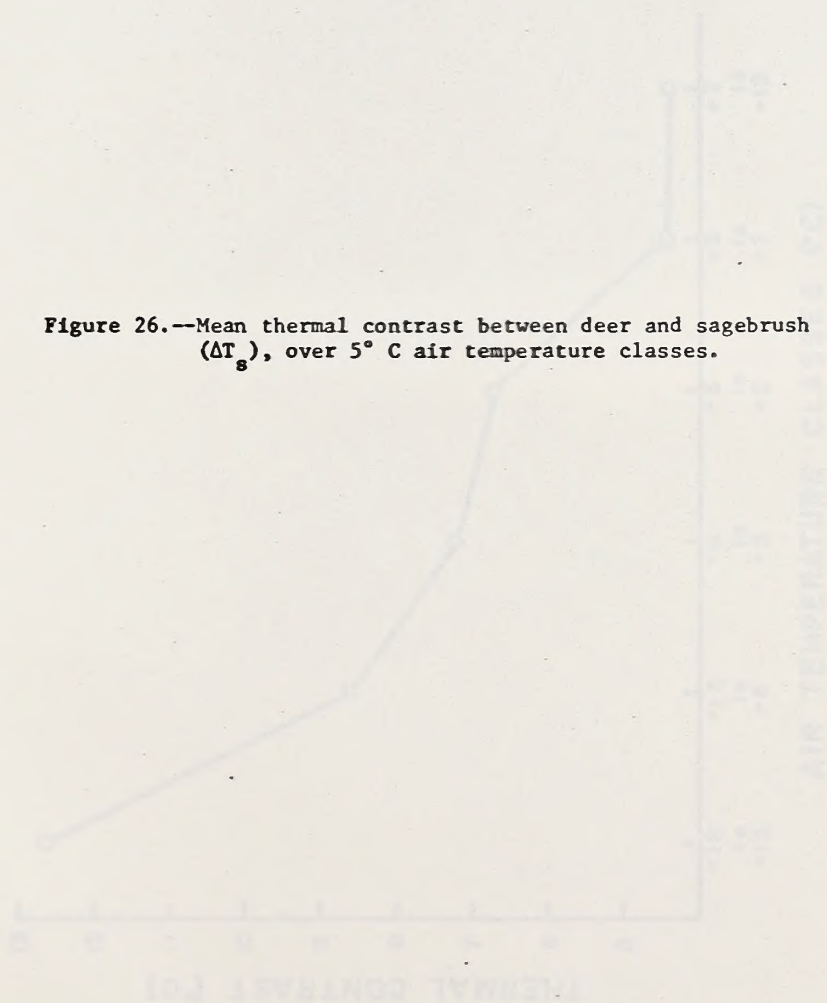


Figure 26.--Mean thermal contrast between deer and sagebrush (ΔT_s), over 5° C air temperature classes.



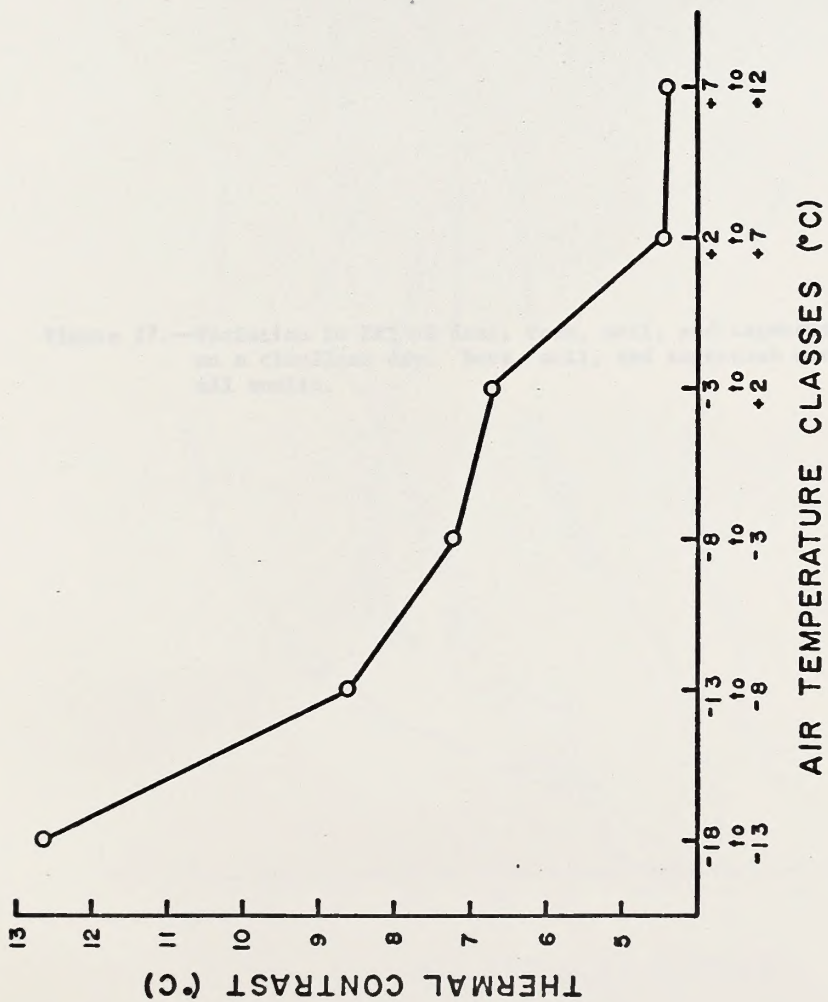
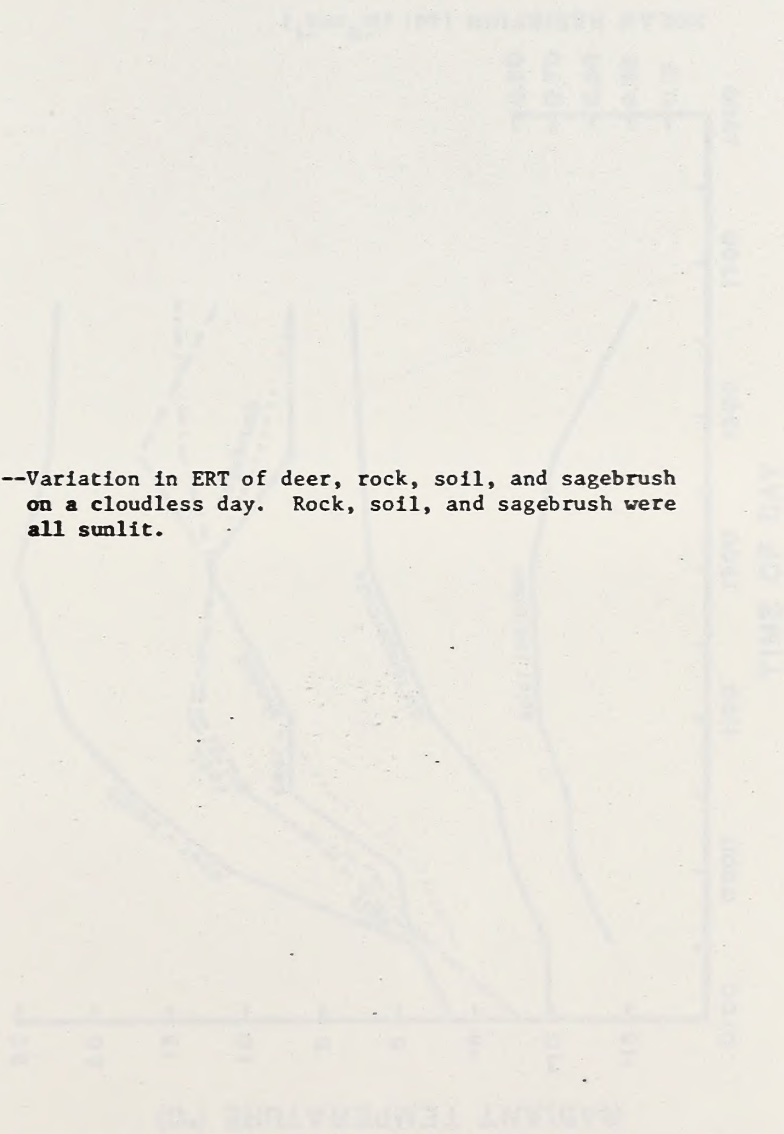


Figure 27.--Variation in ERT of deer, rock, soil, and sagebrush on a cloudless day. Rock, soil, and sagebrush were all sunlit.



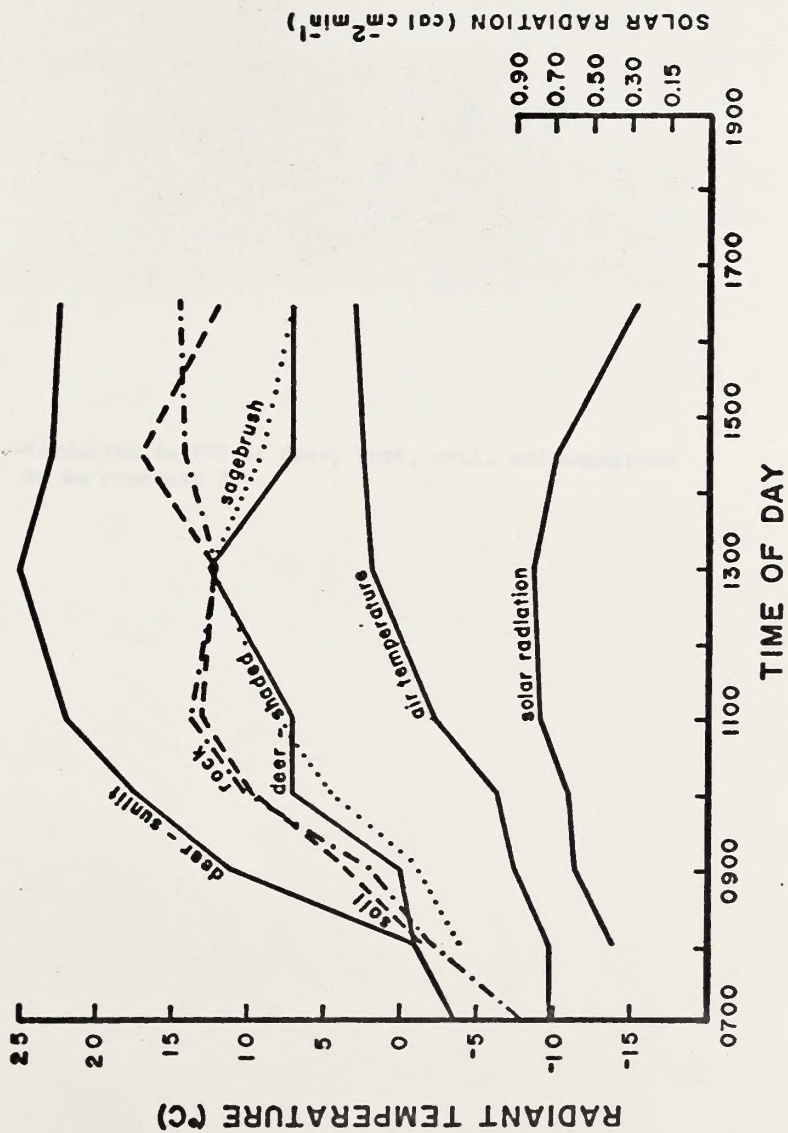
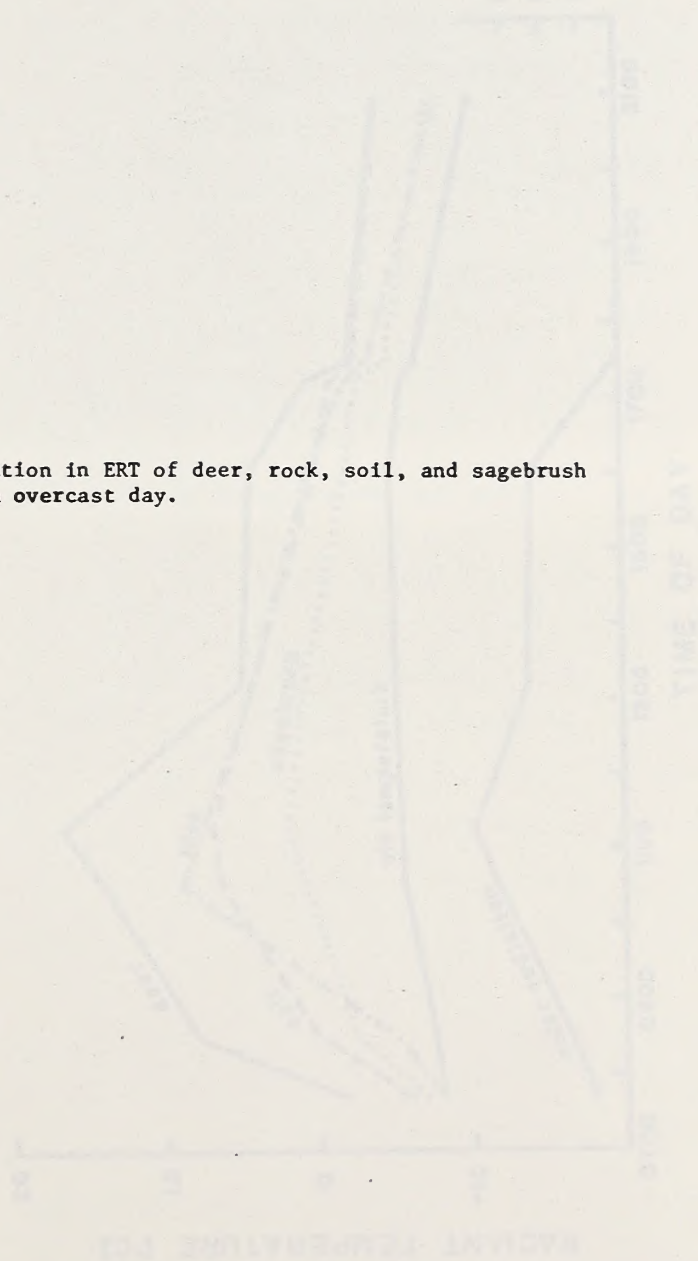


Figure 28.--Variation in ERT of deer, rock, soil, and sagebrush on an overcast day.



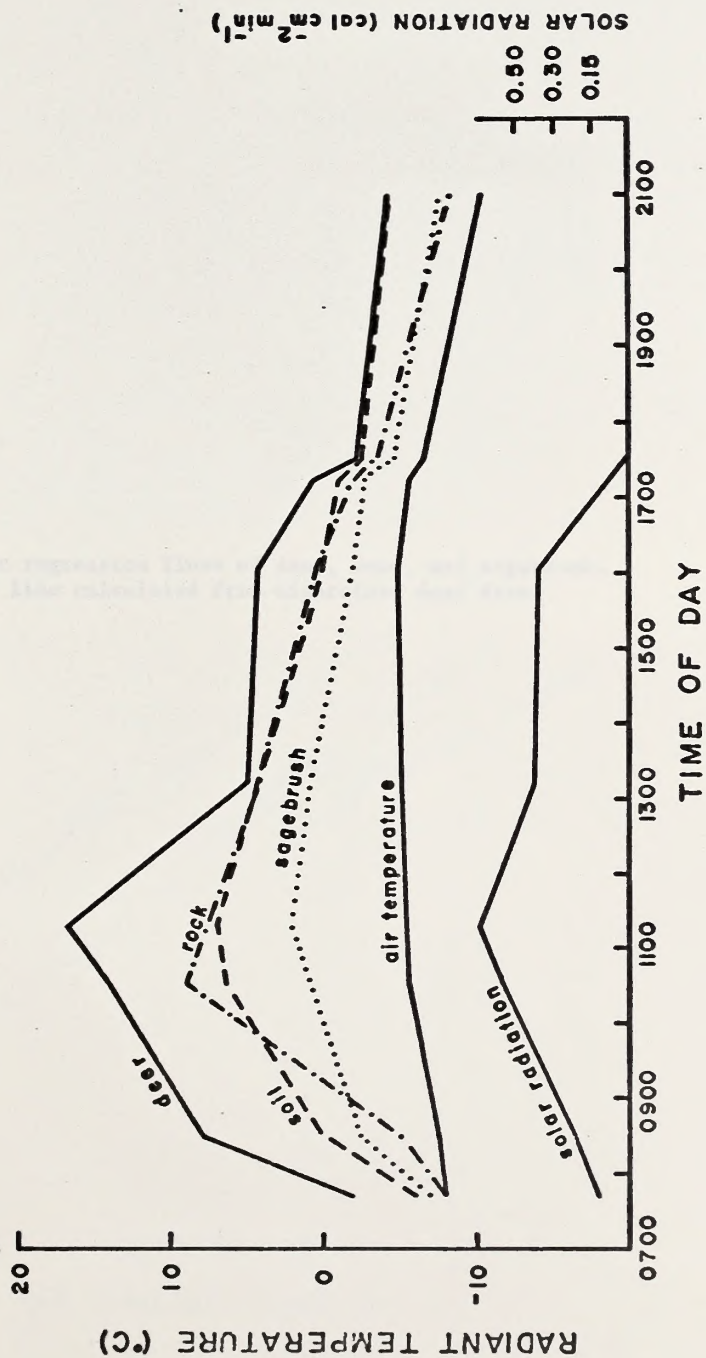
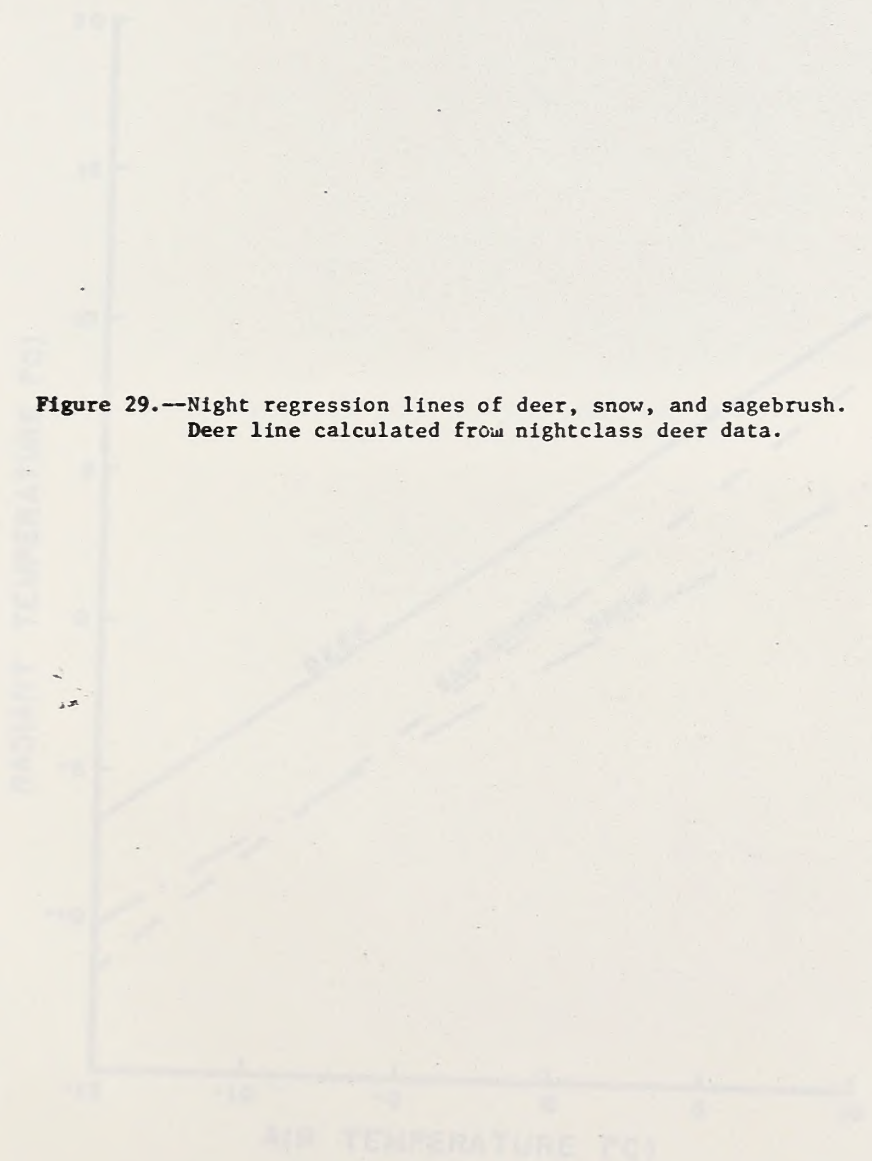
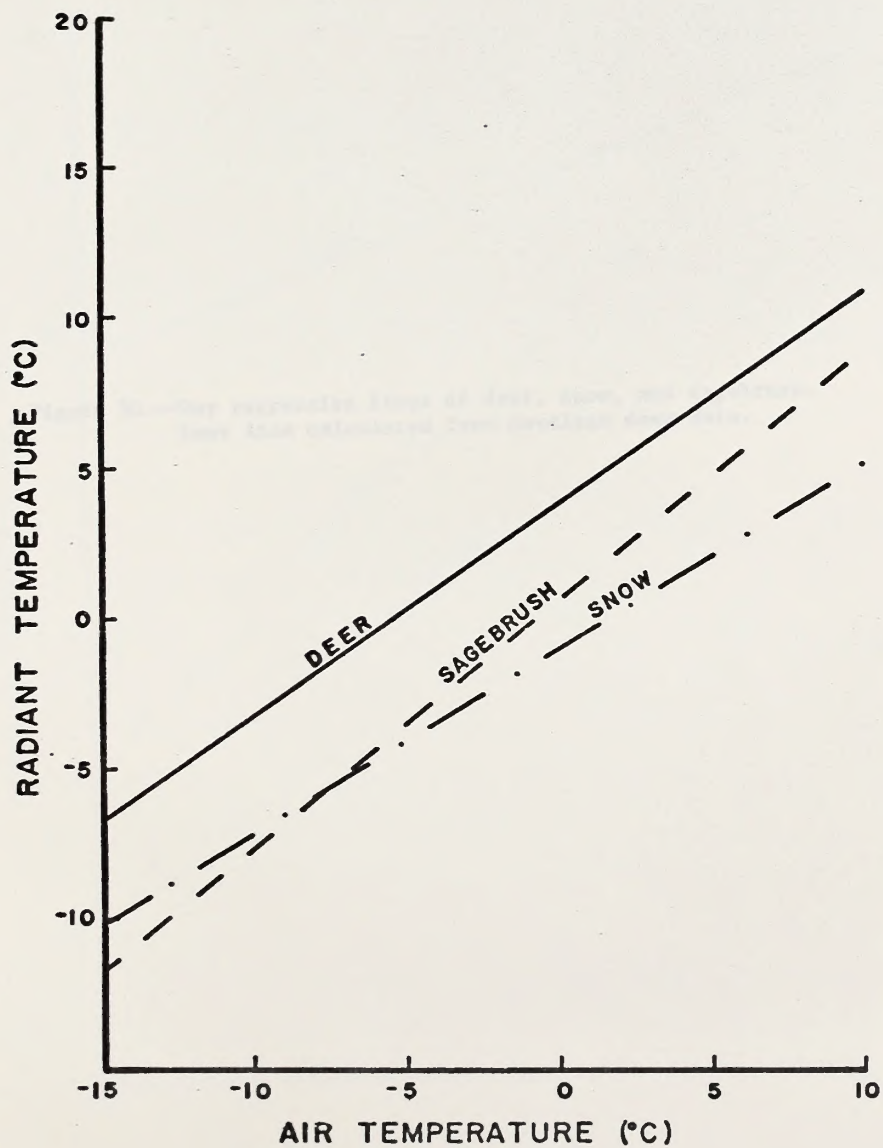


Figure 29.--Night regression lines of deer, snow, and sagebrush.
Deer line calculated from nightclass deer data.





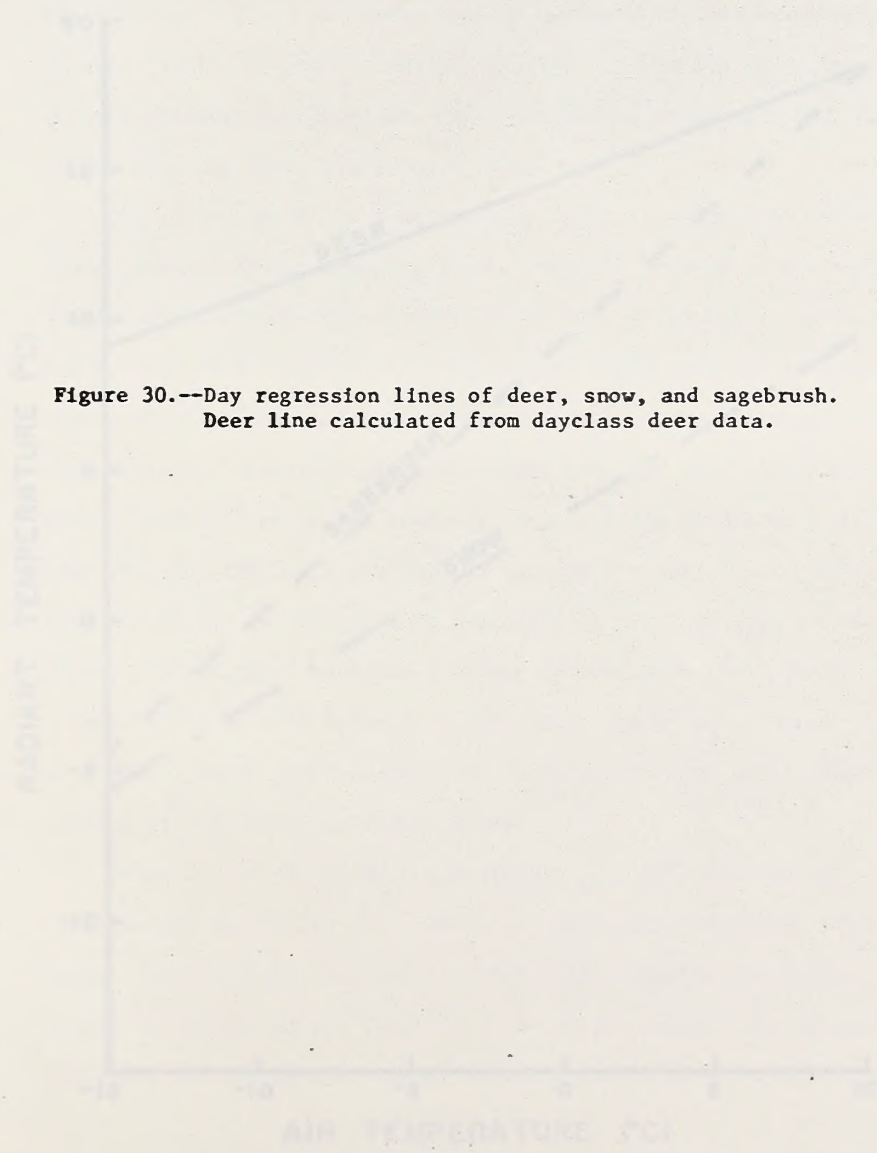
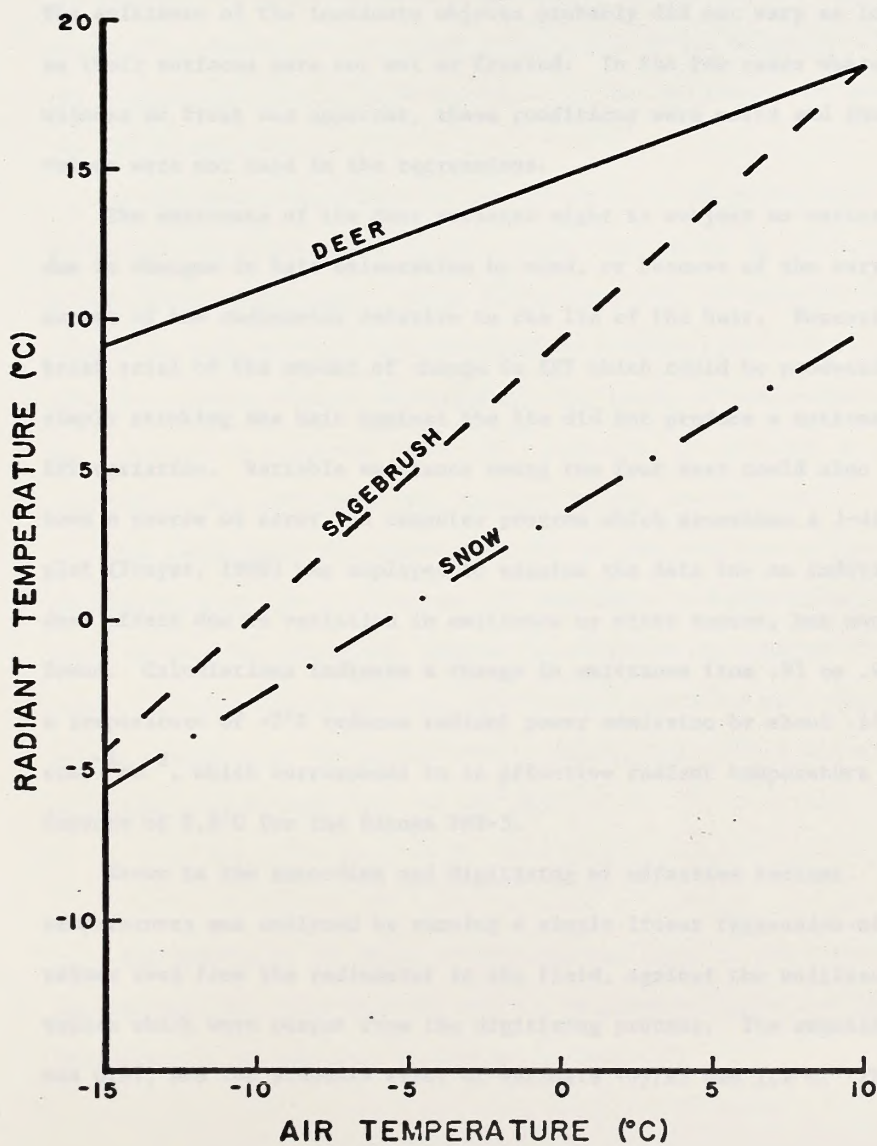


Figure 30.--Day regression lines of deer, snow, and sagebrush.
Deer line calculated from dayclass deer data.



Potential Error Sources

The measurement of effective radiant temperatures is subject to error due to possible variation in emittance of the surfaces measured. The emittance of the inanimate objects probably did not vary as long as their surfaces were not wet or frosted. In the few cases where wetness or frost was apparent, these conditions were noted and the ERT values were not used in the regressions.

The emittance of the deer surfaces might be subject to variation due to changes in hair orientation by wind, or because of the varying aspect of the radiometer relative to the lie of the hair. However, a brief trial of the amount of change in ERT which could be produced by simply stroking the hair against the lie did not produce a noticeable ERT variation. Variable emittance among the four deer could also have been a source of error. A computer program which generates a 3-dimensional plot (Frayer, 1968) was employed to examine the data for an individual deer effect due to variation in emittance or other causes, but none was found. Calculations indicate a change in emittance from .95 to .90 at a temperature of -2°C reduces radiant power emission by about $.14 \text{ mw ster}^{-1} \text{ cm}^{-2}$, which corresponds to an effective radiant temperature difference of 2.8°C for the Barnes PRT-5.

Error in the recording and digitizing of effective radiant temperatures was analyzed by running a simple linear regression of ERT values read from the radiometer in the field, against the unitless digital values which were output from the digitizing process. The resulting R^2 was 0.97, and the standard error of estimate (σ_y/x) was 1.1°C . The

generated regression equation was used to convert the digital values to temperature ($^{\circ}\text{K}.$). Therefore, the average error of the tape-recorded ERT values was $1.1^{\circ}\text{C}.$ The mean error of the final ERT values used in the analyses was probably less, since whenever possible, the taped ERT values were checked and corrected by reference to the original field data. ERT values were read and hand-recorded from the radiometer for about half the ERT's measured.

Little data processing error was possible in the measurement of windspeed. The anemometers produced electrical pulses at a frequency proportional to windspeed. These pulses were tape-recorded and later counted by computer over time intervals of 4 seconds duration, coincident with the 4-second digital ERT records. The number of pulses per second was converted to windspeed in cm sec^{-1} manually, by reference to calibration curves for each anemometer supplied by the manufacturer.

The response of the pyranometer, in voltage output as a function of rate of incident solar radiation, was nonlinear. A calibration curve was drawn by hand to convert the digital record values to original millivolt output from the instrument, and then to solar radiation rate in $\text{cal cm}^{-2} \text{min}^{-1}$, according to the manufacturer's calibration. Error was estimated to be not greater than $0.03 \text{ cal cm}^{-2} \text{min}^{-1}$.

CONCLUSIONS

The results of the Phase I investigations lead to the following conclusions with respect to the surface temperature regime and theoretical detectability of mule deer in winter, in Colorado:

- 1) The erratic nature of the effect of direct solar radiation causes the ERT of deer to be highly unpredictable during daylight hours under clear skies.
- 2) In the absence of direct solar radiation, the ERT of deer and dry background surfaces measured is closely associated with and always greater than, air temperature.
- 3) On the average, deer ERT will exceed the ERT of all background materials measured, during periods of no direct solar illumination, by an amount inversely proportional to air temperature.

These conclusions are believed valid as generalities. However, some qualifications must be made in order to relate them to dependability of detection.

There were no environmental conditions under which deer ERT always exceeded the ERT of the background materials, except when the background was snow. Exceptions to the trends in ERT indicated by the regression lines could always be found. Therefore, there would always be a certain amount of error associated with the quantitative detection of wild deer. However, this error is not constant throughout the day; there are periods when it may approach zero.

To consider the diurnal error variation, the day may be divided into four categories based on the direct and indirect effects of solar radiation. These categories are here defined as follows:

- 1) Day - sunrise to sunset.
- 2) Night - the hours of darkness.
- 3) Post-sunset - the period from sunset to darkness.
- 4) Pre-sunrise - the period from darkness to sunrise.

The day category is the period of greatest average thermal contrast, according to the regression equations. But, it also is the period when the potential type II error is at a maximum on clear days, due to solar heating of background materials. In addition, type I error would be proportional to the number of deer which happened to be shaded during the scanning. They probably would not be detected against a sunlit background.

The post-sunset period is free from the direct effects of bright sunlight, but the residual heat remaining in rocks and perhaps bare soil, tends to sustain the daytime potential for type II error until well after dark.

The night period, after dissipation of residual solar heat, is probably the best time for detection, since the only sources of heat are the animals. Although overall thermal contrast is reduced during this period, the data show it is still sufficient for detection. However, as a practical matter, flying safely at low altitude during the dark is impossible over most of Colorado's deer winter range.

The pre-sunrise period probably represents the optimum time for detection. The advantages of the night period in regard to error are maintained until sunrise, and there is sufficient diffuse light for visual navigation. The pre-sunrise period was the time selected to flight test a thermal scanner in Phase II.

The existence of total cloud cover during the day period offers one additional set of environmental conditions which may be desirable for deer detection. Overcast skies were mentioned by Croon (1967) as desirable, and these results tend to support him. However, from the standpoint

of practical utility of the thermal scanning technique, the requirement of total overcast represents a much more specialized set of environmental conditions than does the specification of time and air temperature, only. It is unlikely that the required equipment and personnel could be made available on a stand-by basis for an indefinite time period, waiting for cloud cover which is total, yet high enough to permit visual navigation.

Chapter IV

PHASE II: THERMAL SCANNING TESTS

EXPERIMENTAL PROCEDURE

Fort Collins Test

The Fort Collins test was preliminary to the more extensive Middle Park Test, and was conducted for the purpose of gaining experience in thermal scanner data acquisition and analysis to aid in the planning of the Middle Park Test. Although thermal characteristics of the scanned area were different from those studied in Phase I, the actual flying, scanning, and analysis procedures were similar.

The test occurred on August 20, 1971. A Bendix, Model 7M/LN-2-LW scanner, mounted in a North American Rockwell Aerocommander 500B, was flown over several deer holding pens just west of Fort Collins on the foothills campus of Colorado State University (Figure 31). Characteristics of the thermal scanner, as quoted by the manufacturer, were:

Instantaneous Angular Field of View (IFOV): 2.5 milliradians

Total Angular Field of View: 120°

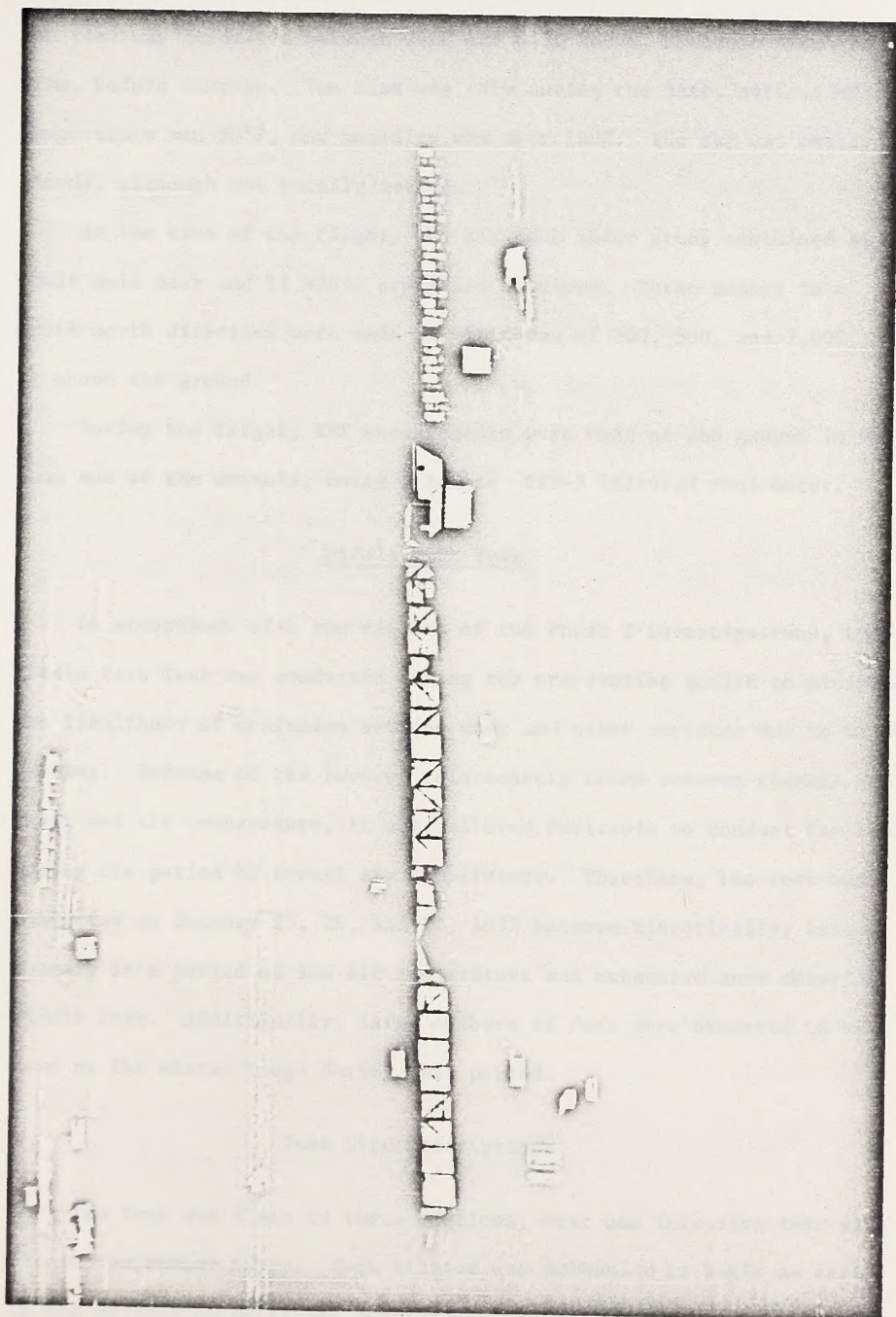
Detector: MCT (Mercury-Cadmium-Telluride)

Thermal Sensitivity: 0.2°C

Wavelength Response: 8.0 - 13.0 micrometers

Data Output Mode: 70 mm filmstrip

Figure 31.--Deer pens on the foothills campus at Colorado State University.



The test was conducted between 0400 and 0430 hours, Mountain Standard Time, before sunrise. The wind was calm during the test, surface air temperature was 56°F, and humidity was near 100%. The sky was mostly cloudy, although not totally overcast.

At the time of the flight, the six pens under study contained 55 adult mule deer and 11 adult pronghorn antelope. Three passes in a north-south direction were made at altitudes of 300, 500, and 1,000 ft above the ground.

During the flight, ERT measurements were made of the ground in the pens and of the animals, using a Barnes PRT-5 infrared radiometer.

Middle Park Test

In accordance with the results of the Phase I investigations, the Middle Park Test was conducted during the pre-sunrise period to minimize the likelihood of confusion between deer and other surfaces due to solar heating. Because of the inverse relationship found between thermal contrast and air temperature, it was believed desirable to conduct the test during the period of lowest air temperature. Therefore, the test was conducted on January 25, 26, and 27, 1972 because historically, late January is a period of low air temperature and extensive snow cover in Middle Park. Additionally, large numbers of deer were expected to be down on the winter range during this period.

Test Site Descriptions

The test was flown in three missions, over one intensive test site and two extensive sites. Each mission was scheduled to begin as early in the morning as possible, consistent with safe flying.

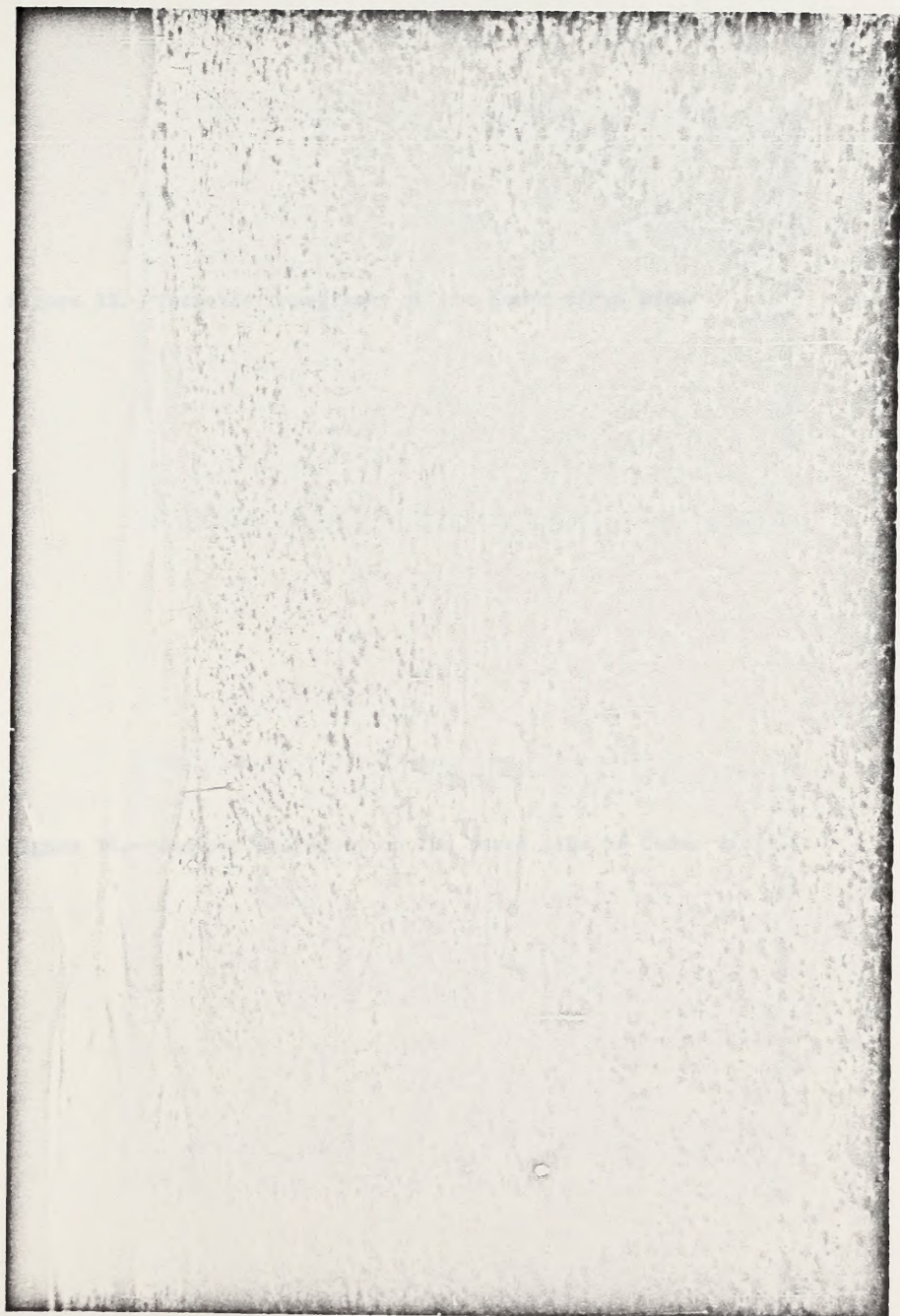
The intensive test area was near the location of the radiometric data acquisition in 1970, on the southwest slope of Junction Butte. A 330 X 610-ft deer enclosure, built by the Colorado Division of Game, Fish and Parks, was used to hold six tame mule deer, three bucks and three does, while the area was scanned. The deer, all 19 months old, weighed 90, 96, 116, 124, 152, and 155 pounds on the morning of the flight. They were put into the pen on January 19.

The first of the extensive sites flown was an area of about 2 square miles, along Jensen Creek, north of Parshall, Colorado (Figure 32). The area was selected because, historically, large numbers of mule deer concentrate on it during part of the winter (R. Bruce Gill, 1971, Private communication). Also, the area has little topographic relief (about 400 ft), compared to much of Middle Park, and there is no coniferous overstory. Most of the Jensen Creek area is open, slightly rolling terrain, characterized by sagebrush and other shrubby species, with a few small pockets of aspen (Populus tremuloides).

The largest of the two extensive sites was Cedar Ridge. This area, southwest of Parshall, is about 7 square miles in size, and is characterized by considerable topographic variation (Figures 33, 34). Elevation varies from approximately 7,600 to 8,400 ft. Bounded on the north by the Colorado River, on the south by a county road, and on the east by the Williams Fork River, the area was described by Gilbert and Grieb (1957) as follows:

"The terrain consists of high rolling ridges with numerous rocky outcrops. There are pockets of dense Douglas-fir (Pseudotsuga menziesii var. glauca) timber on the north-facing exposure and the south-facing

Figure 32.--Mule deer on a portion of the Jensen Creek extensive site.



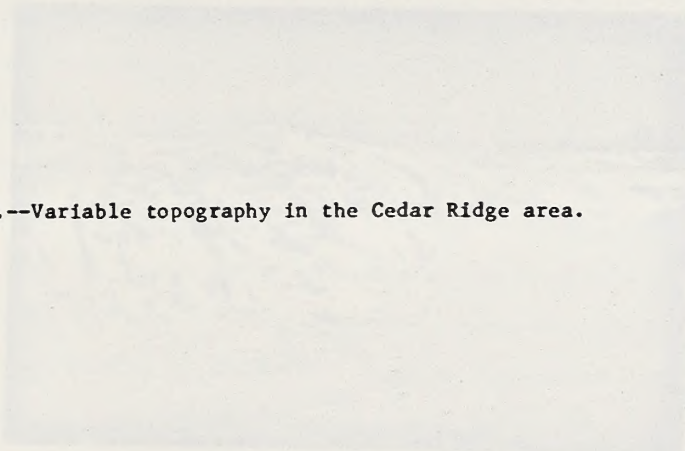


Figure 33.--Variable topography in the Cedar Ridge area.

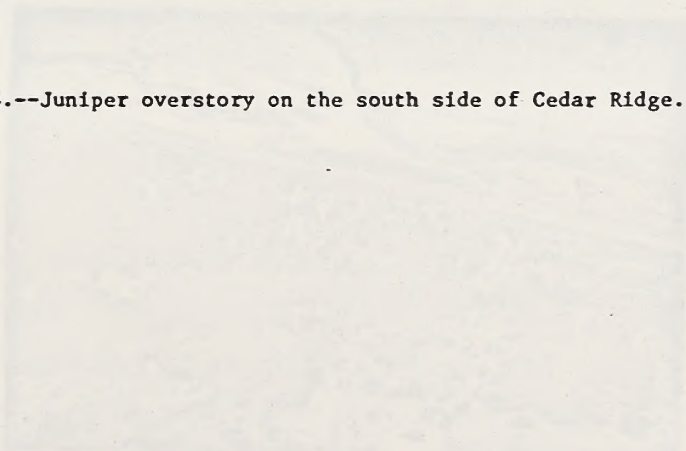
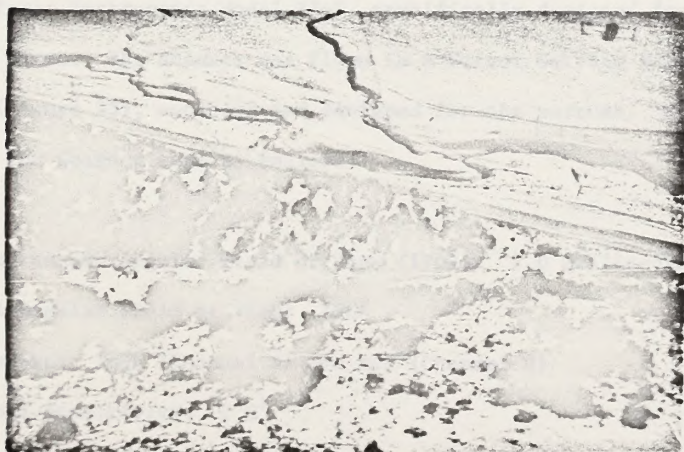
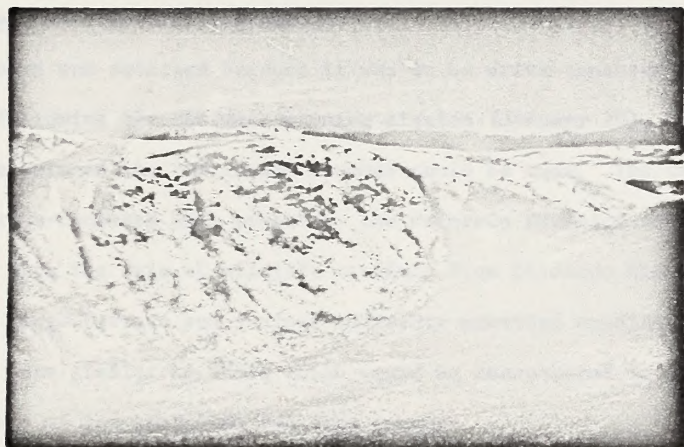


Figure 34.--Juniper overstory on the south side of Cedar Ridge.



slopes support sagebrush (Artemisia tridentata) with an open overstory of juniper (Juniperus monosperma). Patches of aspen (Populus tremuloides var. aurea) are scattered throughout."

The area was selected because it was to be drive-censused on the Saturday following the thermal scanning mission (January 29), and a comparison between the two census methods could be made. The Cedar Ridge area is drive-censused each winter by the Colorado Division of Game, Fish and Parks with the help of wildlife students from Colorado State University. Also, the rough terrain and juniper overstory provided conditions for testing which were similar to those which would be encountered in practical applications of the technique for deer census.

Equipment

The thermal scanner used was a Texas Instruments Model FFS-1, owned by the U.S.D.A. Forest Service, Region I, Missoula, Montana. It was a modified Texas Instruments Model RS-7, specifically designed for detection of forest fires. The scanner was flown in a Forest Service Beechcraft Kingair, (Figure 35), modified and equipped for the purpose. Characteristics of the scanner were as follows:

Instantaneous Angular Field of View (IFOV): 2.0 milliradians

Total Angular Field of View: 120°

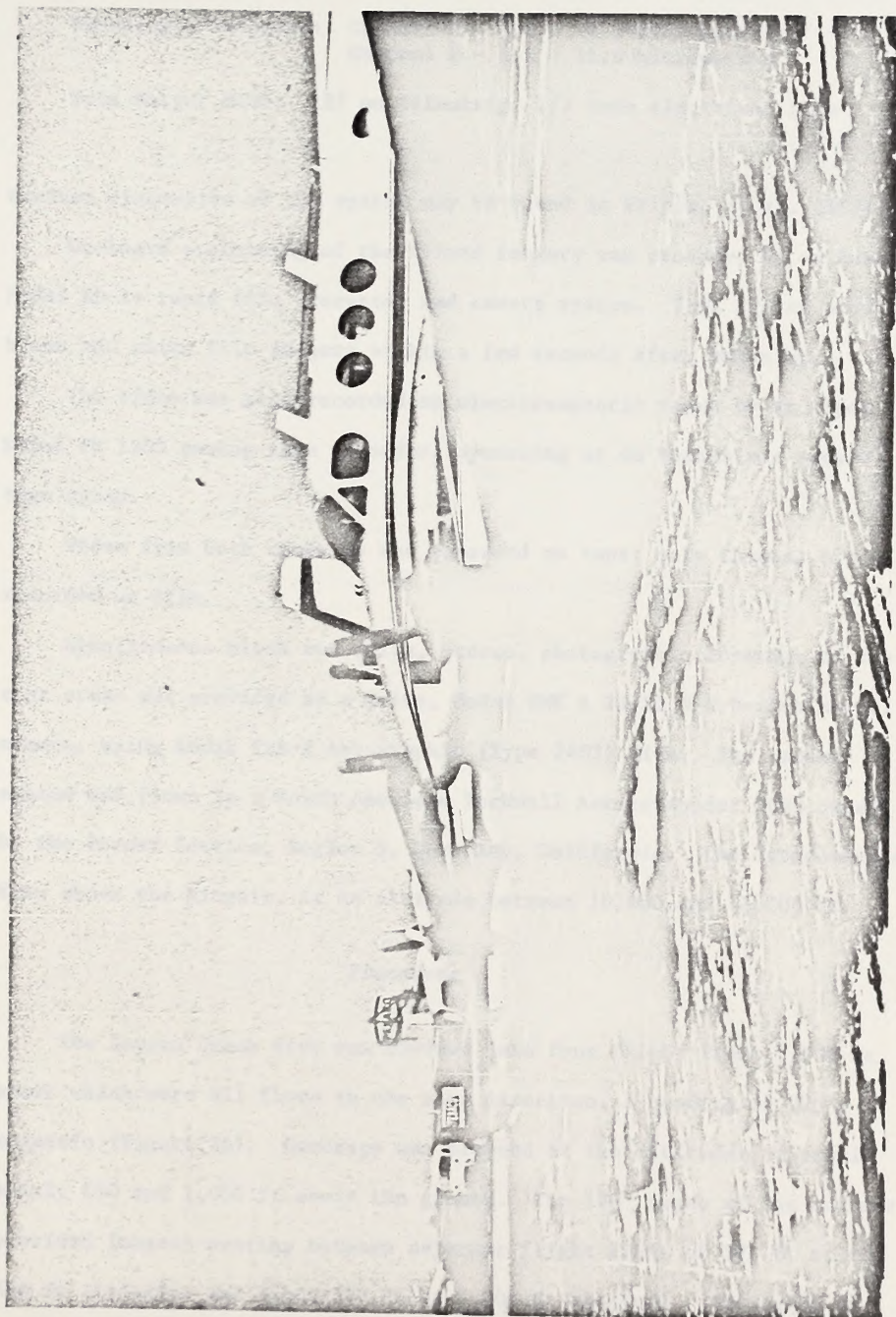
Detectors: InSb (Channel A) and MCT (Channel B)

Thermal Sensitivity: 2°C¹

Scanning Speed (t): .005 sec. per scan line

¹ System NET is 2°C with no overscan. With a 20x overscan, NET is 0.2°C.

Figure 35.--Forest Service Kingair (foreground) and Aerocommander.



Wavelength Response: Channel A - 3.0 - 4.1 micrometers
Channel B - 8.5 - 11.0 micrometers

Data Output Mode: 127 mm filmstrip, 1/2 inch electrical tape

Further discussion of the system may be found in Wilson, et al. (1971).

On-board processing of the filmed imagery was provided by an Ansco Model KD-14 rapid film processor and camera system. This system provides black and white film imagery within a few seconds after scanning.

The video was also recorded on electromagnetic tape, by an Ampex Model FR 1300 analog tape recorder, operating at 60 inches per second tape speed.

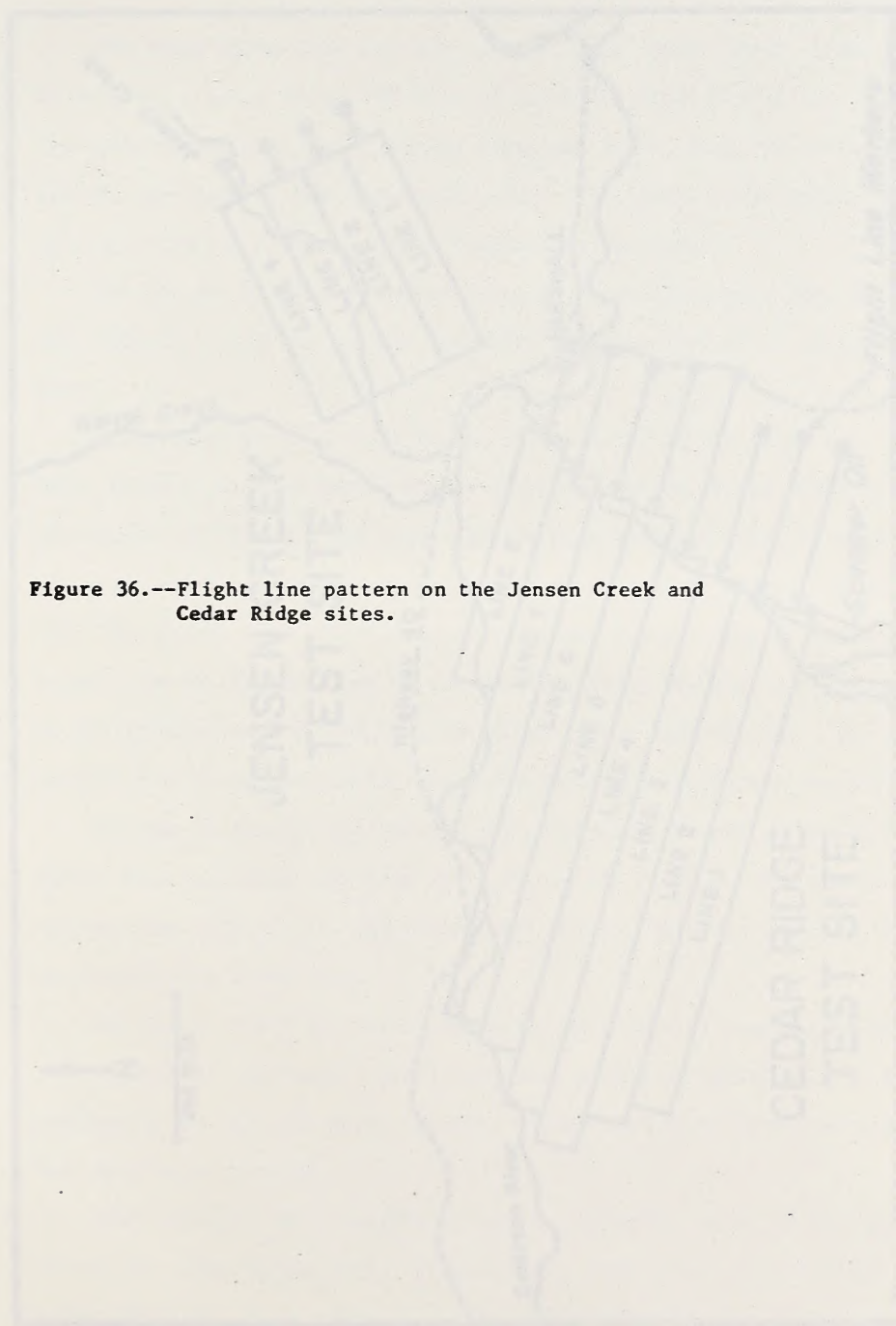
Video from both channels was recorded on tape; only Channel B was recorded on film.

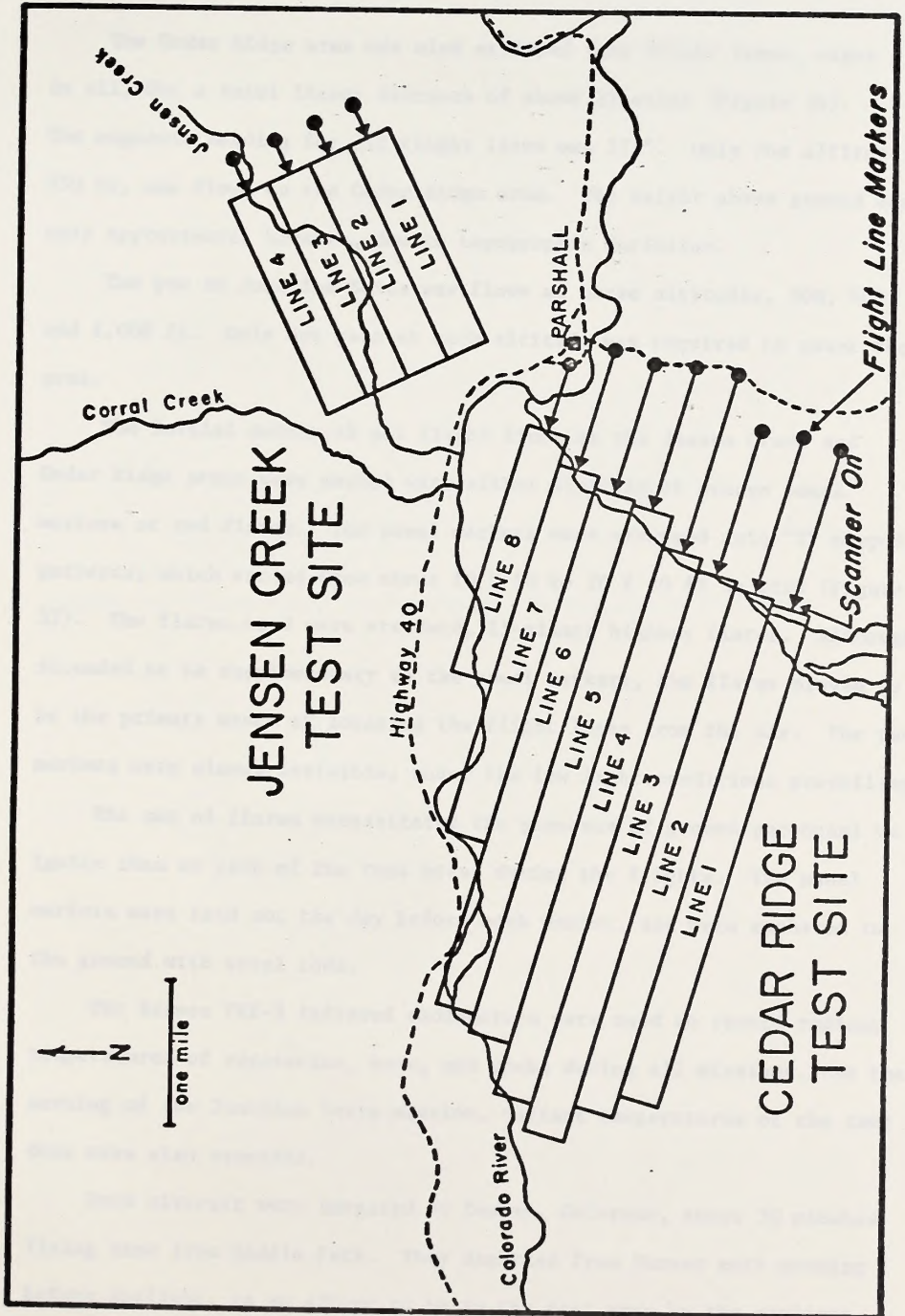
Simultaneous black and white, stereo, photographic coverage of the test areas was provided by a Zeiss, Model RMK A 21/23 9 X 9-inch aerial camera, using Kodak Tri-X Aerographic (Type 2403) film. The camera system was flown in a North American Rockwell Aerocommander 500B owned by the Forest Service, Region 5, Berkeley, California. The Aerocommander flew above the Kingair, at an altitude between 10,000 and 11,000 ft.

Procedure

The Jensen Creek area was divided into four flight lines 1,500 ft apart which were all flown in the same direction, a heading of 229°, magnetic (Figure 36). Coverage was planned at two altitudes, approximately 650 and 1,000 ft above the ground. The 120° sweep of the scanner provided imagery overlap between adjacent flight lines of 375 ft at the 650 ft altitude, and about 577 ft at 1,000 ft altitude. The 1,000 ft altitude was flown first, to minimize disturbance of deer in the area.

Figure 36.--Flight line pattern on the Jensen Creek and Cedar Ridge sites.





The Cedar Ridge area was also stripped into flight lines, eight in all, for a total linear distance of about 22 miles (Figure 36). The magnetic heading for all flight lines was 271°. Only one altitude, 650 ft, was flown on the Cedar Ridge area. The height above ground was only approximate, however, due to topographic variation.

The pen at Junction Butte was flown at three altitudes, 300, 600, and 1,000 ft. Only one pass at each altitude was required to cover the area.

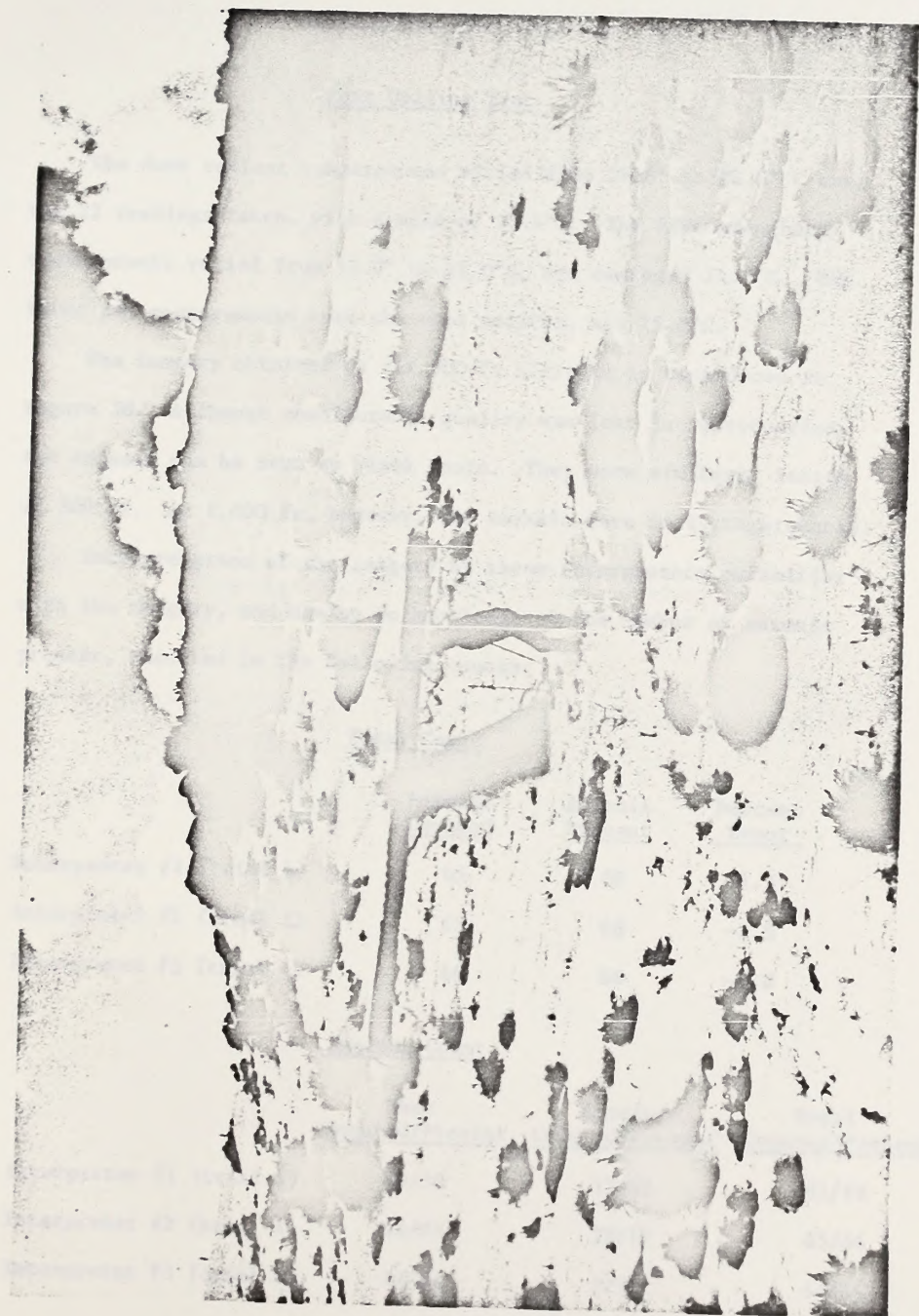
The initial points of all flight lines on the Jensen Creek and Cedar Ridge areas were marked with either fluorescent orange panel markers or red flares. The panel markers were arranged into "T" shaped patterns, which varied from about 10 X 10 to 20 X 20 ft in size (Figure 37). The flares used were standard, 15-minute highway flares. Although intended to be supplementary to the panel markers, the flares proved to be the primary means of locating the flight lines from the air. The panel markers were almost invisible, under the low light conditions prevailing.

The use of flares necessitated the presence of ground personnel to ignite them at each of the test areas during the flights. The panel markers were laid out the day before each mission, and were anchored to the ground with steel rods.

Two Barnes PRT-5 infrared radiometers were used to record radiant temperatures of vegetation, snow, and rocks during all missions. On the morning of the Junction Butte mission, radiant temperatures of the tame deer were also recorded.

Both aircraft were hangared at Denver, Colorado, about 30 minutes flying time from Middle Park. They departed from Denver each morning before daylight, in an effort to be in the test area by the earliest possible flying time.

Figure 37.--Fluorescent panels marking initial points on flight lines.



RESULTS AND DISCUSSION

Fort Collins Test

The deer radiant temperatures varied from 21.0° to 26.0° C over the 12 readings taken, with a mean of 23.4°C. The five pronghorn measurements varied from 19.0° to 23.0°C, and averaged 21.0°C. The three pen measurements were the most uniform, all 15.0°C.

The imagery obtained at the 500-ft altitude is reproduced in Figure 38. Although considerable quality was lost in reproduction, the animals can be seen as black spots. They were similarly imaged at 300 ft. At 1,000 ft, however, the animals were indistinguishable.

Interpretation of the imagery by three interpreters unfamiliar with the imagery, and having no knowledge of the number of animals present, resulted in the following counts:

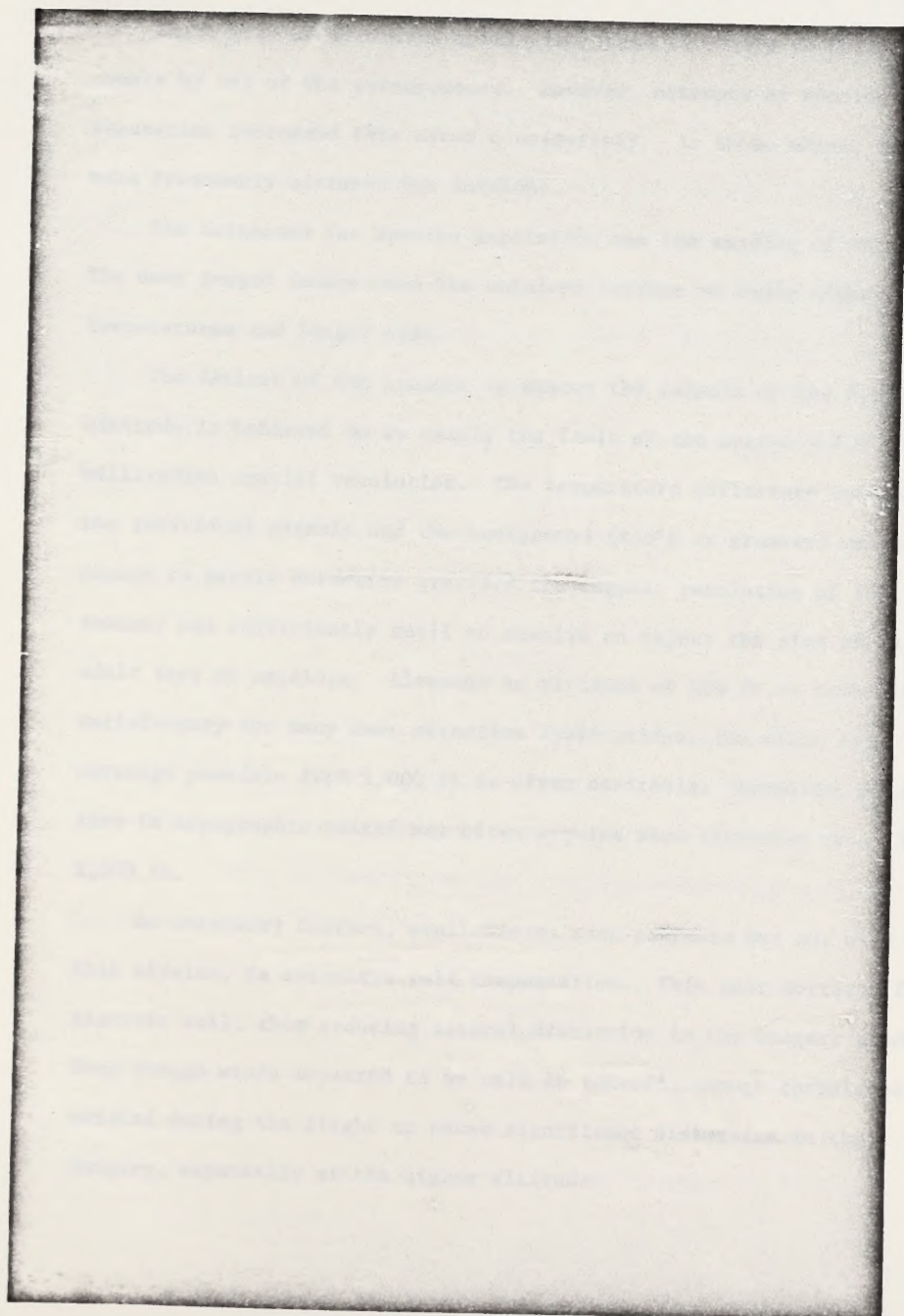
Total Count

	<u>Animals Counted</u>	<u>Animals Present</u>	<u>Percent Error</u>
Interpreter #1 (trial 1)	65	66	-1.5
Interpreter #2 (trial 1)	65	66	-1.5
Interpreter #3 (trial 1)	64	66	-3.0

Species Count

	<u>Deer Counted/Present</u>	<u>Antelope Counted/Present</u>	<u>Total Counted/Present</u>
Interpreter #1 (trial 2)	49/55	12/11	61/66
Interpreter #2 (trial 1)	42/55	23/11	65/66
Interpreter #3 (trial 1)	47/55	17/11	64/66

Figure 38.--Thermal imagery of deer in pens on Colorado State University foothills campus (enlarged approximately 11 times).



There were no errors of commission (type II error) in total counts by any of the interpreters. However, attempts at species separation increased this error considerably. As shown above, deer were frequently mistaken for antelope.

The criterion for species separation was the shading of the spots. The deer imaged darker than the antelope because of their higher temperatures and larger size.

The failure of the scanner to detect the animals at the 1,000-ft altitude is believed to be mainly the fault of the system's 2.5 milliradian spatial resolution. The temperature difference between the individual animals and the background (4.0°C or greater) was great enough to permit detection provided the angular resolution of the scanner was sufficiently small to resolve an object the size of an adult deer or antelope. Although an altitude of 500 ft is probably satisfactory for many deer detection applications, the wider area coverage possible from 1,000 ft is often desirable. Moreover, fluctuation in topographic relief may often require mean altitudes of at least 1,000 ft.

An accessory feature, available on most scanners but not used on this mission, is automatic roll compensation. This unit corrects for aircraft roll, thus reducing lateral distortion in the imagery produced. Even though winds appeared to be calm at takeoff, enough turbulence existed during the flight to cause significant distortion in the imagery, especially at the higher altitudes.

Middle Park Test

Radiant Temperatures

The most comprehensive set of ERT data was obtained at the Junction Butte site on January 26. These measurements, on snow, vegetation, bare soil, and tame deer, were made between 6:00 and 6:30 a.m. (Table 5). Thermal contrast between deer and sagebrush (ΔT_g) averaged 1.6°C , with a minimum potential ΔT_g of 0.5°C . Average ΔT_n (deer vs. snow) was 6.9°C , and average ΔT_{soil} was 4.0°C . Air temperature was 1°C .

Radiometer malfunction rendered ERT measurements on the Jensen Creek and Cedar Ridge sites unusable.

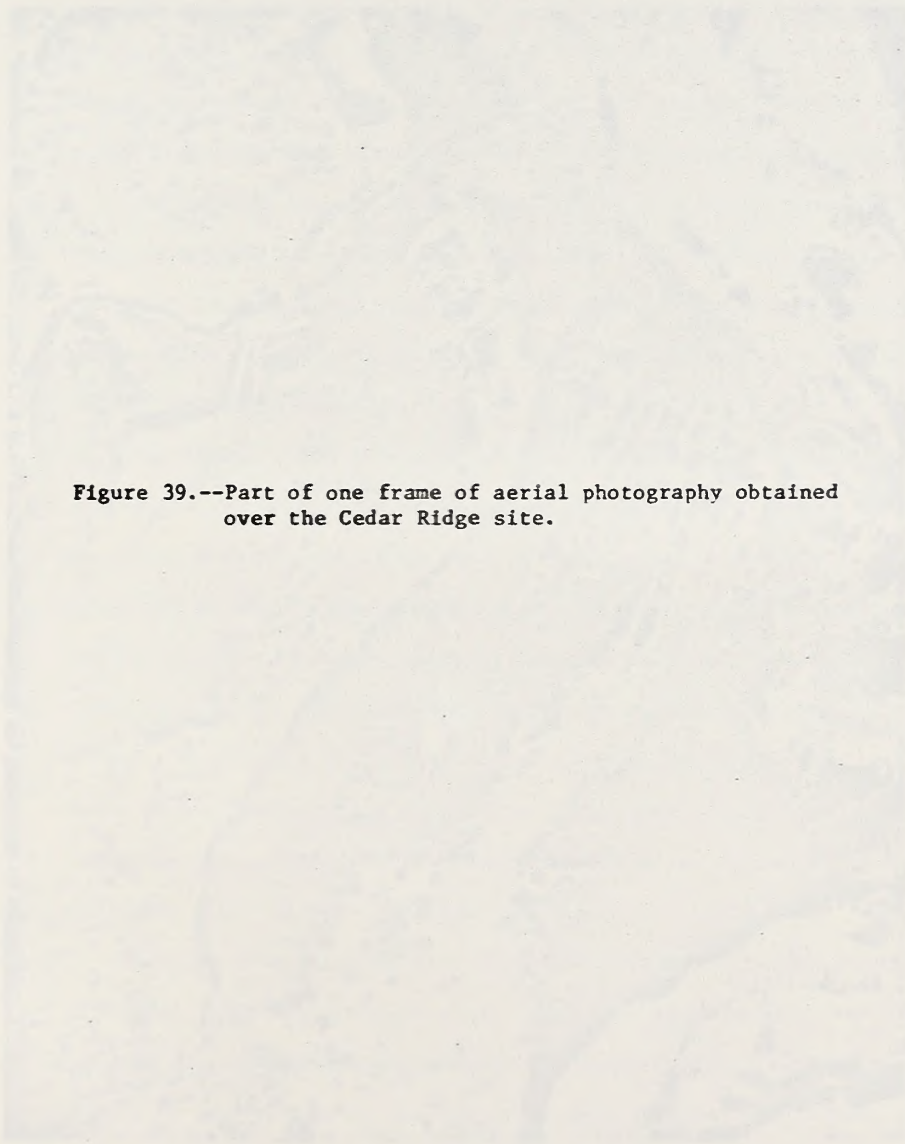
Aerial Photography

A portion of one frame of the aerial photography is shown in Figure 39. It is one of the better frames; much of the photography was incorrectly exposed. The photographic scale varied from about 1:3000 to 1:5000, as camera-to-ground distance varied with terrain elevation. Flight altitude of the Aerocommander was constant at 10,050 ft on the Jensen Creek site, and 10,800 ft over Cedar Ridge.

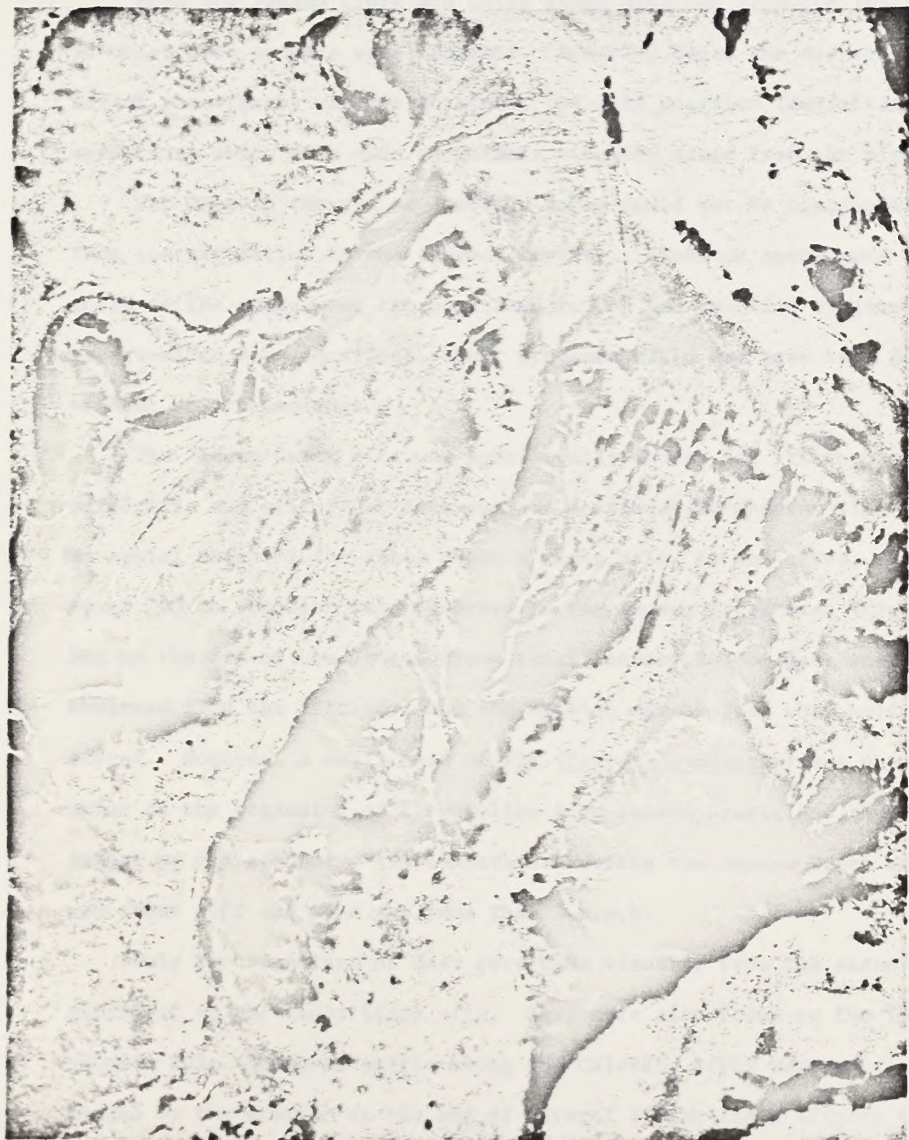
The photographic scale was inadequate to visually detect deer in the photos, under the prevailing low light conditions. Neither could cattle present along the Colorado River be seen. Scale, however, was near the minimum of 1:5000 in the low areas bordering the river.

Table 5.--ERT measurements at Junction Butte on January 26, 1972,
6:00 a.m.

Snow	ERT (°C)		
	Vegetation	Bare Soil	Tame Deer
-9.0	-3.5	-2.0	-2.5
-9.0	-3.0	-7.0	-2.5
-9.0	-3.5	-6.5	-1.0
-9.5	-3.0	-6.5	-2.0
-9.0	-3.5	-6.0	
-9.0	-5.5	-7.0	
-8.5	-4.0	-7.0	
-8.5	-3.0		
Mean = -8.9	Mean = -3.6	Mean = -6.0	Mean = -2.0



**Figure 39.--Part of one frame of aerial photography obtained
over the Cedar Ridge site.**



Thermal Imagery

Both the Jensen Creek and Cedar Ridge missions produced imagery in which some animals were apparent. However, since the corroborating aerial photography was not obtained, the only positive identifications were those which were made on animals visually noted from the aircraft.

The deer in the pen at Junction Butte could not be distinguished from the vegetation in the thermal imagery. Although spots were noted in the imagery at the positions in the pen recorded by ground observers as deer locations, their presence would not have been detected without prior knowledge.

The Jensen Creek site was specifically chosen for its topographic uniformity and history of deer use, as mentioned in Chapter III. During an aerial check of the sites about 6 weeks prior to the tests, an estimated 200 to 300 deer were observed in the Jensen Creek area (Figure 32). But on the day of the Jensen Creek test, January 26, no deer were observed from the aircraft, and the mission was aborted when half completed. However, a small band of elk (Cervus canadensis) was seen just prior to the beginning of flight line 4 on Jensen Creek, and they were imaged by the scanner. Air temperature during the Jensen Creek mission was about -6°C and wind was less than 5 m.p.h.

Only two sightings of deer were made visually from the scanning aircraft, on the Cedar Ridge site. They were also found on the imagery (Figure 40). Numerous cattle along the Colorado River were successfully imaged by the scanner at the end of several flight lines (Figure 41).

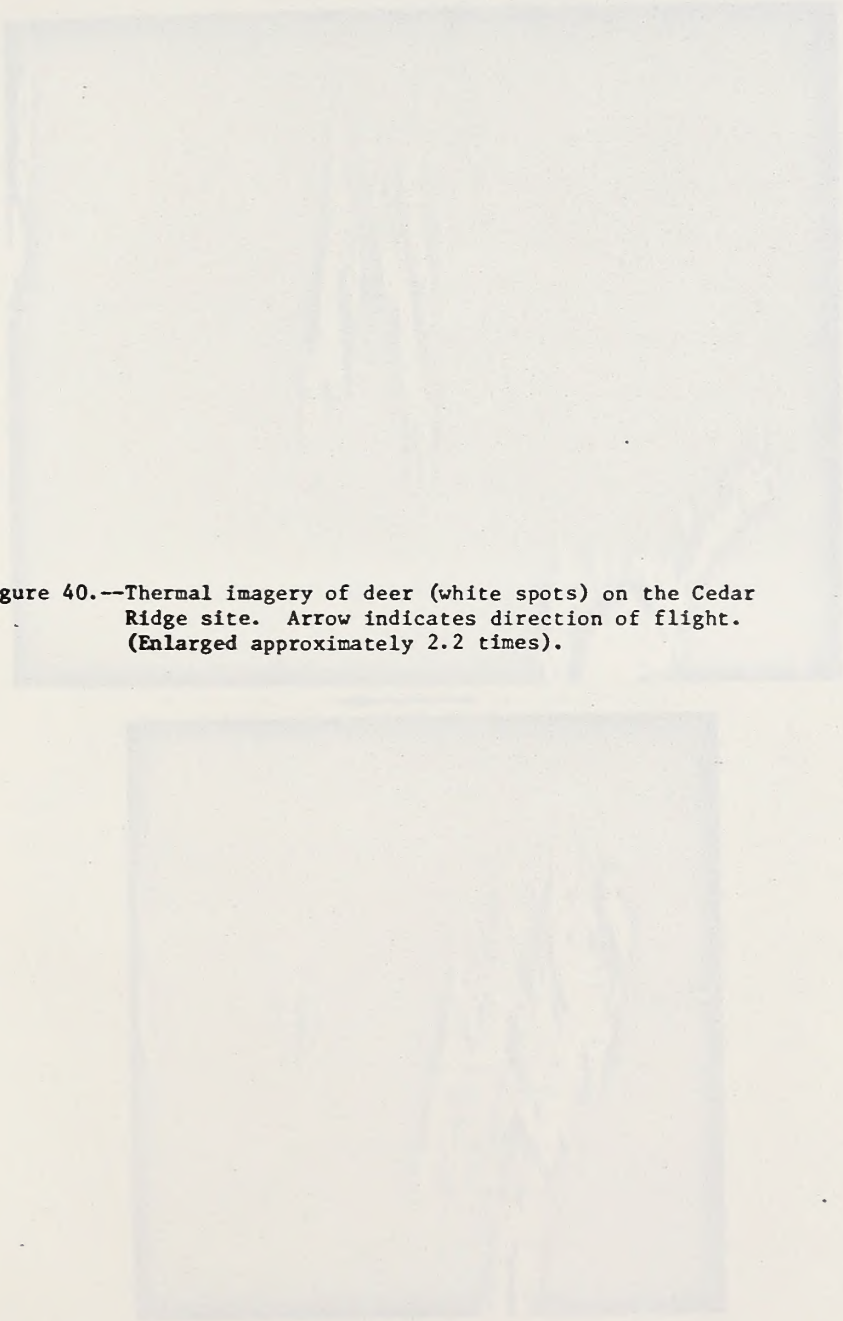
The image consists of two large, rectangular, light gray areas stacked vertically, representing thermal imagery. These areas are very faded and lack detail, appearing as uniform light gray blocks. The caption text is positioned between these two blocks.

Figure 40.--Thermal imagery of deer (white spots) on the Cedar Ridge site. Arrow indicates direction of flight. (Enlarged approximately 2.2 times).

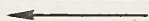
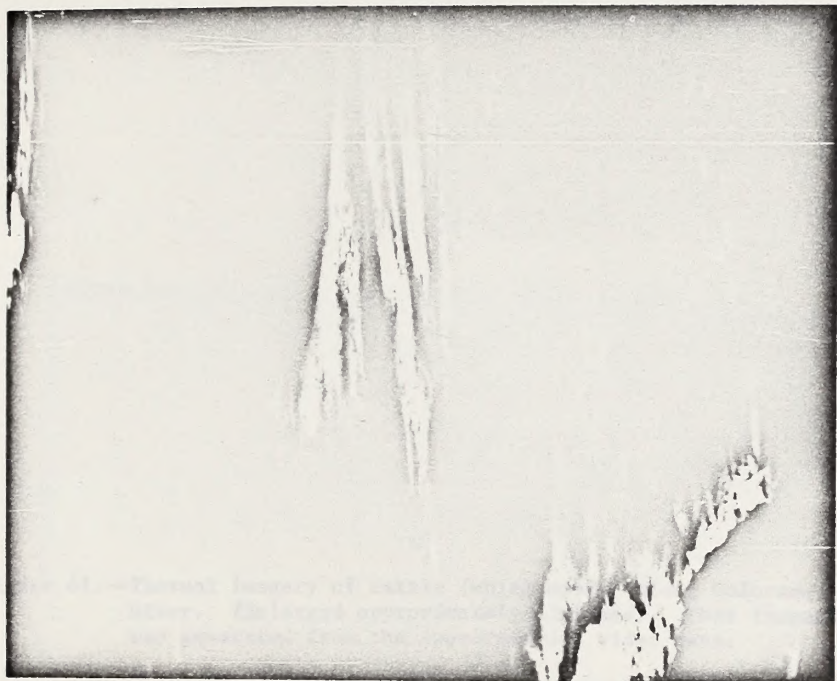
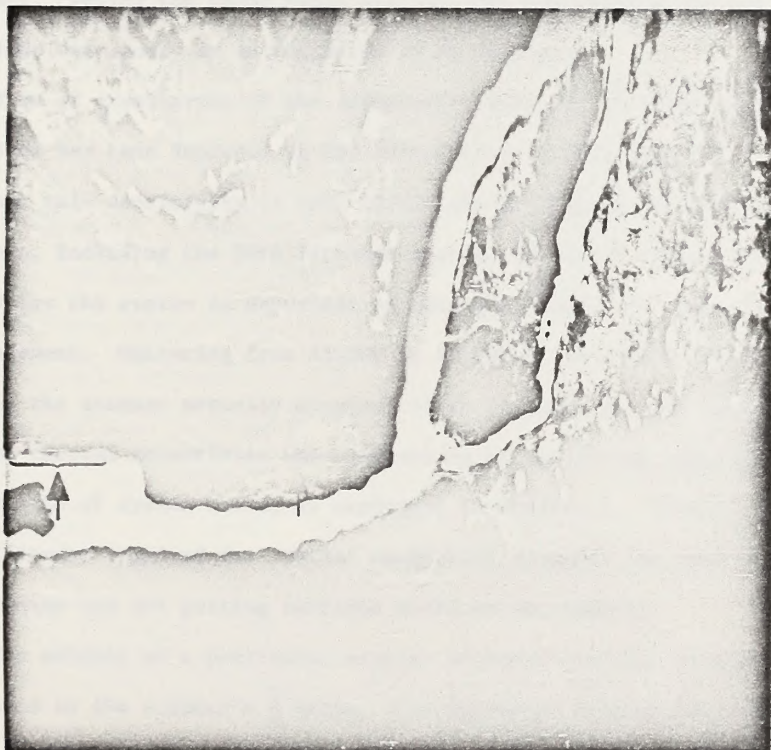


Figure 41.--Thermal imagery of cattle (white spots) along Colorado River. (Enlarged approximately 2.2 times). This imagery was generated from the tape-recorded video data.



Again, since no photography was available to compare with the thermal imagery, there was no way of knowing how many deer were actually detected by the scanner. Many spots were apparent in the Cedar Ridge imagery which could have been deer. The drive census by the Colorado Game, Fish and Parks Division on January 29, produced a count of about 480 deer. During the Cedar Ridge mission, air temperature was -5°C , and winds were gusty at an estimated 10 to 20 m.p.h.

From an examination of the radiometric data, it is clear that detection may have depended on ERT differences of less than 2°C . Although this sensitivity is well within the capability of most modern scanners, including the USFS Firescan System, the 0.5°C resolution quoted for the system is dependent on multiple "looks" at each resolution element. Operating from 15,000 to 20,000 ft as a fire detection system, the scanner normally obtained 15 to 20 looks at each element, and the thermal sensitivity was enhanced by virtue of the statistical integration of system noise, as explained in Chapter I. However, at the low altitudes required for spatial resolution adequate for deer detection, the scanner was not getting multiple looks at the terrain.

The ability of a particular scanner to obtain terrain overscan is expressed by the scanner's $\frac{V}{H}$ ratio, a relationship between aircraft speed, scanning speed, altitude, and IFOV. Since scanning speed (t) and IFOV (β) are constant in most scanners, equation 3 from page 19, may be rearranged to indicate the constancy of $\frac{V}{H}$.

$$Vt = \beta h$$

$$\frac{V}{H} = \frac{\beta}{t} \quad (25)$$

Therefore, the minimum altitude (H) for contiguous scanning is a function of aircraft groundspeed (V). For the Forest Service Firescan system, $\frac{V}{H}$ is 0.4. Using 120 knots as the minimum safe airspeed for the Kingair, the minimum altitude for contiguous coverage is about 591 ft. Put in terms of terrain overscan, 591 ft was the altitude at which overscan was equal to zero. Similarly, there was no underscanning. Although more altitude was desirable to obtain overscan, the spatial resolution consideration was believed more important than thermal sensitivity, and the test was flown at the lowest altitude commensurate with safety and total ground coverage. To allow for error in V and H, 650 ft was the planned primary altitude.

Thermal sensitivity of the firescan system with no overscan was 2.0°C (Wilson, et al., 1971). Therefore, a deer would have to have been at least 2.0°C above the temperature of the background materials around him to have been detected.

Since, on the Junction Butte site, both deer and vegetation ERT's were greater than 2°C above snow ERT, both were imaged against the snow background, but they could not be separated in the imagery.

Although no terrain overlap was achieved, scan-line overlap did occur in the on-board film imagery. The exact amount of overlap varied with scanner-to-ground distance. But, from 2 to 4 scan-lines were estimated to have been "stacked up" on the imagery. This overlap resulted

not only in longitudinal compression of the imagery, but also tended to mask some of the deer imaged, with the images of vegetation and other surfaces which may have been near deer temperature, on adjacent scan lines.

To understand this effect, it is necessary to examine the relationships between film transport speed, aircraft speed and scanning speed. For this purpose, another $\frac{V}{H}$ ratio in terms of the film transport system, must be considered. The $\frac{V}{H}$ ratio defined previously referred to the scanner speed, and the ability of the scanner to cover the terrain. Unlike the scanner $\frac{V}{H}$ ratio, film $\frac{V}{H}$ is usually variable, by virtue of operator control over film transport speed. The range of the film $\frac{V}{H}$ ratio expresses the speed latitude of the film transport system, and therefore its capability to produce undistorted imagery over a range of data input rates.

The $\frac{V}{H}$ range of the Forest Service firescan system film transport was 0.6 to 65.0, where V is aircraft groundspeed in knots, and H is altitude in thousands of ft. Using 120 knots for V and 0.65 as H in $\text{ft} \times 10^{-3}$,

$$\frac{120}{.65} = 184.6 \quad (26)$$

Or, a $\frac{V}{H}$ of 184.6 would have been required to obtain imagery in the correct aspect ratio at an altitude of 650 ft. Conversely, with a $\frac{V}{H}$ limitation of 65, each scan line on the ground was superimposed on top of about two others in the film imagery. Thus, longitudinal compression averaged approximately 1:3 along the flight lines. This figure is not

exact for all the imagery because of variation in H due to variable terrain relief, and variation in aircraft groundspeed.

Where the deer were considerably warmer than their surroundings, as against a snow background, this overlap did not seriously affect their detectability because of considerable gray-scale contrast between deer and snow on the film. However, when the animals were located amidst vegetation or rocks, the small thermal contrast which existed was not evident in the imagery.

Realizing that an unknown number of animals could have been masked by the superimposition of other surface images, some of the tape-recorded video was converted to film imagery with the aid and equipment of National Aeronautics and Space Administration personnel at the Manned Spacecraft Center, Houston, Texas. Their tape-to-film conversion equipment allowed video reproduction in the proper aspect ratio, and provided means for adjusting gain and intensity to enhance any portion of the gray scale. Unfortunately, however, other problems were encountered in this process.

The video tape record was recorded on an Ampex FR-1300 recorder, in the direct mode, at 60 inches per second tapespeed. Synchronization pulses, roll gate, and audio were recorded FM. The bandwidth range of the FR-1300 in direct record, was 300 hz to 300 Khz. The highest potential frequencies which could have been generated by the scanner were within the recording range of the FR-1300. But the lowest frequency generated in the video signal was about 200 hz, the number of scan lines generated each second. The 300 hz limitation of the recorder resulted

in a variable, increasing voltage reference level from the beginning to the end of each scan line. Therefore, the film imagery had an artificial gradation in image density laterally across the flight lines. Due to the very small gray shading difference between the deer and some background materials, this gradation caused the deer images to be difficult or impossible to see in the film. As a result, the original imagery produced in flight was, overall, the best imagery obtained.

Chapter V

OVERALL CONCLUSIONS

Based on the results of both phases of this study, thermal scanning for wild deer detection remains a feasible technique. But, its effectiveness will vary with the sophistication of the scanning and data analysis equipment used, in relation to the physical characteristics of topography and thermal environment, of the area under investigation.

It is clear that large thermal contrasts may not be depended on, under the conditions studied. However, there is little doubt that, on the average, the animals' surfaces will be warmer than their backgrounds, at least by a small margin. Therefore, a scanning system which can differentiate between targets of small (0.5° to 1.0°C) thermal contrast at relatively low absolute temperatures ($250\text{--}275^{\circ}\text{K}$), may be required. The success of the Fort Collins test was believed due mainly to the uniform background temperatures and the 6 to 9°C thermal contrast which existed between the animals and the background. Such large ΔT 's were not encountered, nor would they be expected in a cold winter environment according to the radiometric data from Phase I. The Fort Collins test results, considered in light of the seasonal variation in fasting metabolic rate reported by Silver et al. (1969) (page 36), suggest the possibility that greater thermal contrast may exist in summer, despite warmer background temperatures. Further study

may therefore show that the summer season affords better conditions for detection of species such as the pronghorn antelope, which inhabit open areas of little tree overstory.

However, practical application of thermal scanning for deer census imposes the constraints of area coverage and limited overstory which preclude summer censusing. Therefore, at least in Colorado, the thermal characteristics of deer and their background on winter range must be the basis on which scanning system requirements are specified.

In elaborating the requirements of a scanning system which would be required to detect deer under natural conditions similar to those of the Cedar Ridge test, it is important to consider the interactions and technological trade-offs which are inherent in thermal scanner design. Specific engineering details of such a system are beyond the scope of this study. But, some system parametric requirements are apparent from the Phase II results.

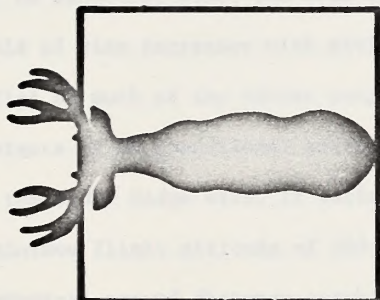
The relationship between thermal sensitivity and spatial resolution was explained in Chapter I. The Kremmling Test afforded an opportunity to see the impact of this relationship in a real situation, where the images of rock and vegetation were frequently as dark (light in the positive prints), as were deer images, even though the deer were probably warmer (Table 5, page 149).

The importance of spatial resolution can be seen in figure 42, where the contribution of deer ERT to resolution element ERT is depicted. As shown, reduction in resolution element size (increase in spatial resolution), improves the effective thermal contrast between the animal and its surroundings, as seen by the scanner. In the Kremmling test,

Figure 42.--The contribution of deer ERT to integrated resolution element ERT, as a function of the instantaneous angular field of view (IFOV).

a)

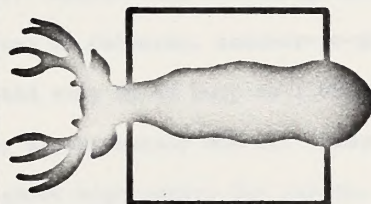
IFOV = 30 MILLIRADIANS



	DEER	BACK-GROUND	RESOL. ELEMENT
AREA	2.1 FT ²	6.9 FT ²	9 FT ²
ERT	8° C.	4° C.	4.5° C.

b)

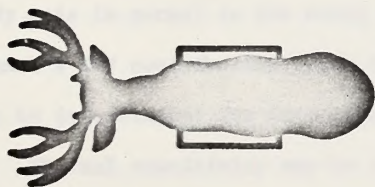
IFOV = 20 MILLIRADIANS



	DEER	BACK-GROUND	RESOL. ELEMENT
AREA	2.1 FT ²	1.9 FT ²	4 FT ²
ERT	8° C.	4° C.	5.5° C.

c)

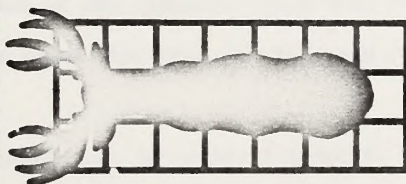
IFOV = 10 MILLIRADIANS



	DEER	BACK-GROUND	RESOL. ELEMENT
AREA	0.8 FT ²	0.2 FT ²	1.0 FT ²
ERT	8° C.	4° C.	7.2° C.

d)

IFOV = 0.5 MILLIRADIANS



	DEER	BACK-GROUND	RESOL. ELEMENT
AREA	0.8 FT ²	0.2 FT ²	1.0 FT ²
ERT	8° C.	4° C.	7.2° C.

patches of vegetation, rock and bare soil appeared to be as warm or warmer than the deer because of their larger horizontal areas. Their contribution to resolution element ERT may have been greater because of their greater area - not because of higher temperatures.

Spatial resolution also limits the altitude from which animals may be detected, since the area subtended by the instantaneous angular field of view increases with altitude. Considering the topographic relief of much of the winter range area in Colorado, scanner-to-ground distance of an operational system could vary by as much as 1,000 ft. On the Cedar Ridge site, it varied by approximately 800 ft. Added to a minimum flight altitude of 500 ft above high points for safety, scanner-to-ground distance reaches a potential of 1,500 ft at the nadir. For off-nadir points, the distance is even greater.

Another aspect of the spatial resolution problem concerns the orientation of the animals relative to the scan lines. Resolution element size should be small enough to be filled by an animal whose long body axis is normal to the sweep plane of the scanner. Otherwise the animal's ERT contribution, when integrated with that of its background, may be insufficient for detection.

Thermal sensitivity may be considered as inversely related to spatial resolution, since improvement of one degrades the other. This relationship exists as a function of the incident radiation which is required to produce a response by the detector above the system noise level. The amount of radiation incident on a detector at constant altitude, from a surface of constant temperature, varies directly with the solid angle through which the surface is observed (IFOV). Thus, a

larger IFOV allows more emitted energy to impinge on the detector surface and produces a greater response. The difference in detector response between surfaces of different temperature is not, however, of constant proportion as IFOV decreases. In other words, as IFOV decreases, detector response per unit energy (photons), decreases, and the flux density of energy required to produce a video signal above the noise level, increases. This means that, as IFOV is decreased, a surface temperature limit is approached below which a target of constant temperature cannot be detected, regardless of the magnitude of the existing thermal contrast. A similar effect is caused by increasing scanner-to-ground distance. Although resolution element size increases with altitude, the resulting increase in radiation at the detector is linear, whereas the decrease in flux density is exponential, by virtue of the inverse-square law (Appendix A). For these reasons, a combination of spatial resolution and thermal sensitivity which is optimized for a specific detection purpose may not embody the best of either parameter.

The minimum ΔT which can be detected is also a function of the absolute temperatures of the target and background. For example, a ΔT of 0.5°C from 25.0° to 25.5°C is more easily detected than the same ΔT from 0° to 0.5°C . Batuschek (1970) presents an excellent discussion of this relationship.

The dwell time of radiation on the detector surface is also important, since the detector responds to power fluctuations. Dwell time can be increased by slowing the speed of the scan mirror shaft, but then the advantages of overscanning may not be realized. Overscan may be improved by the use of more scan mirrors, but then dwell time decreases.

Exactly how a thermal scanner optimized for deer detection should be designed is an engineering problem of no small magnitude. The complexity of determining how well a thermal scanner will perform on a specific detection problem prompted Batuschek (1970) to make the following observation:

"In many instances, the imagery obtained during a particular data collection flight is usable for the intended purpose almost by chance."

However, based on the results of this study, two requirements may be stated:

- 1) Spatial resolution should be at least 6" at 1,000 ft.

(IFOV = 0.5 milliradians)

- 2) Thermal sensitivity should be 0.5°C

These stringent requirements are intended to apply to a thermal scanner for general use over rough terrain, where a non-uniform background exists. Over complete snow cover, with little or no relief, they could be relaxed considerably.

Overall, this study shows there is thermal contrast between mule deer and their surroundings, but that the large ΔT 's which may be intuitively suggested do not exist, under the conditions studied. There is little doubt that deer could be reliably detected against a complete snow background. However, this requirement limits the technique considerably, since total snow cover of all terrain features is a rare occurrence in most temperate regions, because of protruding rocks and vegetation. From the practical standpoint then, successful deer detection

hinges on the capability of the scanner to detect small ERT differences, and at present, on the ability of the imagery interpreter to discriminate between surfaces imaged.

It should be understood, however, that thermal scanners now exist which can detect such small contrasts, and that the interpretation problem is temporary, only. The fact that deer could not be discerned in some of the Phase II imagery can only be attributed to shortcomings in the equipment. Albeit small, thermal contrast did exist, and there is no reason to believe a more sophisticated scanner could not have detected it.

Stingelin (1968) said, "...unclassified scanning systems remain far behind the state-of-the-art in infrared imaging technology...." Today, state-of-the-art systems, including multiple detector and forward-looking infrared (FLIR) devices, remain beyond the reach of most users.

But if, as this study indicates, exploitable natural radiation phenomena do exist, then technological improvements coupled with a continued research effort can only result in eventual success in the application of remote sensing to large animal inventory. Anyone who would doubt the importance of that effort, need only review game management history, and realize that the need for management information is not quelled by its lack.

"Sheep, goats and domestic cattle on the open range can be counted through a gate. Even buffalo on the wildlife refuges can be herded and enumerated accurately. But how is one to tally so wild and nervous an animal as the mule deer? For the deer must be counted, or at least some adequate approximation to numbers arrived at, before one can think seriously of management It is hoped and altogether likely, that more effective methods can and will be developed in the future...."

- Taylor, 1956

LITERATURE CITED

- Banfield, A. W. F., D. R. Flook, J. P. Kelsall, and A. G. Loughrey. 1955. An aerial survey technique for northern big game. Trans. N. Am. Wildl. Conf. 20: 519-523.
- Batuschek, C. P. 1970. Ground temperature and thermal infrared. Photogramm. Eng. 36(10): 1064-1072.
- Bear, G. D. 1970. Evaluation of aerial antelope census technique. Colo. Div. Game, Fish and Parks. Game Inf. Leaflet. 69.
- Bergerud, A. T., and F. Manuel. 1969. Aerial census of moose. J. Wildl. Manage. 33(4): 910-916.
- Birkebak, R. C. 1966. Heat transfer in biological systems. Int. Rev. Gen. and Exp. Zool. 2: 269-344.
- Blaxter, K. L., N. McGraham, F. W. Wainman, and D. G. Armstrong. 1958. Environmental temperature, energy metabolism and heat losses in sheep. II. The partition of heat losses in sheep. J. Agric. Sci. 62(1): 25-40.
- Bligh, J. D., L. Ingram, R. D. Keynes, and S. G. Robinson. 1964. The deep body temperature of an unrestrained Welsh Mountain sheep recorded by a radiotelemetric technique during a 12 month period. J. Physiol. 176: 136-144.
- Bligh, J., and A. M. Harthoorn. 1965. Continuous radiotelemetric records of the deep body temperature of some unrestrained African mammals under near-natural conditions. J. Physiol. 176: 145-162.
- Brockway, J. H., and G. M. O. Maloiy. 1967. Energy metabolism of the red deer. J. Physiol. 194: 22-24.
- Brooks, F. A. 1959. An introduction to physical microclimatology. Davis, Calif.: Assoc. Students Store. 264 p.
- Cain, S. A. 1966. Current and future needs for remote sensor data in ecology. Proc. 4th Symp. Rem. Sens. Environ. April 12, 13, 14. Ann Arbor, Mich. 871 p.
- Croon, G. W. 1967. The application of infrared line scanners to big game inventories. Univ. Mich. 36 p.

- Croon, G. W., D. R. McCullough, C. E. Olson, Jr., and L. M. Queal. 1968. Infrared scanning techniques for big game censusing. *J. Wildl. Manage.* 32(4): 751-759.
- Evans, C. D., W. A. Troyer and C. J. Lensink. 1966. Aerial census of moose by quadrat sampling units. *J. Wildl. Manage.* 30(4): 767-776.
- Eyal, E. 1963. Shorn and unshorn Awassi sheep. I. Body temperature. *J. Agric. Sci.* 60: 159-168.
- Frank, E. C., and R. Lee. 1966. Potential solar beam irradiation on slopes: Tables for 30° to 50° latitude. U.S.D.A. Forest Serv. Pap. RM-18. Rocky Mt. Forest and Range Exp. Stn., Fort Collins, Colo. 115 p.
- Franzmann, A. W., and D. M. Hebert. 1971. Variation of rectal temperature in bighorn sheep. *J. Wildl. Manage.* 35(3): 488-494.
- Frayer, W. E. 1968. Snoop: A computer program for 2- and 3-dimensional plotting. U.S.D.A. Forest Serv. Res. Pap. NE-91. Northeast. Forest Exp. Stn., Upper Darby, Pa. 24 p.
- Garvin, L. E., F. D. Beatty, and A. J. Zanon. 1964. Infrared detection of moose. Interp. and Anal. Sect., Rome Air Dev. Cent. 40 p.
- Gates, D. M. 1961. Winter thermal radiation studies in Yellowstone Park. *Science* 134: 32-35.
- Gates, D. M. 1962. Energy exchange in the biosphere. New York: Harper and Row, Inc. 151 p.
- Gates, D. M. 1969. Infrared measurement of plant and animal surface temperature and their interpretation. In P. A. Johnson (Editor), *Remote Sensing in Ecology*. Univ. Ga. Press, Athens, Georgia. 244 p.
- Gates, D. M. 1970. Physical and physiological properties of plants. In *Remote Sensing, with Special Reference to Agriculture and Forestry*. Washington, D. C. Natl. Acad. Sci. 424 p.
- Gilbert, P. F., and J. R. Grieb. 1957. Comparison of air and ground deer counts in Colorado. *J. Wildl. Manage.* 21(1): 33-37.
- Goss, J. R., and F. A. Brooks. 1956. Constants for empirical expressions for downcoming atmospheric radiation under cloudless sky. *J. Meteorol.* 13: 482-488.
- Grzimek, M., and B. Grzimek. 1960. Census of plains animals in the Serengeti National Park, Tanganyika. *J. Wildl. Manage.* 24(1): 27-37.

- Gubareff, G. G., J. E. Janssen, and R. H. Torborg. 1960. Thermal radiation properties survey, 2nd ed. Minneapolis, Minn.: Minneapolis-Honeywell Regulator Co. 293 p.
- Hackforth, H. L. 1960. Infrared radiation. New York: McGraw-Hill Book Company, Inc. 303 p.
- Hammel, H. T. 1955. Thermal properties of fur. *Am. J. Physiol.* 182: 369-376.
- Hammel, H. T. 1956. Infrared emissivity of some arctic fauna. *J. Mammal.* 37: 375-378.
- Hardy, J. D., and Alice M. Stoll. 1954. Measurement of radiant heat load on man in summer and winter Alaskan climates. *J. Appl. Physiol.* 7: 200-211.
- Hart, J. S., O. Heroux, W. H. Cottle, and J. A. Mills. 1961. The influence of climate on metabolic and thermal responses of infant caribou. *Can. J. Zool.* 39: 845-856.
- Hatfield, H. S., and L. G. C. Pugh. 1951. Thermal conductivity of human fat and muscle. *Nature* 168: 918-919.
- Hirsch, S. N., R. L. Bjornsen, F. H. Madden, and R. A. Wilson. 1968. Project firescan fire mapping final report. U.S.D.A. Forest Serv. Res. Pap. INT-49. Intermountain Forest and Range Exp. Stn., Ogden, Utah. 56 p.
- Irving, L., and J. Krog. 1955. Temperature of skin in the Arctic as a regulator of heat. *J. Appl. Physiol.* 7: 355-364.
- Kelly, C. F., T. E. Bond, and H. Heitman, Jr. 1954. The role of thermal radiation in animal ecology. *Ecology* 35(4): 562-569.
- Lambert, J. L. 1970. Thermal response of a plant canopy to drifting cloud shadows. *Ecology* 51(1): 143-149.
- Lentz, C. P., and J. S. Hart. 1960. The effect of wind and moisture on heat loss through the fur of newborn caribou. *Can. J. Zool.* 36: 979-682.
- Leopold, A. 1933. Game management. New York: Charles Scribner's Sons. 481 p.
- List, R. J. 1958. Smithsonian meteorological tables. Smithsonian Inst. Pub. 4014 (rev. ed. 6). 527 p.
- Maloiy, G. M. O. 1968. The physiology of digestion and metabolism in the red deer (*Cervus elaphus* L.) Ph.D. Thesis. Rowett Research Inst., Aberdeen Scotland. 192 p.

- Marble, Harriet P. 1967. Radiation from big game and background: A control study for infrared scanner census. M.S. Thesis. Univ. of Montana.
- McCain, R., and W. P. Taylor. 1956. Methods of estimating numbers of mule deer. In W. P. Taylor (editor). The Deer of North America. Harrisburg, Pa.: The Stackpole Co. 668 p.
- McCullough, D. R., C. E. Olson, and L. M. Queal. 1969. Progress in large animal census by thermal mapping. In P. A. Johnson (Editor), Remote Sensing in Ecology. Univ. Ga. Press, Athens, Ga. 244 p.
- McEwan, E. H., A. J. Wood, and H. C. Nordan. 1965. Body temperature of barren ground caribou. Can. J. Zool. 43(5): 683-687.
- McGinnis, S. M., Virginia A. Finch, and A. M. Harthoorn. 1970. A radio-telemetry technique for monitoring temperatures from unrestrained ungulates. J. Wildl. Manage. 34(4): 921-925.
- Moen, A. N. 1968. Energy exchange of white-tailed deer, western Minnesota. Ecology 49(4): 676-682.
- Monteith, J. L., and G. Szeicz. 1962. Radiative temperature in the heat balance of natural surfaces. Q. J. R. Meteorol. Soc. 88: 496-507.
- Moote, Irene. 1955. The thermal insulation of caribou pelts. Textile Res. 25: 832-837.
- Myers, V. I., and M. D. Heilman. 1969. Thermal infrared for soil temperature studies. Photogramm. Eng. 35(4): 1024-1032.
- Olson, C. E. 1967. Accuracy of land-use interpretation from infrared imagery in the 4.5 to 5.5 micron band. Ann. Am. Assoc. Geogr. 57: 382-388.
- Parker, H. D., and J. C. Harlan. 1972. Solar radiation affects radiant temperatures of a deer surface. USDA Forest Serv. Res. Note RM-215. Rocky Mt. Forest and Range Exp. Stn., Fort Collins, Colo.
- Pennycuik, C. J. 1969. Methods of using light aircraft in wildlife biology. Proc. Workshop on the Use of Light Aircraft in Wildlife Management in East Africa. Dec. 1968. Special Issue: East Afr. Agric. and Forest. J.
- Porter, W. P., and D. M. Gates. 1969. Thermodynamic equilibria of animals with environment. Ecol. Monogr. 39(3): 227-244.
- Reichert, D. W. 1972. Rearing and training deer for food habits studies. USDA Forest Serv. Res. Note RM-208. Rocky Mt. Forest and Range Exp. Stn., Fort Collins, Colo.

- Reifsnnyder, W. E., and H. W. Lull. 1965. Radiant energy in relation to forests. U. S. Dep. Agric. Tech. Bull. 1344. 111 p.
- Sauberer, F., and Inge Dirmhirn. 1958. Das strahlungsklima. In Klimatographie von Österreich, Vienna Akad. Wiss. Denkschr. des Gesamtakademi. 3: 13-102.
- Scholander, P. F., R. Hock, V. Walters, F. Johnson, and L. Irving. 1950. Heat regulation of some arctic and tropical mammals and birds. Woods Hole Biol. Bull. 99: 237-258.
- Silver, Helenette, N. F. Colovos, and H. H. Hayes. 1959. Basal metabolism of white-tailed deer- a pilot study. J. Wildl. Manage. 23(4): 434-438.
- Silver, Helenette, N. F. Colovos, J. B. Holter, and H. H. Hayes. 1969. Fasting metabolism of white-tailed deer. J. Wildl. Manage. 33(3): 490-498.
- Silver, Helenette, J. B. Holter, N. F. Colovos, and H. H. Hayes. 1971. Effect of falling temperature on heat production in fasting white-tailed deer. J. Wildl. Manage 35(1): 37-46.
- Siniff, D. B., and R. O. Skoog. 1964. Aerial censusing of caribou using stratified random sampling. J. Wildl. Manage. 28(2): 391-401.
- Stephens, Deborah, and A. N. Moen. 1970. Functional aspects of wind as an ecological and thermal force. Trans. N. Am. Wildl. and Nat. Resour. Conf. 35: 106-114.
- Stingelin, R. W. 1969. Operational airborne thermal imaging surveys. Geophysics 34(5): 760-771.
- Taylor, W. P. 1956. The deer of North America. Harrisburg, Pa.: The Stackpole Co. 668 p.
- Texas Instruments, Inc. 1971. Infrared systems highlighting IR mappers and real-time IR sensors. In Remote Sensing for Forest Fire Control. Div. Forest Fire and Atmos. Sci. Res., U.S.D.A. Forest Serv.
- Thomas, D. C. 1967. Population estimates of barren-ground caribou March to May, 1967. Can. Wildl. Serv. Rep. 9. 44 p.
- Tibbals, E. C., Ellen K. Carr, D. M. Gates, and F. Kreith. 1964. Radiation and convection in conifers. Am. J. Bot 51(5): 529-538.
- Turner, M. I. M., and R. M. Watson. 1964. A census of game in Ngorongoro Crater. East Afr. Wildl. J. 2: 165-168.
- Watson, G. W., and R. F. Scott. 1969. Aerial censusing of the Nelchina caribou herd. Trans. North Am. Wildl. Conf. 21: 499-510.

- Weaver, D. K., W. E. Butler, and C. E. Olson. 1969. Observations on interpretation of vegetation from infrared imagery. In P. A. Johnson (Editor), Remote Sensing in Ecology. Athens, Georgia: Univ. Ga. Press. 244 p.
- Werner, H. D., and F. A. Schmer. 1971. Application of remote sensing techniques to monitoring soil moisture. Rem. Sens. Inst. Tech. Rep. RSI -71-4. South Dak. State Univ. 133 p.
- Wilson, R. A., S. N. Hirsch, F. H. Madden, and B. J. Losensky. 1971. Airborne infrared forest fire detection system; final report. U.S.D.A. Forest Serv. Res. Pap. INT-93. Intermountain Forest and Range Exp. Stn., Ogden, Utah. 102 p.
- Wolfe, W. L. (ed.). 1965. Handbook of military infrared technology. Wash. D. C.: U. S. Gov. Print. Off.
- Yates, H. W., and J. H. Taylor. 1960. Infrared transmission of the atmosphere. NRL Rep. 5453. 45 p. U. S. Nav. Res. Lab., Wash. D.C.

APPENDIX A

Properties of Infrared Radiation

Infrared radiation is emitted by all materials above the temperature of absolute zero (0°K. , -273°C. , -459°F.). It is caused by the rotational and vibrational motion of the atoms and molecules which compose the emitting material. The wavelength distribution of radiation emitted depends on the temperature of the emitting surface (Figure 43).

The disposition of radiation incident on a surface depends on the properties of the surface and the wavelength of radiation. It may be absorbed by the surface, reflected from the surface, or transmitted through the surface. Kirchoff's law relates these three phenomena.

$$\alpha + \rho + \tau = 1.0 \quad (27)$$

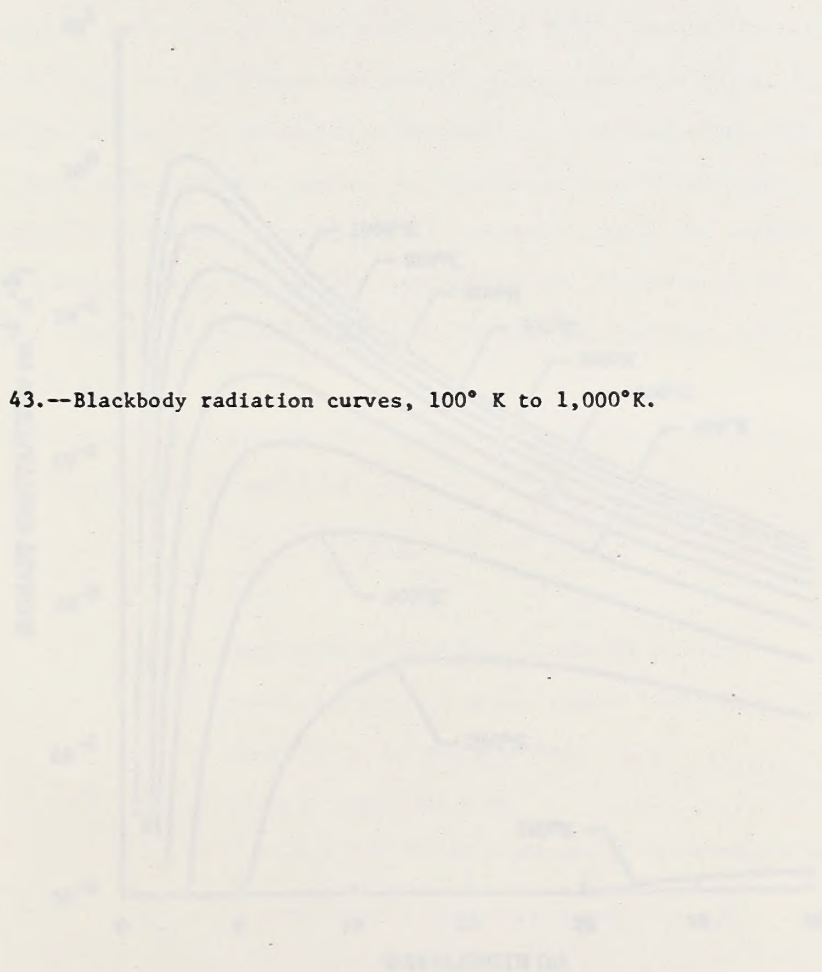
α = absorptance

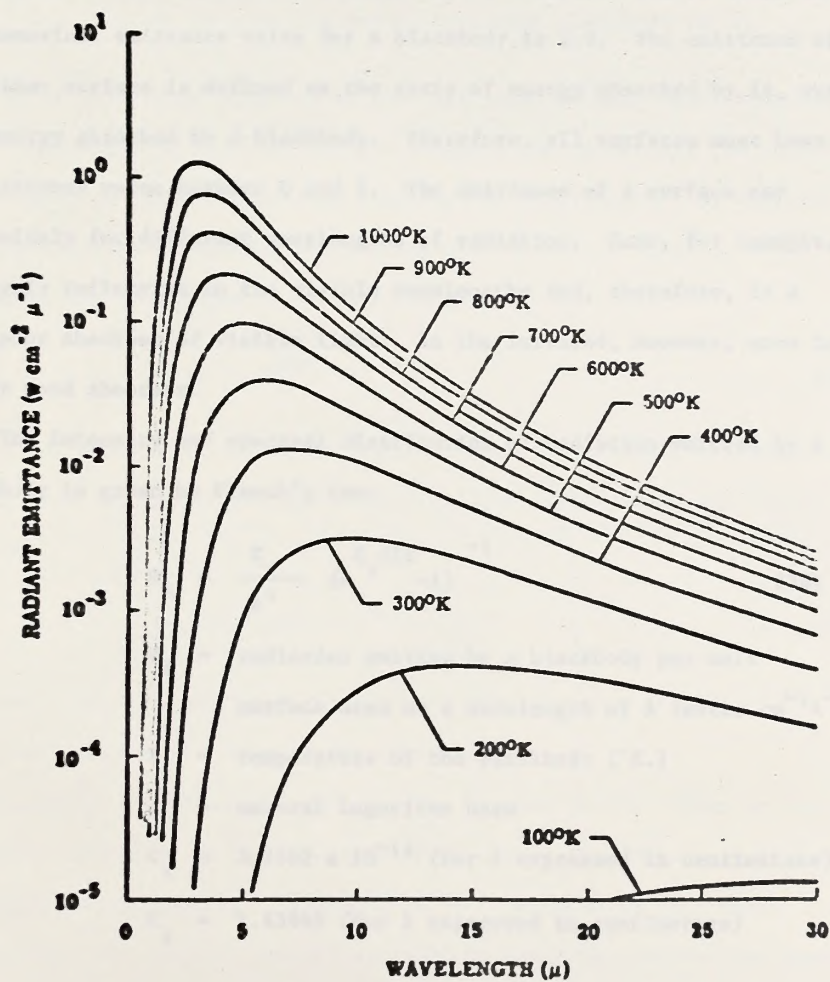
ρ = reflectance

τ = transmittance

Kirchoff's Law also states that under conditions of temperature equilibrium, emittance (ϵ) equals absorptance ($\epsilon = \alpha$). Therefore, a surface which is a good absorber of radiation is also a good emitter of radiation.

Figure 43.--Blackbody radiation curves, 100° K to 1,000°K.





A blackbody, by definition, is any object which absorbs all of the radiation which is incident on it. This is an idealized concept; no surface is a perfect blackbody. However, it is useful as a standard against which the absorptance (emittance) of materials can be compared. The numerical emittance value for a blackbody is 1.0. The emittance of any other surface is defined as the ratio of energy absorbed by it, over the energy absorbed by a blackbody. Therefore, all surfaces must have an emittance value between 0 and 1. The emittance of a surface may vary widely for different wavelengths of radiation. Snow, for example, is highly reflective in the visible wavelengths and, therefore, is a very poor absorber of visible light. In the infrared, however, snow is a very good absorber.

The intensity and spectral distribution of radiation emitted by a blackbody is given by Planck's Law:

$$W_{\lambda} = \frac{C_1}{\lambda^5} (e^{\frac{C_2}{\lambda T}} - 1)^{-1} \quad (28)$$

W_{λ} = radiation emitted by a blackbody per unit surface area at a wavelength of λ (watts $\text{cm}^{-2}\lambda^{-1}$)

T = temperature of the blackbody ($^{\circ}\text{K}$.)

e = natural logarithm base

C_1 = 3.7402×10^{-12} (for λ expressed in centimeters)

C_2 = 1.43848 (for λ expressed in centimeters)

Integration of Planck's Law over all wavelengths produces the Stefan-Boltzmann equation:

$$W_t = \sigma T^4 \quad (29)$$

W_t = total radiation emitted over all wavelengths

σ = Stefan-Boltzmann constant

T = temperature of radiating blackbody in °K.

It is clear from equation 29 that the total radiant power emission from a blackbody is dependent on its temperature. Likewise, the wavelength of peak radiation is also dependent on temperature. By differentiating the Planck equation and setting the derivative equal to zero, we obtain the wavelength of maximum radiation:

$$\lambda_{\max} = \frac{2897}{T} \quad (30)$$

Since real surfaces are not perfect blackbodies, their emittance (ϵ) is less than unity and their total radiant emittance is reduced as follows:

$$W_t = \epsilon \sigma T^4 \quad (31)$$

Note that the emittance term affects the intensity of radiation only--wavelengths of radiation are unchanged.

A comment on terminology is in order at this point. There is considerable confusion in the literature surrounding the difference between emittance and emissivity. According to the standards in electrical terminology, the suffix "-ivity" attached to radiation properties, should be reserved for properties which are independent of size, shape or surface condition. The suffix "-ance" should be used in reference to radiation

properties of materials with specific values for these characteristics. An example is "emissivity applied to a highly polished, uniform metal surface, whereas the same property for a particular surface of the same metal where surface condition is less than perfect, should be termed "emittance". This distinction in terminology has been approved by the American Institute of Physics (Gubareff, et al., 1960), and by the Optical Society of America (Wolfe, 1965). Since, among natural, biotic surfaces such as animals and vegetation, no "perfect" surface exists from the standpoint of radiation properties, it is the author's opinion that use of the term "emissivity" should be discontinued entirely in reference to natural surfaces. Accordingly, "emittance" is used exclusively in this thesis.

The intensity of radiation received from a point source on a surface of fixed area varies inversely with the square of the distance between the surface and the source. This relationship is known as the inverse-square law. Thus, if the distance between the source and detector is halved, the radiation intensity is quadrupled. The radiation received by the detector also depends on the view angle of the detector relative to the plane of the radiating surface. This relationship is expressed by Lambert's cosine law which states that the intensity of radiation emitted varies as the cosine of the angle (θ) between a line from the detector to the radiating surface and a perpendicular to that surface. Equation 32 combines the Stefan-Boltzmann equation with the inverse square law and Lambert's cosine law.

$$W_e = \frac{W_t A}{2\pi d^2} \cos \theta \quad (32)$$

W_e = radiation received by detector

W_t = total radiation emitted by source

A = area of source

d = distance from source to detector

APPENDIX B

MODES OF HEAT TRANSFER

Conduction

Conduction is the transfer of heat in a solid or between solids in contact. It arises from the existence of thermal gradients between the points of heat transfer. For the general, steady-state case, the rate of heat conduction is given by Fourier's heat conduction equation.

$$\frac{dQ}{dt} = KA \frac{dT}{dx} \quad (33)$$

The rate of conduction ($\frac{dQ}{dt}$) is determined by the conductance of the material (K), the area across which conduction is occurring (A), and the temperature difference (dT) associated with the distance dx. The net heat exchange will always be from the higher temperature to the lower temperature region.

Convection

Convection is the transfer of heat between a solid and a fluid in contact. It is a combination of conduction at the molecular level, and mass transport of the fluid resulting in the mixing of fluid molecules of different temperatures. Molecules in contact with the solid surface obtain heat by conduction from the surface. In turn, these molecules lose heat to others as they come in contact by the mixing action. The greater the rate of mixing, the more rapid is the heat transfer.

There are two types of convection: 1) natural or free convection, in which mixing is caused only by density differences resulting from temperature differentials within the fluid, and 2) forced convection, where mixing is caused by external forces, such as wind.

Convection only occurs in a narrow thickness of the fluid adjacent to the solid called the boundary layer. Heat is transferred by conduction into the boundary layer from the solid surface, and by convection, through the boundary layer. Under steady-state conditions, conduction from the solid must equal convection through the boundary layer. Otherwise, there would be a net heat gain or loss within the boundary layer.

As with conduction alone, the amount of heat transferred by convection is proportional to the temperature difference between the solid and the fluid.

$$\frac{dQ}{dt} = hA (T_a - T_s) \quad (34)$$

The rate of heat transfer $\left(\frac{dQ}{dt}\right)$ is proportional to the temperature difference between the solid and the fluid $(T_a - T_s)$, the solid surface area (A) , and a proportionality constant (h) , which is dependent on several properties of the solid and the fluid. Among these properties are: 1) shape of the solid, 2) orientation of the solid, 3) surface finish of the solid, 4) fluid density, 5) fluid viscosity, 6) thermal conductance of the fluid, and 7) fluid velocity over the solid surface. Thus, h is extremely difficult or impossible to formulate for unsteady-state, natural surfaces.

If conduction from the solid must equal convection through the boundary layer (for the steady-state case), then equations 33 and 34 may be equated.

$$\frac{dQ}{dt} = KA \frac{dT}{dx} = hA (T_a - T_s) \quad (35)$$

$$\text{or, } KA \left(\frac{T_a - T_s}{x} \right) = hA (T_a - T_s)$$

$$\frac{k}{x} = h$$

Equation 35 is a simplification of the derivation of h ; analytical procedures are insufficient to describe h for most real situations. Several semiempirical variables have been formed, however, which serve to define h for some specific cases. Among these are the Nusselt number, Prandtl number, and Grashof number. Further discussion of their formulations and applications may be found in Gates (1962) and Birkebak (1966).

Radiation

There is a fundamental difference between radiant heat transfer and conductive or convective heat transfer. Both conduction and convection depend on the existence of a thermal gradient as the driving force for heat transfer. Radiation, however, occurs continuously, regardless of existing gradients, provided the radiating body is above the temperature of absolute zero.

Although the net heat transfer over any time period depends on the temperature difference between mutually radiating bodies, the rate of radiant energy transfer from a particular surface is a function of surface

temperature and emittance of the radiating surface (equation 28).

In order to determine the net rate of radiant heat transfer to or from a particular surface, it is necessary to examine both energy loss and gain, since they are always simultaneous processes.

The total radiant heat loss from a surface, per unit radiating surface area, is given by equation 31.

To obtain total radiant heat loss from a particular surface (S_1) equation 31 is multiplied by radiating surface area (A_1).

$$W_t = A_1 \epsilon_1 \sigma_1 T^4 \quad (36)$$

If we assume S_1 is receiving radiation from a single other source S_2 , then the net radiant energy transfer for S_1 may be expressed as follows:

$$W_{net} = F_1 A_1 \epsilon_1 \sigma_1 T^4 - F_2 A_2 \epsilon_2 \sigma_2 T^4 \quad (37)$$

In this equation F_1 and F_2 are geometrical constants to account for the shapes and orientations of the mutually radiating surfaces, S_1 and S_2 . If thermal equilibrium exists, $W_{net} = 0$, and there is no net gain or loss. In this case,

$$F_1 A_1 \epsilon_1 T_1^4 = F_2 A_2 \epsilon_2 T_2^4 \quad (38)$$

More practically, any real surface is actually receiving radiation from a vast array of radiating bodies simultaneously, resulting in an energy system so complex as to defy analytical description. According to Birkebak (1966), "...it is necessary to rely on measured values for the performance of calculations to radiation exchange between solid surfaces."

AREA OIL SHALE OFFICE
CENTRAL LIBRARY

Form 1279-3
(June 1984)

BORROWER

OL 737 . USS F
Parker, H. De
Airborne infr
of deer

DATE LOANED	BORROWER

USDI - ELM

Bureau of Land Management
Library
Bldg. 50, Denver Federal Center
Denver, CO 80225

